Article

C-6# vs C-7#-Substituted Steroidal Aromatase Inhibitors: Which is Better? Synthesis, Biochemical Evaluation, Docking Studies and Structure-Activity Relationships

Fernanda Maria Fernandes Roleira, Carla Varela, Cristina Amaral, Saul C. Costa, Georgina Correia-da-Silva, Federica Moraca, Giosuè Costa, Stefano Alcaro, Natercia Almeida Teixeira, and Elisiário J. Tavares da Silva

J. Med. Chem., **Just Accepted Manuscript** • Publication Date (Web): 09 Mar 2019

C-6α *vs* C-7α-Substituted Steroidal Aromatase Inhibitors: Which is Better? Synthesis, Biochemical Evaluation, Docking Studies and Structure-Activity Relationships

Fernanda M. F. Roleira[a,b], Carla Varela[a,b], Cristina Amaral[c], Saul C. Costa[a], Georgina Correia-da-Silva[c], Federica Moraca[d,e], Giosuè Costa[d], Stefano Alcaro[d], Natércia A. A. Teixeira[c], and Elisiário J. Tavares da Silva[a,b*]*

[a] Laboratory of Pharmaceutical Chemistry, Faculty of Pharmacy, University of Coimbra, 3000-548 Coimbra, Portugal

[b] CIEPQPF Centre for Chemical Processes Engineering and Forest Products, University of Coimbra, 3030-790 Coimbra, Portugal

[c] UCIBIO.REQUIMTE, Laboratory of Biochemistry, Department of Biological Sciences, Faculty of Pharmacy, University of Porto, 4050-313 Porto, Portugal

[d] Laboratorio di Chimica Farmaceutica, Dipartimento di Scienze della Salute, Università Magna Græcia di Catanzaro, 88100 Catanzaro, Italy

[e] Department of Chemical Sciences, University "Federico II" of Napoli, via Cinthia, 4, 80126, Napoli, Italy

*Corresponding authors. Tel.: +351 239 488 400; fax: +351 239 488 503; e-mail addresses: froleira@ff.uc.pt (Fernanda M. F. Roleira) and etavares@ff.uc.pt (Elisiário J. Tavares da Silva)

Abstract

C-6α and C-7α androstanes were studied to disclose which position among them is more convenient to functionalize in order to reach superior aromatase inhibition. In the first series, the study of C-6 *vs* C-7 methyl derivatives led to the very active compound **9** with IC_{50} of 0.06 μM and Ki = 0.025 μM (competitive inhibition). In the second series, the study of C-6 *vs* C-7 allyl derivatives led to the best aromatase inhibitor **13** of this work with IC_{50} of 0.055 μM and Ki = 0.0225 μM (irreversible inhibition). Beyond these findings, it was concluded that position C-6α is better to functionalize than C-7α, except when there is a C-4 substituent simultaneously. In addition, the methyl group was the best substituent, followed by the allyl group and next by the hydroxyl group. To rationalize the structure-activity relationship (SAR) of the best inhibitor **13**, molecular modelling studies were carried out.

Introduction

Among the various types of cancer, breast cancer is one of the most expression today, being considered one of the cancers that presents a higher incidence rate and constitutes one of the main causes of death of Women around the World.[1] Most breast cancers are hormone-dependent and 80% of these cancers have estrogen receptors (ER^+), which allows them to use these hormones for their growth. Estrogens are produced in the body through a cascade of steroid compound reactions that starts from cholesterol. The latter reaction of this cascade is catalysed by an enzyme called aromatase, which converts the enone function present on the A ring of testosterone and androstenedione into the phenolic aromatic ring present in estradiol and estrone, respectively. For this reason, the enzyme aromatase, which belongs to the cytochrome P450 superfamily, is a very valuable therapeutic target for the selective treatment of estrogen-dependent breast cancer.[2] There are currently only three aromatase inhibitors in clinical use for the treatment of this type of breast cancer. Letrozole and anastrozole are two of these inhibitors and belong to the group of azole derivatives, while exemestane is the only inhibitor of the steroid group marketed (Figure 1). These three third generation aromatase inhibitors are part of the first-line arsenal for the treatment of breast cancer (ER^+) after menopause,[3] being very potent as anti-tumor and very selective for aromatase. However, all of these inhibitors have side effects resulting from their use for very long periods (five years). The most serious side effects are the progressive loss of bone density (osteoporosis) associated with increased risk of bone fractures and bone pain, as well as cardiovascular problems resulting from reduced levels of estrogens.[4, 5] Other type of side effects causing by the prolonged administration of these inhibitors relate to the phenomenon of resistance acquired by the tumor cells leading to tumors regrow and, consequently, to the progression of cancer.[6] In order to overcome these drawbacks it has become necessary to develop novel aromatase inhibitors. Recently, very important works related to nonsteroidal AIs have been reported.[7-9] However, the investigation on steroidal AIs has been less explored, though steroidal AIs are more selective, highly enzyme specific and less toxic[10] due to its structural similarity with the aromatase substrate, androstenedione. In addition, the use of the combination of exemestane with other drugs has been proposed for the treatment

of women with metastatic breast cancer, when acquired resistance to nonsteroidal AIs appears.[11, 12] Further, it has been suggested that, among the AIs in clinical use, exemestane is the only one that has shown to be less aggressive in osteoblasts *in vitro*[13] mainly due to its androgenic activity, leading to reduced side effects associated with loss of bone density.[5, 14, 15] Our previous work has been focused on the study of several new steroidal compounds modified with convenient groups in their A-, B- and D-rings. Some of our new molecules have potent anti-aromatase activity,[16-20] causing anti-proliferative effects and resensitizing resistant breast cancer cells to aromatase inhibition.[21-23] In the present project we are particularly interested in studying steroids substituted in positions 6 and 7, because some studies propose that alkyl or phenyl functions attached at the C-6 or C-7 positions of the androstane backbone may be effective in inhibiting the enzyme aromatase,[24-28] once functional groups at these positions are capable of promoting interactions with the active site of the enzyme. In addition, Ghosh *et al.*[29, 30] described the existence of an access channel cavity located near the C-4 and C-6 positions of the androstenedione complexed with aromatase. They also developed very potent C-6 substituted steroids with alkyl and alkynyl side chains capable of being anchored in the described access channel cavity of the enzyme, resulting in very efficient inhibition.[28] Further, recent studies from our group[18] revealed that C-7α allyl derivatives of androstenedione strongly interact with aromatase leading to its inhibition. However, despite all these studies, the best position to functionalize among positions 6 and 7 of androstane framework still remains unknown. For these reasons, it is our intention to do analog design by preparing new series of steroidal androstanes (Schemes 1-8), based on the most potent and promising hit compounds previously developed by our team,[16-18] namely those with double bonds or epoxide functions at positions C-1, C-3 or C-4, having additional C-6 or C-7 methyl, allyl or hydroxyl groups. After preparation, the new compounds will be evaluated for their inhibitory activity against aromatase, aiming to construct robust structure-activity relationships (SAR) with respect to the referred positions, and ultimately discover hit compounds which can establish a base to develop new lead and drug candidates steroidal AIs for the therapy of ER^+ breast cancer.

Results

Chemistry

The first series synthesized was the methyl series (Scheme 1). Accordingly, the synthesis of 6α-methyl derivatives **1a**, **3a** and **9** was achieved following the strategy reported at scheme 2. Direct alkylenation of androstenedione (**22**) was performed by sodium acetate, phosphoryl chloride and formaldehyde dimethyl acetal in chloroform under reflux temperature.[31] Column chromatography purification allowed isolating **23** in 17% yield. Compound **9** was prepared in 71% yield through reaction of **23** in refluxing solution of ethanol/cyclohexene and catalysis by 5% Pd-C.[32] The follow up of this reaction was easily made by UV spectroscopy once the starting material absorbs at λ_{max} of 260 nm while the desired product absorbs at λ_{max} of 240 nm. This reaction allowed obtaining stereoselectively the 6α-methyl derivative **9,** with the methyl group in the more stable equatorial conformation, which structure was assigned by comparing the NMR and melting point data with that referred in the literature.[32] Alternatively, compound **9** could also be prepared from compound **30** in 47% yield, as discussed later (scheme 4). Compound **9** was then reduced under reflux by zinc dust in glacial acetic acid through a *Clemmenson* reaction,[33] leading to an isomeric mixture of 5α- and 5β-olefins **1a** and **1b** (1.7:1), respectively. Separation of this mixture by column chromatography allowed isolating the pure isomer **1b** in 13% yield. Isomer **1a** was obtained in mixture with **1b** in 90% purity. The stereochemistry of the 5α (**1a**) and 5β (**1b**) stereoisomers was assigned with basis in the chemical shifts observed for the ^{1}H NMR signals for C-19 protons (δ = 0.80 ppm for **1a** and δ = 0.97 ppm for **1b**.[34-36] In the next reaction, the mixture of **1a** and **1b** was treated with performic acid generated *in situ*[35] affording the corresponding mixture of epoxides **3a** and **3b** which after purification by column chromatography afforded **3a** in 44% yield and **3b** in 29% yield. The stereoselectivity of the addition of the peracid on the α-face of 5α-olefin (**1a**) and on the β-face of 5β-olefin (**1b**) was already expected. In fact, the β-face of the olefin **1a** is sterically hindered due to the proximity of the 10β-methyl group. On the other hand, in the 5β-olefin **1b**, the constraint caused by the flexing of ring A on ring B of this isomer renders its β-face more accessible to

the peracid. The stereochemistry of **3a** and **3b** isomers was established based on the chemical shifts shown by the C-19-methyl and C-3 and C-4 proton signals, as well as based on the coupling constants between the C-3 protons and C-4 with the protons C-2 and C-5, respectively.[34-36]

Scheme 3 presents the strategy followed to prepare the studied 7α-methyl compounds. In the first reaction, androstenedione (**22**) was dehydrogenated with chloranil, in *tert*-butanol at reflux temperature.[37] This allowed obtaining **24** in 48%, after purification by column chromatography. Compound **24** was then submitted to a 1,6-conjugate addition using trimethylaluminium in the presence of a catalytic amount of CuBr and trimethylsilyl chloride, in tetrahydrofuran (THF), at room temperature.[37, 38] This reaction produced both C-7 methyl isomers which were separated by column chromatography giving the pure **10a** (30% yield) and **10b** (8% yield). The stereoselectively observed for this step is in accordance with that described for this kind of reaction, affording a major amount of the 7α-methyl isomer **10a**. The stereochemistry of the 7α–methyl (**10a**) and 7β–methyl (**10b**) groups was assigned with basis in the chemical shifts and coupling constants observed for the ^{1}H NMR signals for C-7 methyl protons.[37] After this step, two different paths were followed, one to prepare the Δ^4-olefin **6** (path 1) and another to prepare the Δ^3-olefins **2a** and **2b** (path 2) (Scheme 3). In path 1, compound **10a** was treated with sodium borohydride in trifluoroacetic acid, glacial acetic acid and acetonitrile under nitrogen atmosphere,[39] affording the pure **6** in 10% yield accompanied by its C-17 hydroxyl derivative **25** in 62 % yield, after column chromatography purification. Subsequent reoxidation of compound **25** with Jones reagent allowed its conversion in **6** in 98% yield. Compound **8** was prepared by reaction of **6** with *m*-chloroperbenzoic acid (*m*-CPBA) in dichloromethane at room temperature,[40] being isolated in 90% yield after column chromatography. The stereochemistry of the 4α,5α-epoxide **8** was attributed based on the chemical shift of the C-19 protons.[17] In path 2, compound **10a** was reduced with zinc dust in glacial acetic acid under reflux affording the Δ^3-olefin isomers 5α **2a** and 5β **2b**, in mixture with the Δ^4-olefin **6**. Compounds **2a** and **2b** could not be isolated. However, after sequential column chromatography, some fractions could be enriched in compound **2b** (76%), combined with compound **6** (24%). Oxidation of this mixture with performic acid[35] in dichloromethane at room temperature

afforded, after column chromatography, the 3,4-epoxyde **4** in 56% yield. The stereoselectivity observed in the formation of the olefins **2a** and **2b** was similar to that observed for the formation of **1a** and **1b**. In the formation of epoxide **4**, the same type of stereoselectivity previously discussed for the formation of epoxy derivatives **3a** and **3b** was observed, with the addition of the peracid on the stereochemically free β-side of 5β-olefin **2b**.The stereochemistry of the 5α (**2a**) and 5β (**2b**) stereoisomers was assigned with basis in the chemical shifts observed for the ^{1}H NMR signals for C-19 protons (δ = 0.81 ppm for **2a** and δ = 1.0 ppm for **2b**. Likewise, the stereochemistry of the epoxide derivative **4** was attributed based on the chemical shifts of the C-19, C-3, C-4 and C-7 methyl group protons, as well as their coupling constants.[34-36] The synthesis of compound **5** and its epoxide derivatives **7a** and **7b** was carried out following the strategy presented in scheme 4. Dehydroepiandrosterone (**26**) was submitted to a reduction of the C-17 carbonyl group with sodium borohydride in methanol at 0 ºC[41] leading to the Δ^5-3β,17β-diol **27** in 76% yield. This diol was later set to react under epoxidation conditions using *m*-CPBA in dichloromethane at room temperature[40] affording epoxide **28** (84%). Compound **28** was submitted to nucleophilic attack of methylmagnesium bromide in THF under reflux[41, 42] giving the tertiary alcohol **29** with the methyl group in the C-6 position, in 50% yield. Compound **30** was produced by submitting **29** to Jones oxidation in acetone at 0 ºC.[43] Dehydration of **30** by acid catalysis with HCl in acetic acid at room temperature[44] allowed simultaneous formation of the double bond at C-4 and isomerization of the 6β- to the 6α-methyl group, affording compound **9** in 47% yield. The synthesis of the 3-deoxo derivative **5** was performed by reaction of **9** with a mixture of sodium borohydride in trifluoroacetic acid, glacial acetic acid and acetonitrile under nitrogen atmosphere.[39] In this reaction, **5** was obtained in 14% yield and its C-17 hydroxyl derivative **31**, in 42% yield. Subsequent reoxidation of **31** with Jones reagent allowed its reconversion in **5** in 79% yield. Oxidation of **5** at room temperature with formic peracid[35] gave a mixture of epoxides **7a** and **7b** in 39% and 61% yields, respectively, as determined by NMR. The referred epoxides were separated by column chromatography giving 4α,5α-epoxide **7a** in 31% and 4β,5β-epoxide **7b** in 38% yield. The stereoselectivity observed in the preparation reaction of epoxide derivatives **7a** and **7b** from olefin **5** was expected, based on the results published

previously by the authors for the same type of compounds. The stereochemistry of **7a** and **7b** was attributed based on the chemical shifts of the C-4 and C-19 protons.[17]

The second series synthesized was the allyl series (Scheme 5). Thus, the synthesis of the 6α-allyl substituted derivatives **13, 15** and **17** was carried out through the strategy presented in scheme 6. The first step of the sequence was the protection of the hydroxyl groups of the epoxide **28**. Actually, when the Grignard reaction was performed directly in **28** the yield was very small with many by-products. However, this problem was overcome by using *tert*-butyldimethylsilyl protecting groups for the C-3 and C-17 alcohols. For this, **28** was submitted to reaction with *tert*-butyldimethylsilyl chloride, imidazole and dimethylformamide, at room temperature[45] affording 80% yield of **32**. Grignard reaction of **32** with allylmagnesium bromide in THF at reflux[27] gave the pure compound **33** in 82% yield, after column chromatography. Acid hydrolysis of **33** in ethanol at room temperature afforded the trihydroxylated derivative **34** as an oil, which was directly used to the next reaction. In this reaction, **34** was submitted to Jones oxidation in a mixture of acetone and dioxane[43] leading to the pure **35** in 61% yield, after column chromatography. Acid catalysed dehydration of **35** with HCl in acetic acid at room temperature[44] gave compound **15** in 74% yield. As observed before for other compounds, this reaction occurred with simultaneous formation of the C-4 double bond and isomerization of the 6β- to 6α-allyl group. The α-configuration of the C-6 allyl substituent was assigned on the basis of the ^{1}H NMR spectroscopy. The signal of the olefinic proton at C-4 of the 6α-substituted steroid **15** appears as a doublet ($J_{4\text{-}6\beta}$ = 1.1 Hz) at 5,08 ppm.[27] In order to introduce an additional double bond at C-1/C-2 positions of A-ring, **15** was treated with 2,3-dichloro-5,6-dicyano-1,4-benzoquinone (DDQ) and benzoic acid in toluene, at reflux,[46] allowing the formation of the pure **13** in 81% yield, after alumina filtration followed by column chromatography. To synthesize the 3-deoxo derivative **17**, compound **15** was set to react with a mixture of sodium borohydride in trifluoroacetic acid, glacial acetic acid and acetonitrile under nitrogen atmosphere.[39] These conditions allowed obtaining the pure **17** in 20% yield, and the pure

C-17 hydroxyl derivative **36** in 65% yield, after column chromatography. Reoxidation of **36** with Jones reagent allowed its reconversion in **17**, in 40% yield.

To prepare compound **12** it was followed a six-step strategy depicted in scheme 7. The first reaction consisted in dibromination of androstenedione (**22**) with bromine in acetic acid in diethyl ether at 0º C,[47] leading to an isomeric mixture of 2α,6α- and 2α,6β-dibromoenone **37a** and **37b** in 70% yield. Compound **38** was obtained through an elimination reaction of both **37a** and **37b**, followed by rearrangement, under reflux in an ethanolic solution of potassium acetate[48] in 92 % yield, after crystallization from acetone/*n*-hexane. Acid catalysed hydrolysis of the enol-acetate **38** with a 5% HCl ethanolic solution,[49] led to the diosphenol **39** in 85% yield. After this, protection of the C-4 hydroxyl group of **39** was carried out with acetic anhydride in pyridine at room temperature affording **40** in 69% yield, after column chromatography. This compound was then submitted to a Sakurai reaction with allyltrimethylsilane in anhydrous dichloromethane using $TiCl_4$ as catalyst,[50] giving **41** in 30% yield, after preparative TLC followed by ethyl acetate crystallization. Finally, the acid catalysed hydrolysis of **41** by refluxing in ethanolic HCl solution, afforded the pure **12** in 62% yield.

To prepare compound **11** an eight-step strategy was developed starting from the available testosterone (**42**) (Scheme 8). Reduction of **42** by sodium borohydride in methanol at room temperature yielded the pure **43** in 21% yield, after crystallization.[17] The epoxidation of **43** was performed by reaction with performic acid generated *in situ* and afforded **44** in 71% yield, after purification by column chromatography. Acetylation of **44** with acetic anhydride in pyridine afforded compound **45** in 64% yield. Reaction of epoxide **45** with 75% aqueous CrO_3 in butanone at room temperature afforded the α-ketol **46** in 62% yield.[51] Dehydration of **46** with thionyl chloride in anhydrous pyridine at 0 ºC[52] afforded **47** in 73% yield, after column chromatography followed by diethyl ether/methanol crystallization. The subsequent introduction of the allyl group at C-6 position was achieved through a Sakurai reaction. For that, **47** was set to react in dichloromethane with allyltrimethylsilane and $TiCl_4$ as catalyst at -78 ºC[50, 53] through a 1,4-type addition, affording **48** as a clear oil, in 55% yield. Treatment of **48** with a 5% aqueous NaOH in methanol and acetone, at room temperature gives **49** in 76% yield, after

diethyl ether/*n*-hexane crystallization. The α-configuration of the C-6 allyl substituent of compound **49** was also assigned on the basis of the ^{1}H NMR spectroscopy. The signal of the olefinic proton at C-6 of steroid **49** appears as a double doublet ($J_{6\beta\text{-}7\alpha}$ = 12.9 Hz, $J_{6\beta\text{-}7\beta}$ = 7.8 Hz) at 3.23 ppm. The magnitude of 12.9 Hz for the coupling constant with one of the two C-7 protons and 7.8 Hz with the other reveals interactions of the type 6β-axial/7α-axial and 6β-axial/7α-equatorial. For this reason the C-6 allyl group will have a 6α–equatorial configuration. During the alkaline hydrolysis of **48**, the corresponding C-3/C-17 diol formed rearranges to the more stable diosphenol **49**. The last step of this strategy consisted in the selective Swern type oxidation of the C-17 hydroxyl group of **49** with DMSO activated with trifluoroacetic anhydride (TFAA) and triethylamine in anhydrous dichloromethane at -60 ºC.[54] Purification of the obtained crude by preparative TLC with diethyl ether/toluene gave the pure **11**, in 64% yield.

Biochemistry

The anti-aromatase activity of the synthesized steroidal compounds was determined using human placental microsomes as source of the enzyme and the radiometric method of Thompson and Siiteri[55] in which the ^3H_2O released during aromatization of [1β-^{3}H] androstenedione allows measuring the rate of estrogen formed. Firstly, a screening test was run by determining the percentage of aromatase inhibition (%) for all compounds (Table 1), in relation to the absence of the inhibitor. Formestane (99.22 ± 0.1%) and exemestane (98.91 ± 0.6%) were used as reference AIs. Except steroids **4**, **7a**, **7b**, **8** and **21**, the majority of compounds presented an aromatase inhibition higher than 80%, being steroid **9** (98.73 ± 0.1%) the most potent AI. The IC_{50} value in human placental microsomes was determined for steroids with aromatase inhibition higher than 80%, using [1β-^{3}H] androstenedione at 100 nM concentration (Table 1, Figure 2). Steroids **3a**, **5**, **9**, **12**, **13** and **15** presented IC_{50} values lower than 0.2 μM. The AIs **9** and **13** demonstrate to be the most potent AIs, since they presented an IC_{50} value of 0.060 μM and 0.055 μM, respectively, being these IC_{50} values similar to formestane (0.042 μM)[17] and exemestane (0.050

μM).[19] The anti-aromatase activity in MCF-7aro cells, an aromatase overexpressing ER^+ breast cancer cell line that is considered the best *in vitro* cell model to study AIs,[56, 57] was also studied for the most potent AIs. As presented in Table 1, except for compounds **5** and **12** that induced the formation of crystals in cell culture, the results demonstrate that the majority of these steroids present an anti-aromatase activity higher than 80%. Steroids **9** and **13** were the most potent AIs, since they show an aromatase inhibition of around 98% in cells. For the latter AIs, were additionally carried out kinetic studies aiming to define its binding type with the active site of the enzyme. Moreover, apparent inhibition constants (Ki) were measured, in diverse ranges of concentrations of inhibitor (0.02 – 0.4 μM) and of [1β-^{3}H] androstenedione (10-30 nM) (Table 2). AI **9** revealed to be a competitive inhibitor (Ki = 0.025 μM) while steroid **13** demonstrates to be an irreversible inhibitor (Ki = 0.0225 μM), a behavior similarly to exemestane.[5, 58] As exemestane, compound **13** presents the 1,2-double bond which, according Lombardi P,[59, 60] acts as a latent alkylating group by stabilizing the covalent bond formed between the inhibitor and the enzyme,[59, 60] turning it an irreversible inhibitor. On the other hand, compound **9** not having the 1,2-double bond will not form an irreversible binding with the enzyme, being a competitive inhibitor. Both AIs presented a Ki similar to exemestane (Ki = 0.026 μM),[5, 60] being considered potent AIs. Figure 3 shows representative Lineweaver−Burk and Dixon curves for these AIs.

Docking using GRID Molecular Interaction Fields (MIFs)

Compounds **4**, **7a**, **7b**, **8, 11**, **12**, **13**, **14** and **21** were docked using the FLAPdock tool[61] into the aromatase binding site defined by the FLAPsite utility[62] (Supporting Information, Figures S2). Docking results were ranked according to the FLAP-S Score function, an algorithm that evaluates the overlap similarity between the H (shape), O (H-bond acceptor), N1 (H-bond donor) and DRY (Hydrophobic) MIFs with the compound predicted poses. Looking at the best FLAP S-score poses, it can be observed generally that compounds **11**, **12**, **13** and **14** bind at the active site similarly to the endogenous aromatase substrate, androstenedione (Supporting Information, Figure S4), with the steroidal moiety well overlapping the hydrophobic environment (DRY probe) of the binding pocket, the β-face oriented

toward the heme group and their A- and D-rings positioned toward the Asp309 and the Met374 residues, respectively. This binding orientation was experimentally demonstrated also for the well-known aromatase inhibitor exemestane (Supporting Information, Figure S5)[28] and it is coherent with the proposed catalytic mechanism of aromatase.[63] Nevertheless, the GRID-guided docking method revealed significant differences in the binding geometries adopted by each ligand. Indeed, looking at the energy minimized FLAP S-score poses, it can be clearly observed that, while the 17-keto oxygen atom of the D-ring engages one hydrogen bond with the backbone amide of Met374 as reported for others steroidal inhibitors, the 3-keto oxygen atom of the A-ring adopts, among all ligands, different binding geometries. Indeed, the 3-keto oxygen atom of **13** is the closest to the carboxylate group of Asp309 (3.7 Å) (Figure 4). This distance is almost similar to that reported experimentally in literature for the inhibitor exemestane (3.0 Å) (Supporting Information, Figure S5),[28] the parent compound of **13**. A further analysis of other binding geometric properties (dihedrals and angles) (Supporting Information, Table S5) support the very similar binding mode adopted by **13** with respect to the bioactive conformation of exemestane (Supporting Information, Table S5 and Figure S5). It is worth to mention that all the geometric measurements were taken from the energy minimized FLAPdock poses, in order to take into account both receptor and ligands adjustments. The peculiar geometric features of **13** lead this inhibitor to be a similar competitor of exemestane with the aromatase endogenous substrate androstenedione. We cannot exclude that an important contribution is given by the better planarity of the A-ring of **13**, conferred by the 1,2- and 4,5-double bonds, which is an important structural requirement for the anti-aromatase activity.[20] Conversely, the geometrical analysis of the energy minimized docking poses of **11** and **12** (Figures 5 and 6, respectively) reveals that the simultaneous presence of an hydroxyl group at C-4 causes a deeper distortion of the dihedrals C6-C5-C4-C3 and C4-C3-O1-OD2, especially when the allyl side chain is positioned at C-6α (**11**) (Supporting Information, Table S5), probably due to the steric hindrance reasons. The main consequence of this distortion concerns the 3-keto oxygen, which is farther from the carboxylate group of Asp309 (5.0 Å) in the case of **11** and 4.1 Å in the case of **12** (Supporting Information, Table S5) (Figures 5 and 6, respectively). Finally, compound **14** although owns the same

A-ring planarity as **13** and exemestane (Supporting Information, Table S4), its 3-keto oxygen is 6.0 Å far from the OD2 oxygen atom of Asp309 (Figure 7). This is mainly due to steric hindrance of the C-7α allyl side chain with Leu477 and Ser478 residues that it is not able to accommodate within the access channel, similarly to **12** (Figure 6). As concerns the docking poses of the less active compounds **4**, **7a**, **7b** and **8** (Supporting Information, Figure S3), it seems that the loss of activity of these epoxide derivatives could be due to the absence of the 3-keto oxygen atom in the A ring and, in the case of **4**, also to the 5β-stereochemistry, which prevents the establishment of a hydrogen bond with Asp309. The epoxide oxygen atom is led, in fact, very far from the Asp309 (Supporting Information, Figures S3A, S3B, S3C and S3D). In addition, we cannot discard the pronounced deformation of the 4,5-epoxides A-ring, as previously reported by the authors.[20] On the contrary, compound **21** owns the 3-keto oxygen atom in the A ring, but the simultaneous presence of an hydroxyl group at C-7α alters its binding geometry, so that the 3-keto oxygen atom is located almost perpendicularly at a distance of 4.0 Å to the carboxylate group of Asp309, thus disfavouring any hydrogen bond interaction (Supporting Information, Figure S3E). A further explanation of the lower activity of **21** lies in the binding geometry of the hydroxyl group, which falls in a hydrophobic region of the binding pocket (Supporting Information, Figure S6), thus disfavouring its interactions.

Discussion and Conclusions

As referred, the best position to functionalize, among positions C-6 and C-7 of androstane framework, to reach efficient aromatase inhibition, still remains unknown. That is why we invested in the design and synthesis of series of new steroidal androstanes, with different substituents in position C-6 and C-7. An analog design was performed based in the most potent hit compounds previously developed by our group as models. Structural properties of the aromatase active site, near the C-4, C-6, and C-7 positions of androstenedione[28] were also taken into consideration.

One of the series designed and synthesized was the C-6/C-7 methyl series (Scheme 1). In this series there are a number of compounds with a methyl group in position C-6 and also a number of

analogous compounds with a methyl group in position C-7. Looking at the aromatase inhibitory activity of these compounds (Table 1), it is possible to conclude that, generally, C-6 methyl derivatives are better AIs than the corresponding C-7 methyl derivatives, either in microsomes or in breast cancer cells. By comparing the pairs **5**/**6** (IC_{50}= 0.17/0.40 μM) and **9**/**10a** (IC_{50}= 0.06/0.27 μM) this conclusion turns clear. Further, for the pair **9**/**10a**, it is possible to infer the same conclusion from the results obtained in MCF-7aro cells (inhibition %= 98.56/90.77), respectively. In the case of the pair **1a**/**2b** (IC_{50}= 0.56/0.51 μM), it is not possible to do an accurate comparison firstly because compound **2a** (Scheme 3), with 5β stereochemistry, could not be isolated and secondly because compound **2b** was always obtained in mixture with compound **6**, which presents itself an IC_{50} of 0.40 μM. By this reason the activity of **6** must contribute to increase the activity of **2b**, which being a C-5β androstane would reveal low aromatase activity.[16, 17, 64-66] In the case of the pair **3a/4** (inhibition %=96.72/13.66, in microsomes), again it was not possible to do a precise comparison, since the C-5α derivative of **4** could not be isolated. Instead we isolated the C-5β epoxide **4** whose percentage of aromatase inhibition (13.66%), corroborates the low capacity of inhibition of C-5β androstanes. Considering the pair **7a**/**8** (inhibition %=58.69/64.89, in microsomes) it seems that, in this case, C-6 and C-7 methyl derivatives have similar activities, presenting the C-7 methyl derivative a slightly higher activity. When comparing with the other compounds of this series, the pair **7a**/**8** presents an additional structural feature, namely a substitution at C-4/C-5 positions, which may interfere with the interaction of the C-6 substituent with the aromatase active site, as discussed later. In addition, by focusing in the structural features of the A-ring, it is possible to infer that the presence of a 3,4-epoxide is better than a 3,4-olefin for aromatase inhibition, as observed for the pair **1a**/**3a** (IC_{50}=0.56/0.175 μM), but the presence of a 4,5-olefin is better than a 4,5-epoxide, as in pairs **5**/**7a** (inhibition %=96.72/58.69, in microsomes) and **6**/**8** (inhibition %=97.39/64.89, in microsomes). This kind of SAR was already observed for similar compounds without substitution in the B-ring and was thoroughly discussed in previous works of the authors.[17, 20] Considering compounds **7a** and **7b**, it seems that the 4β,5β configuration of the epoxide **7b** favours more the interaction with the aromatase active site as shown also by molecular modelling studies

(Supporting Information, Figure S3C). However, the absence of a 3-keto oxygen atom, deeply decrease its activity. Furthermore, by comparing the pairs **5**/**9** (IC_{50}=0.17/0.06 μM) and **6**/**10a** (IC_{50}=0.405/0.27 μM) it is possible to conclude that the presence of the C-3 carbonyl function is very advantageous for aromatase inhibition. In fact, the presence of a C-3 carbonyl group makes compounds more similar to the natural substrate, androstenedione, allowing the establishment of additional hydrogen bonds with aromatase active site residues, hence favouring enzyme inhibition. Compound **9**, previously prepared as AI by Numazawa *et al*.[27] through a different synthetic strategy, is effectively the most potent aromatase inhibitor of this series, presenting an IC_{50} of 0.06 μM, displaying high affinity to the aromatase (Ki =0.025 μM) and with a competitive type inhibition, showing an IC_{50} and a Ki similar to that of exemestane (IC_{50}=0.05 μM[19] and Ki=0.026 μM[60]) (Table 2). Moreover, this compound also has the ability to efficiently inhibit aromatase (inhibition %= 98.56) in an aromatase overexpressing ER^+ breast cancer cell line, being one of the most potent studied AIs, in these cells.

Other series designed and synthesized was the C-6/C-7 allyl series (Scheme 5). In this series there is a number of compounds with an allyl group in position C-6 and the corresponding analogous compounds with an allyl group in position C-7. As observed for the methyl series, in the allyl series the C-6 allyl derivatives are better AIs than the corresponding C-7 allyl derivatives, either in microsomes or in breast cancer cells, except for the pair **11**/**12** (IC_{50}= 0.52/0.11 μM) (Table 1) where the C-7 allyl derivative is a stronger AI than the analogous C-6. Once again, this pair presents an additional structural feature, namely a C-4 substitution as discussed before for the pair **7a**/**8**. The observation that the pairs **7a**/**8** and **11**/**12** are the only ones that show a stronger aromatase inhibition for the C-7 derivative and that are also the only ones bearing a C-4 substitution, led us to put the hypothesis that the referred substitution may play an significant role in the molecular interaction within the aromatase active site. The case of the pair **11**/**12** was deeply studied by docking simulations showing that, in both compounds **11**/**12**, the simultaneous presence of a hydroxyl group at C-4 and the allyl side chain at C-6α and C-7α, respectively, interferes with the steric hindrance to the A-ring, which is located farther from Asp309 thus preventing the establishment of strong hydrogen bonding between the 3-keto oxygen atom and

Asp309. In any case, the C-7α substitution of the allyl side chain is more favoured, because the A-ring finds closer to Asp309 with respect to **11** (Figures 5 and 6).

Regarding the structural features of the steroidal A-ring, one can say that besides the C-4 double bond, the presence of an additional carbonyl group at C-3 is advantageous for aromatase inhibition, as in pair **15**/**16** (IC_{50}= 0.105/0.59 μM) relatively to pair **17**/**18** (IC_{50}= 0.21/0.745 μM). As said, a C-3 carbonyl group makes compounds more similar to the natural substrate, androstenedione, permitting the formation of additional hydrogen bonds with aromatase active site residues and favouring enzyme inhibition. Further, the inclusion of an additional double bond in C-1 (pairs **13**/**15** and **14**/**16**) has demonstrated to be very advantageous allowing to found a very potent aromatase inhibitor (compound **13**) presenting an IC_{50} of 0.055 μM, showing high affinity to the aromatase (Ki = 0.0225 μM) and with an irreversible type inhibition. Actually, compound **13** is the most potent compound of this series and also of all the other series, in microsomes and in breast cancer cells, showing a behavior very similar to exemestane, which is also an irreversible inhibitor of aromatase with an IC_{50} around 0.050 μM[19] and a Ki of 0.026 μM[60] (Table 2). Docking simulations confirmed the similar behavior of compound **13** and exemestane as described in the results.

In the C-7α substituted compounds **12** and **14** it was detected a steric hindrance of the C-7α allyl side chain with Leu477 and Ser478 residues that it is not able to well accommodate within the access channel of aromatase. This observation can contribute to explain the worst aromatase inhibitory activity of the C-7 substituted steroids.

An additional series analysed was the C-6/C-7 hydroxyl series (Scheme 9). In this short series there is a compound with a hydroxyl group in position 6α (**20**), a compound with the same substitution in position 6β (**19**) and the corresponding analogous with a hydroxyl group in position 7α (**21**). By analysing their aromatase inhibitory activities (Table 1), it is possible to infer, once more, that the C-6 substitution is preferable to the C-7 substitution. Further, the stereochemistry (α *vs* β) of the substituent at C-6 does not seem to influence the aromatase inhibitory activity since their IC_{50} are similar (**20** IC_{50}= 0.88 μM and **19** IC_{50}= 0.84 μM).

Considering all series, it is even possible to ascertain which of the substitutions (methyl, allyl and hydroxyl) is more convenient to achieve compounds with superior aromatase inhibition. This could be done by comparing the activity of compounds **9**/**15**/**20** (IC_{50}= 0.06/0.105/0.88 μM) and **10a**/**16**/**21** (IC_{50}= 0.27/0.59 μM /inhibition %= 49.83). From this, it is clear that the methyl group seems to be the best substituent among those that were studied.

In summary, it was disclosed for the first time, that 6α position, among 6α and 7α of the steroidal androstane framework, is the best to be functionalized in order to reach superior aromatase inhibition. In this work this was always true, except when there is a C-4 substituent, which can compete with the C-6 substituent to protrude into the access channel of the active site of aromatase, making the C-7 substituent more available to bulge in the referred channel, increasing the activity of the C-7 derivatives. The methyl group proved to be the best substituent among those studied, followed by the allyl and finally the hydroxyl group. Besides the presence of a carbonyl group at C-17 and a double bond at C-4, which is known to be important for aromatase inhibition, the existence of an additional carbonyl group at C-3 and a double bond at C-1 is very beneficial for the referred activity. With this study, very potent aromatase inhibitors in human placental microsomes and in an ER^+ breast cancer cell model were found. In particular, compound **13**, which combines the described structural features, showed a potency and affinity to aromatase similar to exemestane, the reference compound used in clinic for ER^+ breast cancer treatment. Finally, molecular modelling studies guided by the GRID MIFs were useful to rationalize the best inhibition potency of **13**, which shares very similar binding geometries with respect to androstenedione and exemestane, especially as concerns the 3-keto oxygen atom of the A-ring. This new hit compound can compete by itself with exemestane and ultimately establish a base to develop new lead and drug candidates AIs for the treatment of ER^+ breast cancer.

Experimental Section

Chemistry

Melting points (Mps) were determined on a Reichert Thermopan hot block apparatus and were not corrected. IR spectra were recorded on a Jasco 420FT/IR or a PerkinElmer Spectrum 400 FT-IR/FT-NIR spectrometers using the universal ATR sampling accessory, $CHCl_3$ solutions in NaCl plates, or KBr disks.

NMR spectra were recorded on a Brucker AMX 300 spectrometer operating at 300 MHz (^1H) and at 75 MHz (^{13}C) or on a Varian Unity 400 operating at 400 MHz (^1H) and at 100 MHz (^{13}C) and are reported in δ values in ppm downfield from TMS, as internal standard. All *J* values are given in Hz and $^1H-^1H$ couplings are assumed to be first-order. Peak multiplicities are reported in the usual manner and b s, b d, b t and b m, means broad singlet, doublet, triplet or multiplet signals. Mass spectra ESI and LC-MS were obtained with mass spectrometers QIT-MS Thermo Finningan, models LCQ Advantage MAX and LXQ coupled to a Liquid Chromatograph of High Performance Thermo Finningan, model Accela. 6β-Hydroxyandrost-4-ene-3,17-dione (**19**), 6α-hydroxyandrost-4-ene-3,17-dione (**20**) and 7α-hydroxyandrost-4-ene-3,17-dione (**21**) were purchased from Steraloids, Inc. (Newport RI, USA). 3β-Hydroxyandrost-5-en-17-one (**26**) and testosterone (**42**) were purchased from Sigma-Aldrich (Schnelldorf, Germany). Reagents and solvents were used as obtained from the suppliers without further purification, unless otherwise indicated. Compounds **14**, **16** and **18**, were prepared as previously described[17].

All compounds evaluated possess a purity superior to 95%, except compound **1a** (90% purity). The purity of the compounds was checked by HPLC with a C18 - reversed phase column (ACE5 C18) and water/acetonitrile (50:50, 40:60) and acetonitrile/methanol (60:40) were used as solvents. The purity of individual compounds was determined from the area peaks in the chromatogram of the sample solution. The results presented for compound **2b** refers to a mixture of **2b** with **6** (7.6:2.4, by ^1H NMR).

6α-Methyl-5α-androst-3-en-17-one (1a) and 6α-methyl-5β-androst-3-en-17-one (1b)

To a boiling solution of **9** (259.3 mg, 0.863 mmol) in glacial acetic acid (40 mL), zinc dust <10 μm (1.48 g, 22.66 mmol) was added in several portions during 1 h. After 3 h another portion of zinc (1.48 g, 22.66 mmol) was added within 1 h and the reaction was left under reflux for a total of 5 h 15 min. The suspension was filtered, the zinc was washed with glacial acetic acid and the filtrate was evaporated to dryness. The obtained residue was diluted with water (100 mL), extracted with diethyl ether (3x 100 mL) and the organic layer washed with 10% aq $NaHCO_3$ (3x 100 mL) and water (3x 100 mL), dried over anhyd Na_2SO_4, filtered and concentrated to dryness. NMR analysis of the crude revealed that it was composed by a 1.7:1 mixture of isomers **1a** and **1b**, respectively. The crude was purified by silica gel column chromatography (hexane/ethyl acetate) allowing isolating in some fractions the pure **1b** as a white solid residue (32.3 mg, 13% yield). In other fractions, mixtures with different proportions of isomers **1a** and **1b** were obtained (193.7 mg, 78% yield). Two sequential chromatographies allowed obtaining compound **1a** in 90% purity.

6α-Methyl-5α-androst-3-en-17-one (1a): IR (NaCl plates, $CHCl_3$) ν_{max} cm^{-1}: 3030 (=C-H), 1740 (C=O), 1651 (C=C). ^1H NMR (400 MHz, $CDCl_3$) δ: 0.80 (3H, s, 19-H_3), 0.87 (3H, s, 18-H_3), 0.93 (3H, d, J=6.1 Hz, 6α-CH_3), 5.61 (1H, ddd, $J_{3\text{-}4}$=10.0 Hz, $J_{3\text{-}2\beta}$=6.5 Hz, $J_{3\text{-}2\alpha}$=3.3 Hz, 3-H), 5.67 (1H, ddd, $J_{4\text{-}3}$= 10.0 Hz, $J_{4\text{-}5\alpha}$=3.9 Hz, $J_{4\text{-}2\alpha}$=2.0 Hz, 4-H). ^{13}C NMR (100 MHz, $CDCl_3$) δ: 12.6 (C-19), 13.9 (C-18), 19.9 (C-20), 20.3, 21.7, 23.2, 29.5, 31.6, 34.2, 34.7, 35.3, 35.8, 35.9, 47.8, 51.4, 52.3, 53.3, 126.2 (C-3), 127.2 (C-4), 221.4 (C-17). ESI: 287.3 ($[M+H]^+$, 100%).

6α-Methyl-5β-androst-3-en-17-one (1b): $Mp_{(hexane/ethyl\ acetate)}$ 84-87 ºC. IR (NaCl plates, $CHCl_3$) ν_{max} cm^{-1}: 3025 (=C-H), 1740 (C=O), 1647 (C=C). ^1H NMR (400 MHz, $CDCl_3$) δ: 0.86 (3H, s, 18-H_3), 0.96 (3H, d, J=6.9 Hz, 6α-CH_3), 0.97 (3H, s, 19-H_3), 2.03 (1H, ddd, $J_{16\alpha\text{-}16\beta}$=19.0 Hz, $J_{16\alpha\text{-}15\beta}$=9.0 Hz, $J_{16\alpha\text{-}15\alpha}$=9.0 Hz, 16α-H), 2.42 (1H, dd, $J_{16\beta\text{-}16\alpha}$=19.0 Hz, $J_{16\beta\text{-}15\beta}$=9.0 Hz, 16β-H), 5.56 (1H, dd, $J_{4\text{-}3}$=10.3 Hz, $J_{4\text{-}5\beta}$=1.7 Hz, 4-H), 5.70 (1H, dd, $J_{3\text{-}4}$=9.8 Hz, $J_{3\text{-}2\alpha}$=3.5 Hz, 3-H). ^{13}C NMR (100 MHz, $CDCl_3$) δ: 13.8 (C-18), 14.1 (C-20), 19.3 (C-19), 20.8, 21.8, 22.3, 22.7, 22.9, 29.3, 31.8, 34.3, 34.5, 35.6, 35.9, 40.8, 49.1, 51.1, 125.7 (C-4), 127.9 (C-3), 221.5 (C-17).

7α-Methyl-5α-androst-3-en-17-one (2a) and 7α-methyl-5β-androst-3-en-17-one (2b)

To a boiling solution of **10a** (150.4 mg, 0.5 mmol) in glacial acetic acid (20 mL), zinc dust <10 μm (2.29 g, 35 mmol) was added in several portions over 22 h. The zinc suspension was filtered, washed with glacial acetic acid and the filtrate was evaporated to dryness. The residue was diluted with water (70 mL) and extracted with diethyl ether (3x 70 mL). The organic layer was washed with 10% aq $NaHCO_3$ (3x 100 mL) and water (3x 100 mL), dried over anhyd $MgSO_4$, filtered and concentrated to dryness giving a yellow oily residue which was purified by silica gel 60 column chromatography (hexane/ethyl acetate). In some fractions an inseparable mixture of **2b** with **6** was obtained (18.53 mg, **2b** (76%) and **6** (24%), by NMR). In other fractions, **2b** was obtained in a mixture with **2a** and **6** (46.4 mg, **2b** (58%), **2a** (15%) and **6** (27%), by NMR).

Although **2a** and **2b** could not be isolated in the pure form, their characterization could be performed by NMR analysis of the mixture.

7α-Methyl-5α-androst-3-en-17-one (2a): ^{1}H NMR (400 MHz, $CDCl_3$) δ: 0.81 (3H, s, 19-H_3), 0.89 (3H, s, 18-H_3), 0.95 (3H, d, *J*=7.1, 7α-CH_3), 5.23 (1H, ddd, $J_{4\text{-}3}$=8.0 Hz, $J_{4\text{-}5\alpha}$=3.8 Hz, $J_{4\text{-}2\alpha}$=1.9 Hz, 4-H), 5.58 (1H, b m, $W_{1/2}$ *ca.* 4 Hz, 3-H).

7α-Methyl-5β-androst-3-en-17-one (2b): ^{1}H NMR (400 MHz, $CDCl_3$) δ: 0.87 (3H, s, 18-H_3), 0.92 (3H, d, *J*=7.4 Hz, 7α-CH_3), 1.00 (3H, s, 19-H_3), 5.53 (2H, s, 3-H and 4-H). ^{13}C NMR (100 MHz, $CDCl_3$) δ: 13.4 (C-18), 15.4 (C-7'), 20.4, 21.6, 21.8, 22.7 (C-19), 29.5, 31.6, 33.2, 34.2, 34.2, 34.4, 35.8, 36.9, 42.9, 47.3, 47.7, 124.1 (C-3), 134.7 (C-4), 221.5 (C-17).

3α,4α-Epoxy-6α-methyl-5α-androstan-17-one (3a) and 3β,4β-epoxy-6α-methyl-5β-androstan-17-one (3b)

To a stirred solution of compounds **1a** and **1b** (112.4 mg, 0.39 mmol) in DCM (30 mL) at room temperature, performic acid generated *in situ* by the addition of 98-100% HCOOH (0.10 mL) and 30% H_2O_2 (0.21 mL) was added and the reaction was stirred until complete transformation of the starting material (9 h 30 min, TLC). DCM (150 mL) was added and the organic layer was washed successively

with 10% aq $NaHCO_3$ (100 mL) and water (4x 100 mL), dried over anhyd Na_2SO_4, filtered and concentrated to dryness giving a slightly yellow oily residue. This residue was purified by a silica gel column chromatography (hexane/ethyl acetate) allowing to isolate 52.0 mg (44%) of the pure 3α,4α-isomer **3a** and 34.6 mg (29%) of the pure 3β,4β-isomer **3b**, as white solids.

3α,4α-Epoxy-6α-methyl-5α-androstan-17-one (3a): $Mp_{(hexane/ethyl\ acetate)}$ 153-156 ºC. IR (NaCl plates, $CHCl_3$) ν_{max} cm^{-1}: 1740 (C=O), 1013 (C-O). ^1H NMR (400 MHz, $CDCl_3$) δ: 0.79 (3H, s, 19-H_3), 0.85 (3H, s, 18-H_3), 1.07 (3H, d, *J*=6.4 Hz, 6α-CH_3), 2.43 (1H, dd, $J_{16\beta\text{-}16\alpha}$=19.2 Hz, $J_{16\beta\text{-}15\beta}$=8.7 Hz, 16β-H), 2.92 (1H, dd, $J_{4\beta\text{-}5\alpha}$=4.1 Hz, $J_{4\beta\text{-}6\beta}$=1.3 Hz, 4β-H), 3.15 (1H, dd, $J_{3\beta\text{-}2\beta}$=3.4 Hz, $J_{3\beta\text{-}2\alpha}$=3.4 Hz, 3β-H). ^{13}C NMR (100 MHz, $CDCl_3$) δ: 13.8 (C-19), 13.9 (C-18), 19.8, 20.6, 20.9, 21.7 (C-20), 29.5, 30.8, 31.5, 34.4, 34.7, 35.9, 40.2, 47.7, 51.2, 51.9, 52.3, 53.3 (C-4), 53.4 (C-3), 221.0 (C-17). ESI: 303.1 ($[M+H]^+$, 100%).

3β,4β-Epoxy-6α-methyl-5β-androstan-17-one (3b): $Mp_{(hexane/ethyl\ acetate)}$ 85-87 ºC. IR (NaCl plates, $CHCl_3$) ν_{max} cm^{-1}: 1738 (C=O), 1050 (C-O). ^1H NMR (400 MHz, $CDCl_3$) δ: 0.84 (3H, s, 18-H_3), 0.87 (3H, s, 19-H_3), 1.06 (3H, d, *J*=6.9 Hz, 6α-CH_3), 2.44 (1H, dd, $J_{16\beta\text{-}16\alpha}$=18.3 Hz, $J_{16\beta\text{-}15\beta}$=8.7 Hz, $J_{16\beta\text{-}15\alpha}$=0.8 Hz, 16β-H), 2.91 (1H, d, $J_{4\alpha\text{-}5\beta}$=3.9 Hz, 4α-H), 3.17 (1H, dd, $J_{3\alpha\text{-}2\alpha}$=2.5 Hz, $J_{3\alpha\text{-}2\beta}$=2.5 Hz, 3α-H). ^{13}C NMR (100 MHz, $CDCl_3$) δ: 13.6 (C-18), 13.7 (C-19), 18.9, 20.2 (C-20), 22.1, 28.9, 29.5, 31.6, 33.6, 35.1, 35.5, 35.80, 35.81, 35.82, 42.6, 48.9, 51.1, 52.9 (C-4), 53.0 (C-3), 220.9 (C-17).

3β,4β-Epoxy-7α-methyl-5β-androstan-17-one (4)

To a solution of **2b** (in mixture with **2a** (15%) and **6** (27%)) (24.6 mg, 0.086 mmol) in DCM (4 mL), a solution of performic acid, generated *in situ* by addition of 98−100% HCOOH (0.015 mL) to 35% H_2O_2 (0.035 mL) was added. The reaction mixture was stirred at room temperature until complete transformation of the starting material (8 h, TLC). DCM (50 mL) was added, and the organic layer was washed successively with 10% aq $NaHCO_3$ (3x 70 mL) and water (4x 100 mL), dried over anhyd $MgSO_4$, filtered and concentrated to dryness. The obtained residue was purified by silica gel 60 column chromatography (hexane/ethyl acetate) allowing isolating 14.6 mg (56%) of **4** as an oil. ^1H NMR (400

MHz, $CDCl_3$) δ: 0.86 (3H, s, 18-H_3), 0.92 (3H, s, 19-H_3), 0.94 (3H, d, *J*=7.4 Hz, 7α-CH_3), 2.45 (1H, ddd, $J_{16\beta\text{-}16\alpha}$=18.3 Hz, $J_{16\beta\text{-}15\beta}$=9.0 Hz, $J_{16\beta\text{-}15\alpha}$=1.1 Hz, 16β-H), 2.96 (1H, d, $J_{4\alpha\text{-}3\alpha}$=3.7 Hz, 4α-H), 3.25 (1H, m, $J_{3\alpha\text{-}4\alpha}$=3.7 Hz, 3α-H). ^{13}C NMR (100 MHz, $CDCl_3$) δ: 12.7 (C-18), 13.5 (C-19), 14.1 (C-7'), 19.3, 19.9, 20.9, 21.6, 27.9, 28.0, 30.8, 31.9, 32.8, 33.1, 35.1, 35.8, 41.4, 46.6, 52.7 (C-4), 56.3 (C-3), 221.0 (C-17). ESI: 303.3 ($[M+H]^+$).

6α-Methylandrost-4-en-17-one (5)

Preparation of **5** was performed by adapting a described strategy.[39]

To a stirred and cooled mixture of trifluoracetic acid (0.36 mL), glacial acetic acid (0.36 mL) and acetonitrile (0.36 mL), sodium borohydride (83.1 mg, 1.48 mmol) was added in small portions followed by a solution of **9** (83.1 mg, 1.48 mmol) in anhyd DCM (8 mL). The reaction was stirred at room temperature under a nitrogen atmosphere until complete transformation of the starting material (2 h, TLC). The reaction mixture was neutralized with 10% aq $NaHCO_3$ and, after dilution with water (50 mL), the aqueous phase was extracted with DCM (3x 50 mL). The organic layer was washed with water (3x 50 mL), dried over anhyd Na_2SO_4, filtered and concentrated to dryness giving an oily residue. This residue was purified by silica gel column chromatography (petroleum ether 60-80ºC/ethyl acetate) affording in some fractions 11.1 mg of the desired pure **5** (14%) and in other fractions 33.8 mg of the C-17 reduced by-product **31** in 42.4% yield. Oxidation of **31**, according to the procedure described below, allowed its reconversion in **5**.

To a stirred and cooled (0 ºC) solution of **31** (33.8 mg, 0.117 mmol) in acetone (8 mL), Jones reagent was added dropwise until a persistent brown colour appears. After 5 min of reaction, the excess of the oxidant was destroyed by addition of 2-propanol, until a green colour appears. The reaction mixture was poured in water (50 mL) and the aqueous phase was extracted with ethyl acetate (3x 50 mL). The organic layer was washed with 10% aq $NaHCO_3$ (2x 50 mL) and water (2x 50 mL), dried over anhyd Na_2SO_4, filtered and concentrated to dryness to give a white solid residue. This residue was purified by silica gel column chromatography (petroleum ether 60-80 ºC/ethyl acetate) allowing isolating an

additional amount of 26.6 mg (79%) of the pure **5**. $Mp_{(petroleum\ ether/ethyl\ acetate)}$ 122-124 ºC. ^{1}H NMR (400 MHz, $CDCl_3$) δ: 0.89 (3H, s, 18-H_3), 1.11 (3H, d, *J*=7.6 Hz, 6α-CH_3), 1.27 (3H, s, 19-H_3), 2.45 (1H, dd, $J_{16\beta\text{-}16\alpha}$=19.2 Hz, $J_{16\beta\text{-}15\beta}$=8.5 Hz, 16β-H), 5.32 (1H, b dd, *J*=2.6 and 2.4 Hz, 4-H). ^{13}C NMR (100 MHz, $CDCl_3$) δ: 13.8 (C-18), 18.9, 19.0 (C-6'), 20.3 (C-19), 20.7, 21.8, 26.0, 31.6, 32.3, 35.3, 35.9, 37.4, 38.4, 40.9, 47.8, 51.2, 54.6, 116.7 (C-4), 147.9 (C-5), 221.3 (C-17). ESI: 287.3 ($[M+H]^+$).

7α-Methylandrost-4-en-17-one (6)

To a stirred and cooled (0 ºC) mixture of trifluoracetic acid (0.5 mL), glacial acetic acid (0.5 mL) and acetonitrile (0.5 mL), sodium borohydride (75.8 mg, 1.97 mmol) was added in small portions followed by a solution of **10a** (120.0 mg, 0.399 mmol) in anhyd DCM (12 mL). The reaction was stirred at room temperature under nitrogen atmosphere until complete transformation of the starting material (3 h 40 min, TLC). The reaction mixture was neutralized with 10% aq $NaHCO_3$ and the aqueous phase was extracted with DCM (2x 50 mL). The organic layer was washed with water (3x 50 mL), dried over anhyd $MgSO_4$, filtered and concentrated to dryness giving an oil residue. This residue was purified by silica gel column chromatography (hexane/ethyl acetate) affording in some fractions 9.6 mg the pure **6** (10%) and in other fractions 71.4 mg of its C-17 reduced derivative, the 7α-methylandrost-4-en-17β-ol **25** (62%) formed as by-product. Oxidation of **25**, according to the procedure described below, allowed its reconversion in **6**.

To a stirred and cooled (0 ºC) solution of **25** (70 mg, 0.24 mmol) in acetone (20 mL), Jones reagent was added dropwise until a persistent brown colour appears. After 5 min of reaction, the excess of the oxidant was destroyed by addition of 2-propanol, until a green colour appears. The reaction mixture was poured in water (70 mL) and the aqueous phase was extracted with ethyl acetate (3x 70 mL). The organic layer was washed with 10% aq $NaHCO_3$ (4x 70 mL) and water (4x 70 mL), dried over anhyd Na_2SO_4, filtered and concentrated to dryness giving 68.5 mg of the pure **6** (98%). $Mp_{(hexane/ethyl\ acetate)}$ 135-137 ºC. ^{1}H NMR (400 MHz, $CDCl_3$) δ: 0.77 (3H, d, *J*=7.0 Hz, 7α-CH_3), 0.88 (3H, s, 18-H_3), 1.04 (3H, s, 19-H_3), 5.28 (1H, b s, 4-H). ^{13}C NMR (100 MHz, $CDCl_3$) δ: 12.3 (C-7'), 13.6 (C-18), 19.2, 19.7

(C-19), 20.6, 21.4, 25.7, 30.2, 31.4, 35.7, 37.3, 37.87, 37.89, 40.0, 46.5, 47.4, 47.7, 121.6 (C-4), 140.9 (C-5), 221.3 (C-17). ESI: 287.3 ($[M+H]^+$).

4α,5α-Epoxy-6α-methylandrostan-17-one (7a) and 4β,5β-epoxy-6α-methylandrostan-17-one (7b)

To a solution of **5** (27.7 mg, 0.097 mmol) in DCM (5 mL), performic acid (generated *in situ* by addition of 98−100% HCOOH (0.05 mL)) and 35% H_2O_2 (0.04 mL), was added. The reaction mixture was stirred at room temperature until complete transformation of the starting material (6 h, TLC). DCM (50 mL) was added, and the organic layer was washed successively with 10% aq $NaHCO_3$ (2x 50 mL) and water (2x 50 mL), dried over anhyd Na_2SO_4, filtered, and concentrated to dryness. The obtained residue was purified by two sequential silica gel 60 column chromatographies (petroleum ether 60-80 ºC/ethyl acetate) and (petroleum ether 60-80 ºC/chloroform) allowing the isolation of 9.2 mg (31%) of the pure **7a** and 11.2 mg (38%) of the pure **7b**.

4α,5α-Epoxy-6α-methylandrostan-17-one (7a). $Mp_{(petroleum\ ether/chloroform)}$ 116-118 ºC. ^1H NMR (400 MHz, $CDCl_3$) δ: 0.71 (3H, d, J=6.7 Hz, 6α-CH_3), 0.89 (3H, s, 18-H_3), 1.02 (3H, s, 19-H_3), 2.45 (1H, dd, $J_{16\beta\text{-}16\alpha}$=19.2 Hz, $J_{16\beta\text{-}15\beta}$=8.7 Hz, 16β-H), 3.1 (1H, dd, J=2.6 and 2.2 Hz, 4β-H). ^{13}C NMR (100 MHz, $CDCl_3$) δ: 13.8 (C-6'), 14.5 (C-18), 14.9, 19.5 (C-19), 20.6, 21.8, 23.1, 29.7, 30.8, 31.4, 34.8, 35.8, 37.1, 38.4, 46.7, 47.8, 51.1, 54.5 (C-4), 67.5 (C-5), 220.9 (C-17). ESI: 303.3 ($[M+H]^+$).

4β,5β-Epoxy-6α-methylandrostan-17-one (7b). $Mp_{(petroleum\ ether/chloroform)}$ 134-137 ºC. ^1H NMR (400 MHz, $CDCl_3$) δ: 0.68 (3H, d, J=6.7 Hz, 6α-CH_3), 0.88 (3H, s, 18-H_3), 1.08 (3H, s, 19-H_3), 2.43 (1H, dd, $J_{16\beta\text{-}16\alpha}$=19.3 Hz, $J_{16\beta\text{-}15\beta}$=8.5 Hz, 16β-H), 3.14 (1H, d, J=3.5 Hz, 4α-H). ^{13}C NMR (100 MHz, $CDCl_3$) δ: 13.8 (C-6'), 14.6 (C-18), 15.8, 17.6 (C-19), 20.0, 21.7, 22.5, 29.4, 31.4, 31.9, 35.2, 35.8, 36.3, 36.6, 47.8, 50.5, 50.7, 56.3 (C-4), 67.2 (C-5), 221.2 (C-17). ESI: 303.3 ($[M+H]^+$).

4α,5α-Epoxy-7α-methylandrostan-17-one (8)

To a solution of **6** (75.1 mg, 0.262 mmol) in DCM (20 mL), *m*-chloroperbenzoic acid ≤77% (68.1 mg, 0.393 mmol) was added. The reaction mixture was stirred at room temperature until complete

transformation of the staring material (2 h, TLC). DCM was added (50 mL) and the organic layer was washed successively with 10% aq $NaHCO_3$ (10x 100 mL) and water (6x 100 mL), dried over anhyd $MgSO_4$, filtered and concentrated to dryness giving a slightly yellow solid residue. This residue was purified by silica gel column chromatography (hexane/ethyl acetate) allowing isolating 68.4 mg (90%) of the pure **8** as a white solid. $Mp_{(hexane/ethyl\ acetate)}$ 139-141 ºC. ^{1}H NMR (400 MHz, $CDCl_3$) δ: 0.89 (3H, s, 18-H_3), 0.94 (3H, d, *J*=7.2 Hz, 7α-CH_3), 1.03 (3H, s, 19-H_3), 2.35 (1H, dd, $J_{16\alpha\text{-}16\beta}$=13.4 Hz, $J_{16\alpha\text{-}15}$=4.8 Hz, 16α-H), 2.46 (1H, ddd, $J_{16\beta\text{-}16\alpha}$=13.4 Hz, $J_{16\beta\text{-}15\beta}$=8.8 Hz, $J_{16\beta\text{-}15\alpha}$=1.0 Hz, 16β-H), 2.94 (1H, d, *J*=4.5 Hz, 4β-H). ^{13}C NMR (100 MHz, $CDCl_3$) δ: 13.3 (C-18), 13.6 (C-7'), 15.7, 19.0 (C-19), 20.6, 21.4, 23.6, 29.7, 29.9 (2 carbons), 31.3, 35.7, 36.8, 37.1, 38.5, 39.0, 47.5, 47.7, 62.4 (C-4), 220.8 (C-17). ESI: 303.3 ($[M+H]^+$).

6α-Methylandrost-4-ene-3,17-dione (9)

Preparation of **9**, as in scheme 4, was performed by adapting a described strategy.[44]

To a solution of **30** (205.1 mg, 0.644 mmol) in 0.5 N HCl/CH_3COOH (13 mL) was stirred at room temperature until total transformation of the starting material (5 h 45 min, TLC). DCM (80 mL) was added and the organic phase washed with 10% aq $NaHCO_3$ (3x 80 mL) and water (3x 80 mL), dried over anhyd Na_2SO_4, filtered and concentrated to dryness giving a yellow oily residue. This residue was purified by silica gel column chromatography (petroleum ether 60-80ºC/ethyl acetate) affording the pure **9** (90.3 mg, 47%) as a white solid. $Mp_{(hexane/ethyl\ acetate)}$ 163-166 ºC [lit.,[27] 166-168 ºC]. IR (NaCl plates, $CHCl_3$) ν_{max} cm^{-1}: 3050 (=C-H), 1739 (C=O), 1671 (C=C). ^{1}H NMR (400 MHz, $CDCl_3$) δ: 0.92 (3H, s, 18-H_3), 1.09 (3H, d, *J*=6.5 Hz, 6α-CH_3), 1.21 (3H, s, 19-H_3), 5.80 (1H, b s, 4-H). ^{13}C NMR (100 MHz, $CDCl_3$) δ: 13.7 (C-18), 18.3 (C-20), 18.4 (C-19), 20.5, 21.7, 31.3, 33.6, 33.7, 35.0, 35.8, 35.9, 38.9, 39.7, 47.5, 50.7, 54.1, 121.6 (C-4), 173.5 (C-5), 199.6 (C-3), 220.3 (C-17). ESI: 301.3 ($[M+H]^+$).

Preparation of **9**, as in scheme 2, described in Supporting Information Section according the previously reported.[32]

7α-Methylandrost-4-ene-3,17-dione (10a) and 7β-methylandrost-4-ene-3,17-dione (10b)

Preparation of **10a** and **10b** was performed by adapting a described strategy.[37, 38]

To a stirred solution of **24** (243.0 mg, 0.85 mmol) in anhyd THF (5 mL), CuBr (5.4 mg, 0.035 mmol) was added under nitrogen atmosphere. Trimethylaluminium (0.97 mL, 1.94 mmol) and trimethylsilyl chloride (0.27 mL, 2.11 mmol) were sequentially added through a syringe. The reaction proceeded with magnetic stirring at room temperature under nitrogen for 2 h 20 min, time after which water (0.18 mL) was added. The reaction was left to react until complete transformation of the starting material (24 h, TLC). THF was removed under vacuum, water (100 mL) was added and the aqueous phase extracted with DCM (150 mL). The organic layer was washed with 10% aq HCl (100 mL), 10% aq $NaHCO_3$ (100 mL) and water (3x 100 mL), dried over anhyd Na_2SO_4, filtered and concentrated to dryness giving a yellow crystalline residue. Silica gel 60 column chromatography (chloroform/diethyl ether) purification afforded the pure **10a** (77.8 mg, 30%) and its isomer **10b** (19.8 mg, 10.6%).

7α-Methylandrost-4-ene-3,17-dione (10a): $Mp_{(chloroform/diethyl\ ether)}$ 177-179 ºC. ^1H NMR (400 MHz, $CDCl_3$) δ: 0.82 (3H, d, *J*=7.1, 7α-CH_3), 0.92 (3H, s, 18-H_3), 1.21 (3H, s, 19-H_3), 5.75 (1H, d, *J*=1.8 Hz, 4-H). ^{13}C NMR (100 MHz, $CDCl_3$) δ: 12.7 (C-7'), 13.6 (C-18), 17.8 (C-19), 20.3, 21.3, 30.4, 31.1, 33.9, 35.6, 35.9, 37.7, 38.8, 40.6, 46.2, 47.2, 47.5, 126.1 (C-4), 168.9 (C-5), 198.9 (C-3), 220.2 (C-17). ESI: 301.4 ($[M+H]^+$).

7β-Methylandrost-4-ene-3,17-dione (10b): $Mp_{(chloroform/diethyl\ ether)}$ 131-133 ºC. IR (ATR) υ_{max} cm^{-1}: 3009 (=C-H), 1737 (C_{17}=O), 1731 (C_3=O), 1678 (C=C). ^1H NMR (400 MHz, $CDCl_3$) δ: 0.92 (3H, s, 18-H_3), 1.13 (3H, d, *J*=5.9 Hz, 7β-CH_3), 1.19 (3H, s, 19-H_3), 5.73 (1H, s, 4-H). ^{13}C NMR (100 MHz, $CDCl_3$) δ: 14.2 (C-18), 17.6 (C-7'), 20.8, 22.9 (C-19), 25.7, 31.4, 33.9, 35.8, 35.9, 37.5, 38.3, 42.5, 42.6, 48.5, 51.4, 54.0, 123.2 (C-4), 169.9 (C-5), 199.3 (C-3), 220.7 (C-17).

6α-Allyl-4-hydroxyandrost-4-ene-3,17-dione (11)

To a stirred and cooled (-60 ºC) solution of anhyd DCM (2 mL) and anhyd dimethyl sulfoxide (DMSO) (0.26 mL, 3.77 mmol) under nitrogen atmosphere, a solution of anhyd trifluoroacetic acid (TFAA) (0.13

mL, 0.934 mmol) in anhyd DCM (1 mL) was added dropwise through a dropping funnel. After 10 min of reaction, a solution of **49** (60 mg, 0.174 mmol) in anhyd DCM (4 mL) was added dropwise through another dropping funnel. After 3 h of reaction, triethylamine (TEA) (0.2 mL) was added, and reaction proceeded for more 15 min. The temperature of the reaction mixture was raised up to room temperature and an aqueous solution of 2N HCl (50 mL) was added. The aqueous phase was extracted with DCM (3x 100 mL) and the organic layer was washed with 10% aq $NaHCO_3$ (50 mL) and water (3x 100 mL), dried with anhyd Na_2SO_4, filtered and concentrated to dryness giving to a yellow oily crude. Preparative TLC (diethyl ether/toluene) allowed the recovery of 21 mg of the starting material and 25 mg (64%) of the pure **11**. $Mp_{(ethyl\ acetate)}$ 138-140 ºC. IR (ATR) υ_{max} cm^{-1}: 3393 (O-H), 1735 (C_{17}=O), 1657 (C_3=O), 1618 (C=C), 1247 (C_4-O). ^{1}H NMR (300 MHz, $CDCl_3$) δ: 0.94 (3H, s, 18-H_3), 1.28 (3H, s, 19-H_3), 3.29 (1H, dd, $J_{6\beta\text{-}7\alpha}$=14.1 Hz, $J_{6\beta\text{-}7\beta}$=6.6 Hz, 6β-H), 5.03 (2H, b m, $W_{1/2}$ *ca.* 23 Hz, -CH=C$\underline{H}_2$), 5.81 (1H, m, b m, $W_{1/2}$ *ca.* 43 Hz, -C$\underline{H}$=CH_2), 6.18 (1H, s, 4-OH, disappears on adding D_2O). ^{13}C NMR (75.5 MHz, $CDCl_3$) δ: 13.8 (C-18), 20.1 (C-19), 20.2, 21.8, 29.6, 31.3, 31.9, 32.3, 32.9, 35.7, 36.8, 37.5, 39.0, 47.5, 50.9, 53.6, 116.2, 137.3, 141.4, 142.2, 193.8 (C-3), 220.7 (C-17). ESI: 343.3 ($[M+H]^+$).

7α-Allyl-4-hydroxyandrost-4-ene-3,17-dione (12)

A solution of **41** (177.0 mg, 0.46 mmol) in ethanol/HCl [95:05] (48 mL) was stirred under reflux for 1h 30 min. After cooling the reaction mixture to room temperature, water (100 mL) was added and the organic layer washed with 10% aq $NaHCO_3$ (3x 100 mL) and water (100 mL), dried over anhyd $MgSO_4$, filtered and concentrated to dryness giving a yellow oily crude which by trituration with cold diethyl ether allowed the isolation of 74 mg (47%) of the pure **12**, as white crystals. $Mp_{(diethyl\ ether)}$ 205-207 ºC. ^{1}H NMR (400 MHz, $CDCl_3$) δ: 0.92 (3H, s, 18-H_3), 1.22 (3H, s, 19-H_3), 3.14 (1H, dd, $J_{6\alpha\text{-}6\beta}$=14.4 Hz, $J_{6\alpha\text{-}7\beta}$=1.8 Hz, 6α-H), 5.04 (1H, b m, $W_{1/2}$ *ca.* 8 Hz, -CH=C$\underline{H}_2$), 5.06 (1H, b m, $W_{1/2}$ *ca.* 6 Hz, -CH=C$\underline{H}_2$), 5.85 (1H, b m, $W_{1/2}$ *ca.* 43 Hz, -C$\underline{H}$=CH_2), 6.07 (1H, s, 4-OH). ^{13}C NMR (100 MHz, $CDCl_3$) δ: 13.5 (C-18), 17.55 (C-19), 17.57, 20.5, 21.3, 26.8, 30.6, 31.2, 31.8, 34.9, 35.6, 35.9, 37.9,

46.9, 47.5, 47.7, 116.2 (-CH=$\underline{C}H_2$), 137.0 (-$\underline{C}$H=CH_2), 137.1 (C-5), 143.1 (C-4), 193.2 (C-3), 220.3 (C-17). ESI: 343.3 ($[M+H]^+$).

6α-Allylandrosta-1,4-diene-3,17-dione (13)

To a stirred solution of **15** (132.7 mg, 0.41 mmol) in toluene (18 mL), under reflux and nitrogen atmosphere, DDQ (219.9 mg, 0.97 mmol) followed by benzoic acid (71.4 mg, 0.58 mmol) were added. The reaction was stirred until complete transformation of the starting material (18 h 30 min, TLC). The reaction mixture was cooled to room temperature and the suspension formed was filtered through an alumina column and eluted with toluene followed by DCM. The obtained fractions were evaporated under vacuum and purified by silica gel column chromatography (petroleum ether 60-80 ºC/ethyl acetate) affording 108.2 mg (81%) of the pure **13**. $Mp_{(petroleum\ ether/ethyl\ acetate)}$ 143-145 ºC. ^{1}H NMR (400 MHz, $CDCl_3$) δ: 0.94 (3H, s, 18-H_3), 1.27 (3H, s, 19-H_3), 5.08 (1H, b m, $W_{1/2}$ *ca.* 5 Hz, -CH=C$\underline{H}_2$), 5.11 (1H, b m, $W_{1/2}$ *ca.* 13 Hz, -CH=C$\underline{H}_2$), 5.80 (1H, b m, $W_{1/2}$ *ca.* 41 Hz, -C$\underline{H}$=CH_2), 6.11 (1H, b s, 4-H), 6.25 (1H, dd, $J_{2\text{-}1}$=10.2 Hz, $J_{2\text{-}4}$=1.8 Hz, 2-H), 7.05 (1H, d, $J_{1\text{-}2}$=10.2 Hz, 1-H). ^{13}C NMR (100 MHz, $CDCl_3$) δ: 13.8 (C-18), 18.9 (C-19), 21.9, 22.2, 31.2, 35.1, 35.6, 35.9, 38.4, 38.5, 43.8, 47.7, 50.3, 53.5, 117.2 (-CH=$\underline{C}H_2$), 121.8 (-$\underline{C}$H=CH_2), 127.3 (C-4), 135.9 (C-2), 156.0 (C-1), 170.0 (C-5),186.1 (C-3), 219.8 (C-17). ESI: 325.3 ($[M+H]^+$).

7α-Allylandrosta-1,4-diene-3,17-dione (14)

Compound **14** was prepared as previously described.[17]

6α-Allylandrost-4-ene-3,17-dione (15)

A solution of **35** (204.1 mg, 0.59 mmol) in 0.5N HCl in CH_3COOH (7 mL) was stirred at room temperature until complete transformation of the starting material (17 h 30 min, TLC). The reaction mixture was neutralized with 10% aq $NaHCO_3$ and the aqueous phase was extracted with ethyl acetate (2x 100 mL). The organic layer was washed with 10% aq $NaHCO_3$ (100 mL) and water (2x 100 mL),

dried over anhyd $MgSO_4$, filtered and concentrated to dryness giving an oily residue. The residue was purified by silica gel column chromatography (petroleum ether 60-80 ºC/ethyl acetate) affording 142.2 mg (74%) of the pure **15**. $Mp_{(petroleum\ ether/ethyl\ acetate)}$ 100-102 ºC. ^1H NMR (400 MHz, $CDCl_3$) δ: 0.91 (3H, s, 18-H_3), 1.24 (3H, s, 19-H_3), 5.06 (1H, b m, $W_{1/2}$ *ca.* 12 Hz, -CH=C$\underline{H}_2$), 5.08 (1H, b t, $W_{1/2}$ *ca.* 4 Hz, -CH=C$\underline{H}_2$), 5.77 (1H, b m, $W_{1/2}$ *ca.* 41 Hz, -C$\underline{H}$=CH_2), 5.08 (1H, d, $J_{4\text{-}6\beta}$=1.1 Hz, 4-H). ^{13}C NMR (100 MHz, $CDCl_3$) δ: 13.7 (C-18), 18.4 (C-19), 20.5, 21.7, 31.2, 33.5, 35.1, 35.71, 35.74, 36.3, 36.8, 38.3, 39.2, 47.6, 50.7, 54.1, 117.0 (-CH=$\underline{C}H_2$), 121.8 (C-4), 136.1 (-$\underline{C}$H=CH_2), 172.1 (C-5), 199.5 (C-3), 220.3 (C-17). ESI: 327.3 ($[M+H]^+$).

7α-Allylandrost-4-ene-3,17-dione (16)

Compound **16** was prepared as previously described.[17]

6α-Allylandrost-4-en-17-one (17)

To a stirred and cooled (0 ºC) mixture of trifluoracetic acid (0.12 mL), glacial acetic acid (0.12 mL) and acetonitrile (0.12 mL), sodium borohydride (21.1 mg, 0.48 mmol) was added in small portions followed by a solution of **15** (32.0 mg, 0.098 mmol) in anhyd DCM (4 mL). The reaction was stirred at room temperature under nitrogen atmosphere until complete transformation of the starting material (1 h 30 min, TLC). The reaction mixture was neutralized with 10% aq $NaHCO_3$ and, after dilution with water (50 mL), the aqueous phase was extracted with DCM (3x 20 mL). The organic layer was washed with water (2x 100 mL), dried over anhyd $MgSO_4$, filtered and concentrated to dryness. The residue obtained was purified by silica gel column chromatography (hexane/ethyl acetate) affording in some fractions 6.1 mg the desired **17** (20%) as an oil and in other fractions 20 mg (65%) of the C-17 reduced derivative 6α-allylandrost-4-en-17β-ol (**36**) formed as by-product. Oxidation of **36**, according to the procedure described below, allowed its reconversion in **17**.

To a stirred and cooled (0 ºC) solution of **36** (13.7 mg, 0.044 mmol) in acetone (5 mL), Jones reagent was added dropwise until a persistent brown colour appears. After 5 min of reaction, the excess of the

oxidant was destroyed by addition of 2-propanol, until a green colour appears. The reaction mixture was poured in water (50 mL) and the aqueous phase was extracted with ethyl acetate (3x 25 mL). The organic layer was washed with 10% aq $NaHCO_3$ (2x 50 mL) and water (2x 50 mL), dried over anhyd Na_2SO_4, filtered and concentrated to dryness to give a white solid residue. This residue was purified by silica gel column chromatography (hexane/ethyl acetate) allowing isolating an additional amount of 5.5 mg (40%) of the pure **17**. ^{1}H NMR (400 MHz, $CDCl_3$) δ: 0.89 (3H, s, 18-H_3), 1.04 (3H, s, 19-H_3), 5.00 (1H, b m, $W_{1/2}$ *ca.* 8 Hz, -CH=C$\underline{H}_2$), 5.03 (1H, b m, $W_{1/2}$ *ca.* 18 Hz, -CH=C$\underline{H}_2$), 5.32 (1H, dd, $J_{4\text{-}3\alpha}$=2.5 Hz, $J_{4\text{-}3\beta}$=2.5 Hz, 4-H), 5.82 (1H, b m, $W_{1/2}$ *ca.* 41 Hz, -C$\underline{H}$=CH_2). ^{13}C NMR (100 MHz, $CDCl_3$) δ: 13.8 (C-18), 14.1 (C-19), 18.9, 20.3, 20.7, 21.8, 26.1, 29.4, 31.6, 31.9, 35.4, 35.8, 37.2, 37.8, 38.4, 51.2, 54.8, 115.6 (-CH=$\underline{C}H_2$), 117.2 (-$\underline{C}$H=CH_2), 138.2 (C-4), 146.6 (C-5), 221.2 (C-17). ESI: 313.3 ($[M+H]^+$).

7α-Allylandrost-4-en-17-one (18)

Compound **18** was prepared as previously described.[17]

6β-Hydroxyandrost-4-ene-3,17-dione (19)

Compound **19** was purchased from Steraloids, Inc. (Newport RI, USA) and their identity and purity were confirmed according to the physicochemical data (Mp, TLC and ^{1}H NMR spectra) given by the supplier.

6α-hydroxyandrost-4-ene-3,17-dione (20)

Compound **20** was purchased from Steraloids, Inc. (Newport RI, USA) and their identity and purity were confirmed according to the physicochemical data (Mp, TLC and ^{1}H NMR spectra) given by the supplier.

7α-hydroxyandrost-4-ene-3,17-dione (21)

Compound **21** was purchased from Steraloids, Inc. (Newport RI, USA) and their identity and purity were confirmed according to the physicochemical data (Mp, TLC and ^{1}H NMR spectra) given by the supplier.

Androst-4-ene-3,17-dione (22)

Compound **22** was prepared as previously described.[17]

6-Methylenandrost-4-ene-3,17-dione (23)

Preparation of **23** described in Supporting Information Section, according the previously reported.[31]

Androsta-4,6-diene-3,17-dione (24)

Preparation of **24** was performed by adapting a described strategy.[37]

To a stirred solution of **22** (1.0 g, 3.49 mmol) in *tert*-butanol (60 mL), chloranil (2.4 g, 9.77 mmol) was added and the resulting suspension was stirred at reflux for 7 h. The *tert*-butanol was removed under vacuum and DCM (200 mL) was added. The organic layer was washed with 5% aq NaOH (1000 mL) and water (3x 200 mL), dried over anhyd Na_2SO_4, filtered and concentrated to dryness giving a solid crude. This crude was purified by silica gel 60 column chromatography (chloroform/diethyl ether) affording 475.1 mg (48%) of the pure **24**. $Mp_{(chloroform/diethyl\ ether)}$ 165-167 ºC. IR (ATR) υ_{max} cm^{-1}: 3019 (=C-H), 1734 (C_{17}=O and C_3=O), 1653 and 1644 (C=C). ^{1}H NMR (400 MHz, $CDCl_3$) δ: 0.96 (3H, s, 18-H_3), 1.14 (3H, s, 19-H_3), 5.69 (1H, s, 4-H), 6.18 (2H, s, 6-H and 7-H). ^{13}C NMR (100 MHz, $CDCl_3$) δ: 13.7 (C-18), 16.3 (C-19), 19.9, 21.4, 31.2, 33.8, 35.6, 36.1, 36.9, 48.2, 48.7, 50.7, 124.1 (C-4), 128.7 (C-6), 138.3 (C-7), 162.9 (C-5), 199.3 (C-3), 219.4 (C-17).

7α-Methylandrost-4-en-17β-ol (25)

Compound **25** was obtained in 62% yield after silica gel column chromatography (hexane/ethyl acetate) during preparation of **6**, as its C-17 reduced by-product, as previously described. $Mp_{(hexane/ethyl\ acetate)}$ 136-

138 ºC. IR (ATR) υ_{max} cm^{-1}: 3279 (O-H), 3049 (=C-H), 1655 (C=C), 1053 (C-O).^{1}H NMR (400 MHz, $CDCl_3$) δ: 0.72 (3H, d, *J*=6.9 Hz, 7α-CH_3), 0.76 (3H, s, 18-H_3), 1.03 (3H, s, 19-H_3), 3.63 (1H, dd, $J_{17\alpha\text{-}16\alpha}$=8.6 Hz, $J_{17\alpha\text{-}16\beta}$=8.6 Hz, 17α-H), 5.25 (1H, b s, 4-H). ^{13}C NMR (100 MHz, $CDCl_3$) δ: 10.9 (C-20), 12.4 (C-18), 19.3, 19.8 (C-19), 20.9, 22.8, 25.8, 30.4, 30.7, 36.6, 37.3, 37.9, 38.3, 40.2, 42.9, 46.5, 46.8, 81.9 (C-17), 121.2 (C-4), 141.5 (C-5).

3β-Hydroxyandrost-5-en-17-one (26)

Compound **26** was purchased from Sigma-Aldrich (Schnelldorf, Germany) and their identity and purity were confirmed according to the physicochemical data (Mp, TLC and ^{1}H NMR spectra) given by the supplier.

Androst-5-ene-3β,17β-diol (27)

Preparation of **27** was performed by adapting a described strategy.[41]

To a stirred and cooled (0 ºC) solution of **26** (1.00 g, 3.46 mmol) in absolute methanol (110 mL under nitrogen atmosphere, sodium borohydride (120.7 mg, 3.19 mmol) was added in small portions. After 1 h, another portion of sodium borohydride (26.3 mg, 0.66 mmol) was added and the reaction was proceeded until complete transformation of the starting material (1 h 45 min, TLC). After this time, methanol was evaporated under vacuum, water was added (200 mL) and the product extracted with ethyl acetate (4x 100 mL). The organic layer was washed with water (4x 100 mL), dried over anhyd $MgSO_4$, filtered and concentrated to dryness giving the pure compound **27** (763.8 mg, 76%) as a white solid residue. $Mp_{(ethyl\ acetate)}$ 171-174 ºC. IR (ATR) υ_{max} cm^{-1}: 3199 (O-H), 3031 (=C-H), 1683 (C=C), 1041 (C-O). ^{1}H NMR (400 MHz, DMSO-d_6) δ: 0.64 (3H, s, 18-H_3), 0.95 (3H, s, 19-H_3), 3.24 (1H,, b m, $W_{1/2}$ *ca.* 15 Hz, 17α-H), 3.43 (1H, b m, $W_{1/2}$ *ca.* 23 Hz, 3α-H), 4.42 (1H, b s, 17β-OH), 4.59 (1H, b s, 3β-OH), 5.25 (1H, b s, 6-H). ^{13}C NMR (100 MHz, DMSO-d_6) δ: 11.1 (C-18), 19.1 (C-19), 20.2, 23.0, 29.7, 30.9, 31.4, 31.5, 36.1, 36.3, 36.9, 42.1, 42.2, 49.8, 50.8, 69.9 (C-17), 79.9 (C-3), 120.2 (C-6), 141.2 (C-5).

5α,6α-Epoxyandrostane-3β,17β-diol (28)

Preparation of **28** was performed by adapting a described strategy.[40]

To a solution of **27** (751.3 mg, 2.59 mmol) in DCM (100 mL) *m*-chloroperbenzoic acid <77% (674.6 mg, 3.89 mmol) was added. The reaction was stirred at room temperature until complete transformation of the starring material (1 h, TLC). The organic layer was washed successively with 10% aq $NaHCO_3$ (10x 100 mL) and water (6x 100 mL), dried over anhyd $MgSO_4$, filtered and concentrated to dryness giving the pure compound **28** (669.4 mg, 84%) as a white solid residue. MP $_{(\text{ethyl acetate})}$ 195-196.5 ºC. IR (ATR) υ_{max} cm^{-1}: 3401 and 3279 (O-H), 1135 (C-O-C), 1056 and 1043 (C-O). ^{1}H NMR (400 MHz, DMSO-d_6) δ: 0.57 (3H, s, 18-H_3), 0.99 (3H, s, 19-H_3), 2.82 (1H, d, *J*=4.3 Hz, 6β-H), 3.39 (1H, ddd, *J*=8.6, 8.5 and 4.9 Hz, 17α-H) , 3.54 (1H, m, *J*=11.0, 9.7, 4.8, 4.7 and 4.4 Hz, 3α-H), 4.41 (1H, d, *J*=4.8 Hz, 17β-OH), 4.59 (1H, d, *J*=4.9 Hz, 3β-OH). ^{13}C NMR (100 MHz, DMSO-d_6) δ: 11.1 (C-18), 15.6 (C-19), 19.8, 22.8, 27.9, 29.4, 29.6, 30.9, 32.3, 34.4, 36.1, 39.6, 42.3, 42.5, 51.3, 57.8 (C-6), 65.0 (C-5), 66.9 (C-17), 79.7 (C-3).

6β-Methylandrostane-3β,5α,17β-triol (29)

Preparation of **29** was performed by adapting a described strategy.[41, 42]

To a stirred solution of **28** (660.0 mg, 2.15 mmol) in anhyd THF (35 mL) under reflux and nitrogen atmosphere, a 1.4 M solution of methylmagnesium bromide (60.2 mL, 84.3 mmol) was added dropwise during 30 min through a dropping funnel. The reaction was stirred until the maximum transformation possible of the starting material (2 days) and after this time, it was cooled to room temperature and a saturated aq solution of NH_4Cl (200 mL) was added. The resulting solution was extracted with ethyl acetate (3x 100 mL) and the organic layer was washed successively with 10% aq $NaHCO_3$ (3x 100 mL), 5% aq HCl (3x 100 mL) and water (5x 100 mL), dried over anhyd $MgSO_4$, filtered and concentrated to dryness giving an oily crude. This crude was purified by silica gel column chromatography (hexane/ethyl acetate) allowing isolating 347.3 mg (50%) of the pure **29**. Mp$_{(\text{isopropyl ether/ethyl acetate})}$ 116-

119 ºC. IR (ATR) υ_{max} cm^{-1}: 3477, 3383 and 3220 (O-H), 1079, 1056 and 1038 (C-O). ^{1}H NMR (400 MHz, DMSO-d_6) δ: 0.63 (3H, s, 18-H_3), 0.92 (3H, d, *J*=7.6, 6β-CH_3), 0.94 (3H, s, 19-H_3), 3.42 (1H, b m, $W_{1/2}$ *ca.* 23 Hz, 3α-H), 3.82 (1H, b m, $W_{1/2}$ *ca.* 30 Hz, 5α-OH), 4.20 (1H, d, *J*=4.7, 17β-OH), 4.38 (1H, d, *J*=4.1, 3β-OH). ^{13}C NMR (100 MHz, DMSO-d_6) δ: 11.4 (C-18), 17.2 (C-6'), 18.0 (C-19), 20.4, 23.1, 29.8, 30.3, 31.0, 32.6, 33.2, 36.8, 38.5, 40.3, 42.0, 42.6, 45.3, 50.2, 65.8 (C-17), 75.2 (C-5), 80.0 (C-3).

5α-Hydroxy-6β-methylandrostane-3,17-dione (30)

Preparation of **30** was performed by adapting a described strategy.[43]

To a stirred and cooled (0 ºC) solution of **29** (225.6 mg, 0.699 mmol) in acetone (32 mL), Jones reagent was added dropwise until a persistent brown coloration was obtained. After 5 min of reaction, the excess of oxidant was destroyed by addition of 2-propanol until a green color was acquired. Water (100 mL) was added, the aqueous phase was extracted with ethyl acetate (3x 100 mL) and the organic layer was washed with 10% aq $NaHCO_3$ (2x 100 mL) and water (2x 100 mL), dried over anhyd $MgSO_4$, filtered and concentrated to dryness giving a white solid residue. This residue was purified by silica gel column chromatography (hexane/ethyl acetate) allowing isolating 99.1 mg (44%) of the pure **30**. $Mp_{(hexane/ethyl\ acetate)}$ 188-191 ºC. IR (ATR) υ_{max} cm^{-1}: 3433 (O-H), 1738 (C_{17}=O), 1706 (C_3=O), 1020 (C-O). ^{1}H NMR (400 MHz, $CDCl_3$) δ: 0.91 (3H, s, 18-H_3), 1.11 (3H, d, *J*=7.6 Hz, 6β-CH_3), 1.27 (3H, s, 19-H_3), 2.45 (1H, dd, $J_{16β-16α}$=19.3 Hz, $J_{16β-15β}$=8.5 Hz, 16β-H). ^{13}C NMR (100 MHz, $CDCl_3$) δ: 13.9 (C-18), 17.9 (C-19 and C-6'), 20.7, 21.8, 30.2, 31.5, 32.2, 35.6, 35.8, 37.9, 39.6, 41.8, 46.6, 47.8, 50.6, 50.8, 79.9 (C-5), 211.3 (C-3), 220.9 (C-17).

6α-Methylandrost-4-en-17β-ol (31)

Compound **31** was obtained in 42.4% yield after silica gel column chromatography (petroleum ether 60-80ºC/ethyl acetate) during preparation of **5**, as its C-17 reduced by-product, as previously described. $Mp_{(petroleum\ ether/ethyl\ acetate)}$ 137-140 ºC. IR (ATR) υ_{max} cm^{-1}: 3280 (O-H), 3052 (=C-H), 1646 (C=C), 1059

(C-O). ^{1}H NMR (400 MHz, $CDCl_3$) δ: 0.77 (3H, s, 18-H_3), 0.96 (3H, d, *J*=6.5 Hz, 6α-CH_3), 1.02 (3H, s, 19-H_3), 3.62 (1H, dd, $J_{17\alpha\text{-}16\alpha}$=8.6 Hz, $J_{17\alpha\text{-}16\beta}$=8.6 Hz, 17α-H), 5.29 (1H, b dd, *J*=2.2 and 2.2 Hz, 4-H).

3β,17β-bis(*tert*-butyldimethylsilyloxy)-5α,6α-epoxyandrostane (32)

To a solution **28** (1.2 g, 3.9 mmol) in dimethylformamide (11 mL) *tert*-butyldimethylsilyl chloride (2.21 g, 14.6 mmol) and imidazole (0.75 g, 11 mmol) were added. The reaction was stirred at room temperature for 2 h, after which the dimethylformamide was evaporated. The concentrated solution was poured in 300 mL of an ice cooled stirred 10% aq $NaHCO_3$ and the obtained suspension was filtered, washed with water until neutral pH and dried over vacuum, giving 1.99 (80%) of **32** as a white solid. $Mp_{(petroleum\ ether/ethyl\ acetate)}$ 160-163 ºC. IR (ATR) υ_{max} cm^{-1}: 1249 (Si-C), 1128 (C-O), 1093 and 1072 (O-Si), 868 (Si-C). ^{1}H NMR (400 MHz, $CDCl_3$) δ: -0.001 (3H, s, Si-CH_3), 0.005 (3H, s, Si-CH_3), 0.053 (6H, s, Si-$(CH_3)_2$), 0.73 (3H, s, 18-H_3), 0.88 (9H, s, Si-C$(CH_3)_3$), 0.89 (9H, s, Si-C$(CH_3)_3$), 1.27 (3H, s, 19-H_3), 3.56 (1H, dd, $J_{17\alpha\text{-}16\alpha}$=8.3 Hz, $J_{17\alpha\text{-}16\beta}$=8.3 Hz, 17α-H), 3.81 (1H, dd, *J*=3.6 Hz, *J*=1.7 Hz, 6β-H), 4.00 (1H, dddd, $J_{3\alpha\text{-}2\beta}$=10.7 Hz, $J_{3\alpha\text{-}4\beta}$=10.7 Hz, $J_{3\alpha\text{-}2\alpha}$=5.4 Hz, $J_{3\alpha\text{-}4\alpha}$=5.4 Hz, 3α-H). ^{13}C NMR (100 MHz, $CDCl_3$) δ: -4.83 (Si-CH_3), -4.62 (Si-CH_3), -4.50 (Si-$(CH_3)_2$), 11.5 (C-18), 18.1, 18.2, 18.4 (C-19), 20.8, 23.4, 25.8 (Si-C($\underline{C}H_3)_3$), 25.9 (Si-C($\underline{C}H_3)_3$), 30.3, 30.8, 31.0, 33.1, 35.2, 37.1, 39.1, 42.4, 43.4, 46.2, 49.7, 63.7 (C-3*), 68.2 (C-17*), 77.4 (C-5), 81.7 (C-6).

*Interchangeable

6β-Allyl-5α-hydroxy-3β,17β-bis(*tert*-butyldimethylsilyloxy)androstane (33)

To a stirred solution of **32** (734.9 mg, 1.37 mmol) in anhyd THF (15 mL) under reflux and nitrogen atmosphere, a 0.1 M solution of allylmagnesium bromide in diethyl ether (30 mL, 3.0 mmol) was added during 30 min from a dropping funnel. The reaction was stirred until complete transformation of the starting material (40 min, TLC). The reaction mixture was cooled to room temperature and saturated aq NH_4Cl (200 mL) was added carefully. The aqueous phase was extracted with ethyl acetate (300 mL), and the organic layer was washed with 10% aq $NaHCO_3$ (2x 100 mL), 0.1N HCl (30 mL) and water

(100 mL), dried over anhyd $MgSO_4$, filtered and concentrated to dryness giving a slightly yellow oily residue. The crude was purified by silica gel 60 column chromatography (petroleum ether 60-80 ºC/diethyl ether) affording 650.5 mg (82%) of the pure **33**. $Mp_{(petroleum\ ether/diethyl\ ether)}$ 100-103 ºC. IR (ATR) υ_{max} cm^{-1}: 3493 (O-H), 1257 and 1249 (Si-C), 1087(O-Si), 1047 (C-O), 865 (Si-C). ^{1}H NMR (400 MHz, $CDCl_3$) δ: -0.003 (3H, s, Si-CH_3), 0.004 (3H, s, Si-CH_3), 0.06 (6H, s, Si-$(CH_3)_2$), 0.70 (3H, s, 18-H_3), 0.87 (9H, s, Si-C$(CH_3)_3$), 0.89 (9H, s, Si-C$(CH_3)_3$), 1.02 (3H, s, 19-H_3), 3.55 (1H, dd, $J_{17\alpha\text{-}16\alpha}$=8.3 Hz, $J_{17\alpha\text{-}16\beta}$=8.3 Hz, 17α-H), 4.10 (1H, dddd, $J_{3\alpha\text{-}2\beta}$=10.3 Hz, $J_{3\alpha\text{-}4\beta}$=10.3 Hz, $J_{3\alpha\text{-}2\alpha}$=5.1 Hz, $J_{3\alpha\text{-}4\alpha}$=5.1 Hz, 3α-H), 4.96 (1H, dd, *J*=1.4 Hz, *J*=1.4 Hz, CH=C$\underline{H}_2$), 4.99 (1H, dddd, *J*=6.3 Hz, *J*=1.2 Hz, *J*=0.8 Hz, *J*=0.8 Hz, CH=C$\underline{H}_2$), 5.65 (1H, dddd, *J*=16.2 Hz, *J*=10.3 Hz, *J*=8.1 Hz, *J*=5.6 Hz, C$\underline{H}$=CH_2). ^{13}C NMR (100 MHz, $CDCl_3$) δ: -4.77 (Si-CH_3), -4.55 (Si-CH_3), -4.46 (Si-$(CH_3)_2$), 11.5 (C-18), 18.1 (C-19), 18.3, 20.9, 23.6, 25.9 (Si-C($\underline{C}H_3)_3$), 26.0 (Si-C($\underline{C}H_3)_3$), 28.5, 30.7, 30.8, 31.4, 33.6, 34.9, 37.2, 39.1, 42.8, 43.4, 46.9, 47.1, 50.1 (C-3), 68.7 (C-17), 77.9 (C-5), 81.8 (C-6), 115.5 (=CH_2), 138.9 (=CH).

6β-Allylandrostane-3β,5α,17β-triol (34)

A solution of **33** (495.5 mg, 0.86 mmol) in 1.6% ethanolic HCl (16.5 mL) was stirred at room temperature until complete transformation of the staring material (25 h, TLC). The reaction mixture was neutralized with 10% aq $NaHCO_3$ and the aqueous phase was extracted with ethyl acetate (500 mL). The organic layer was washed with 10% aq $NaHCO_3$ (2x 100 mL) and water (2x 100 mL), dried over anhyd $MgSO_4$, filtered and concentrated to dryness giving 440 mg of a white oily residue, which was later used without further purification. ^{1}H NMR (400 MHz, DMSO-d_6) δ: 0.63 (3H, s, 18-H_3), 0.91 (3H, s, 19-H_3), 3.34 (1H, b s, 5α-OH)*, 3.42 (1H, dd, $J_{17\alpha\text{-}16\alpha}$=8.5 Hz, $J_{17\alpha\text{-}16\beta}$=8.5 Hz, 17α-H), 3.85 (1H, dddd, *J*=10.8 Hz, *J*=10.8 Hz, *J*=5.3 Hz, *J*=5.3 Hz, 3α-H), 4.18 (1H, b s, 17β-OH)*, 4.37 (1H, b s, 3β-OH)*, 4.93 (1H, b d, *J*=3.5 Hz, -CH=C$\underline{H}_2$), 4.95 (1H, b d, *J*=10.8 Hz, -CH=C$\underline{H}_2$), 5.63 (1H, dddd, *J*=16.1, *J*=10.1, *J*=8.1, *J*=5.8, -C$\underline{H}$=CH_2). ^{13}C NMR (100 MHz, DMSO-d_6) δ: 11.4 (C-18), 17.6 (C-19), 20.3, 23.1, 27.9, 29.8, 30.2, 31.0, 33.0, 34.5, 36.7, 38.5, 41.9, 42.6, 45.4, 45.8, 50.0, 65.8 (C-3), 75.2 (C-5), 80.0 (C-17), 115.1 (-CH=$\underline{C}H_2$), 139.4 (-$\underline{C}$H=CH_2).

*Interchangeable

6β-Allyl-5α-hydroxyandrostane-3,17-dione (35)

To a stirred and cooled (0 ºC) solution of **34** (360.0 mg, 1.03 mmol) in acetone (26 mL) and dioxane (4 mL), Jones reagent was added dropwise until a persistent brown coloration was obtained. After 5 min of reaction, the excess of oxidant was destroyed by addition of 2-propanol until a green color was acquired. Water (100 mL) was added and the aqueous phase was extracted with ethyl acetate (2x 100 mL). The organic layer was washed with 10% aq $NaHCO_3$ (2x 100 mL) and water (2x 100 mL), dried over anhyd $MgSO_4$, filtered and concentrated to dryness. The residue obtained was purified by silica gel column chromatography (petroleum ether 60-80 ºC/ethyl acetate) affording 216.2 mg (61%) of the pure **35**. $Mp_{(petroleum\ ether/diethyl\ ether)}$ 101-104 ºC. IR (ATR) υ_{max} cm^{-1}: 3416 (O-H), 3060 (=C-H), 1744 (C_{17}=O), 1724 (C_3=O), 1699 (C=C), 1011(C-O). ^{1}H NMR (400 MHz, $CDCl_3$) δ: 0.91 (3H, s, 18-H_3), 1.24 (3H, s, 19-H_3), 4.97 (1H, dd, *J*=13.6 Hz, *J*=2.1 Hz, -CH=C$\underline{H}_2$), 5.01 (1H, dd, *J*=13.6 Hz, *J*=1.9 Hz, -CH=C$\underline{H}_2$), 5.66 (1H, b m, $W_{1/2}$ *ca.* 41 Hz, -C$\underline{H}$=CH_2). ^{13}C NMR (100 MHz, $CDCl_3$) δ: 13.9 (C-18), 17.5 (C-19), 20.6, 21.8, 27.9, 30.2, 31.5, 35.48, 35.5, 35.7, 37.8, 39.6, 46.7, 47.1, 47.8, 50.4, 50.6, 79.8, 116.3 (-CH=$\underline{C}H_2$), 137.9 (-$\underline{C}$H=CH_2), 210.9 (C-3), 220.8 (C-17).

6α-Allylandrost-4-en-17β-ol (36)

Compound **36** was obtained in 65% yield after silica gel column chromatography (hexane/ethyl acetate) during preparation of **17**, as its C-17 reduced by-product, as previously described. IR (ATR) υ_{max} cm^{-1}: 3240 (O-H), 3075 (=C-H), 1642 (C=C), 1058 (C-O). ^{1}H NMR (400 MHz, $CDCl_3$) δ: 0.76 (3H, s, 18-H_3), 1.02 (3H, s, 19-H_3), 3.62 (1H, dd, $J_{17\alpha\text{-}16\alpha}$=8.4 Hz, $J_{17\alpha\text{-}16\beta}$=8.4 Hz, 17α-H), 4.98 (1H, b m, $W_{1/2}$ *ca.* 11 Hz, -CH=C$\underline{H}_2$), 5.01 (1H, b m, $W_{1/2}$ *ca.* 17 Hz, -CH=C$\underline{H}_2$), 5.30 (1H, dd, $J_{4\text{-}3\alpha}$=2.4 Hz, $J_{4\text{-}3\beta}$=2.4 Hz, 4-H), 5.81 (1H, b m, $W_{1/2}$ *ca.* 43 Hz, -C$\underline{H}$=CH_2). ^{13}C NMR (100 MHz, $CDCl_3$) δ: 11.1 (C-18), 18.9, 20.4 (C-19), 23.4, 26.2, 29.7, 30.6, 35.9, 36.8, 37.3, 37.4, 37.6, 38.5, 38.6, 50.8, 54.9, 59.5, 81.9 (C-17), 115.4 (-CH=$\underline{C}H_2$), 116.8 (-$\underline{C}$H=CH_2), 138.3 (C-4), 147-2 (C-5).

2α,6α-Dibromoandrost-4-ene-3,17-dione (37a) and 2α,6β-dibromo-androst-4-ene-3,17-dione (37b)

Preparation of **37a** and **37b** described in Supporting Information Section, according the previously reported.[47]

4,17-Dioxoandrosta-2,5-dien-3-yl acetate (38)

Preparation of **38** was performed by adapting a described strategy.[48]

To a solution of **37** (1.74 g, 3.90 mmol) in acetone (30 mL), an ethanolic solution of potassium acetate (60 mL, 0.02g/mL) was added. The reaction was heated under reflux for 30 min and after cooling the mixture, it was poured over stirred cold water. The aqueous suspension formed was extracted with ethyl acetate (3x 100 mL) and the organic layer was washed with 10% aq $NaHCO_3$ (2x 100 mL), 10% aq HCl (2x 100 mL) and water (3x 100 mL), dried over anhyd Na_2SO_4, filtered and concentrated to dryness. Crystallization from acetone/*n*-hexane gave 1.24 g (92%) of the pure **38**. $Mp_{(acetone/n\text{-hexane})}$ 198-201 ºC. IR (ATR) υ_{max} cm^{-1}: 1757 and 1733 (C=O), 1671 and 1626 (C=C), 1364(C-O). ^1H NMR (400 MHz, $CDCl_3$) δ: 0.82 (3H, s, 18-H_3), 1.12 (3H, s, 19-H_3), 2.18 (3H, s, 3-OAc), 6.68 (1H, dd, $J_{2\text{-}1\alpha}$=6.8 Hz, $J_{2\text{-}1\beta}$=2.2 Hz, 2-H), 6.73 (1H, dd, $J_{6\text{-}7\alpha}$=5.2 Hz, $J_{6\text{-}7\beta}$=2.5 Hz, 6-H). ^{13}C NMR (100 MHz, $CDCl_3$) δ: 13.2 (C-18), 19.7 (C-19), 20.1, 21.0, 21.2, 30.0, 30.1, 30.9, 35.2, 36.4, 38.1, 46.8, 48.2, 50.4, 133.8 (C-2), 135.3 (C-6), 140.9, 144.0, 168.4 (OC=O), 180.3 (C-4), 219.3 (C-17).

4-Hydroxyandrosta-4,6-diene-3,17-dione (39)

Preparation of **39** was performed by adapting a described strategy.[49]

A solution of **38** (0.97 g, 2.80 mmol) in ethanol/HCl [95:05] (100 mL) was heated under reflux for 1 h 30 min. After cooling the reaction mixture, it was poured over stirred cold water and ethyl acetate (250 mL) was added. The organic phase was washed with water (2x 150 mL), dried over anhyd Na_2SO_4, filtered and concentrated to dryness giving 0.73 g (85%) of the almost pure compound **39**. $Mp_{(methanol)}$ 205-207 ºC [lit.,[67] 206-207.5 ºC]. IR (NaCl plates, $CHCl_3$) υ_{max} cm^{-1}: 3380 (O-H), 3040 (=C-H), 1730

(C_{17}=O), 1650 (C_3=O), 1675 and 1615 (C=C), 1215 (C-O). ^{1}H NMR (300 MHz, $CDCl_3$) δ: 0.97 (3H, s, 18-H_3), 1.13 (3H, s, 19-H_3), 6.10 (1H, m, $J_{6\text{-}7}$=9.9 Hz, $J_{6\text{-}8}$=1.8 Hz, 6-H), 6.32 (1H, s, 4-OH), 6.73 (1H, dd, $J_{7\text{-}6}$=9.9 Hz, $J_{7\text{-}8}$=2.7 Hz, 7-H). ^{13}C NMR (75.5 MHz, $CDCl_3$) δ: 13.7 (C-18), 16.4 (C-19), 19.8, 21.4, 31.2, 31.8, 33.1, 35.5, 35.6, 36.6, 48.3, 48.8, 51.2, 122.1 (C-6), 133.8 (C-5), 135.0 (C-7), 140.4 (C-4), 193.6 (C-3), 219.8 (C-17).

3,17-Dioxoandrosta-4,6-dien-4-yl acetate (40)

Preparation of **41** described in Supporting Information Section according the previously reported.[67]

7α-Allyl-3,17-dioxoandrost-4-en-4-yl acetate (41)

To a stirred and cooled (-78 ºC) solution of **40** (90.0 mg, 0.26 mmol) in anhyd DCM (10 mL) under nitrogen atmosphere, titanium tetrachloride (0.7 mL) was added. After 10 min of reaction, a solution of allyltrimethylsilane (1.5 mL, 9.3 mmol) in anhyd DCM (5 mL) was carefully added for 30 min through a dropping funnel. The reaction mixture was allowed to reach -25 ºC (4 h), water was added and the aqueous phase was extracted with DCM (3x 50 mL). The organic layer was washed with 10% aq $NaHCO_3$ (4x 50 mL) and water (4x 50 mL), dried over anhyd Na_2SO_4, filtered and concentrated yielding a yellow oil (147 mg). Silica gel preparative TLC (diethyl ether/toluene) allowed the isolation of the main product formed in the reaction through extraction from the silica gel strip with ethyl acetate. The organic phase was washed with 10% aq $NaHCO_3$ (4x 50 mL) and water (4x 50 mL), dried over anhyd Na_2SO_4, filtered and concentrated leading to an oil that was crystallized from ethyl acetate to afford 43 mg (30%) of the pure **41**. $Mp_{(ethyl\ acetate)}$ 199-201 ºC. IR (ATR) υ_{max} cm^{-1}: 1763 (OC=O), 1734 (C_{17}=O), 1681 (C_3=O), 1628 (C=C), 1370 (C-O). ^{1}H NMR (300 MHz, $CDCl_3$) δ: 0.93 (3H, s, 18-H_3), 1.29 (3H, s, 19-H_3), 2.21 (3H, s, 4-OAc), 2.85 (1H, d, *J*=14.1 Hz 6α-H), 5.05 (2H, b m, $W_{1/2}$ *ca.* 21 Hz, -CH=C$\underline{H}_2$), 5.69 (1H, b m, $W_{1/2}$ *ca.* 41 Hz, -C$\underline{H}$=CH_2). ^{13}C NMR (75.5 MHz, $CDCl_3$) δ: 13.4 (C-18), 17.9 (C-19), 20.29, 20.34, 21.2, 27.6, 30.3, 31.0, 33.3, 34.7 (2 carbons), 35.5, 37.5, 39.1, 46.7, 47.2,

47.4, 116.8 (-CH=$\underline{C}H_2$), 136.9 (-$\underline{C}$H=CH_2), 141.4 (C-4), 153.4 (C-5), 168.6 (OC=O), 190.1 (C-3), 220.1 (C-17).

17β-Hydroxyandrost-4-en-3-one (42)

Compound **42** was purchased from Sigma-Aldrich (Schnelldorf, Germany) and their identity and purity were confirmed according to the physicochemical data (Mp, TLC and ^{1}H NMR spectra) given by the supplier.

Androst-4-ene-3β,17β-diol (43)

Compound **43** was prepared from testosterone (**42**) as previously described.[17]

4β,5β-Epoxyandrostane-3β,17β-diol (44)

To a stirred solution of **43** (946.9 mg, 3.26 mmol) in DCM (50 mL) at room temperature, performic acid (generated *in situ* by addition of 98-100% HCOOH (0.85 mL) to 35% H_2O_2 (1.69 mL)), was added. The reaction was stirred until complete transformation of the starting material (4 h, TLC). DCM (100 mL) was added and the organic layer was washed with 10% aq $NaHCO_3$, (100 mL) and water (4x 100 mL), dried over anhyd Na_2SO_4, filtered and concentrated to dryness. The crude obtained was purified by silica gel 60 column chromatography (hexane/ethyl acetate) affording 707.4 mg (71%) of the pure **44**. $Mp_{(hexane/ethyl\ acetate)}$ 170-172 ºC. IR (ATR) υ_{max} cm^{-1}: 3332 and 3244 (O-H), 1143, 1075 and 1063 (C-O). ^{1}H NMR (400 MHz, DMSO-d_6) δ: 0.64 (3H, s, 18-H_3), 0.93 (3H, s, 19-H_3), 2.93 (1H, d, $J_{4\alpha\text{-}3\alpha}$=3.0 Hz, 4α-H), 3.43 (1H, ddd, $J_{17\alpha\text{-}16\alpha}$=8.5 Hz, $J_{17\alpha\text{-}16\beta}$=8.5 Hz, $J_{17\alpha\text{-}17\beta OH}$=4.8 Hz, 17α-H), 3.85 (1H, ddd, $J_{3\alpha\text{-}3\beta OH}$=6.1 Hz, $J_{3\alpha\text{-}2\alpha}$=4.2 Hz, $J_{3\alpha\text{-}2\beta}$=4.2 Hz, 3α-H), 4.43 (1H, dd, $J_{17\beta OH\text{-}17\alpha}$=4.8 Hz, $J_{17\beta OH\text{-}16}$=1.7 Hz, 17β-OH), 4.60 (1H, dd, $J_{3\beta OH\text{-}3\alpha}$=6.1 Hz, $J_{3\beta OH\text{-}2}$=1.4 Hz, 3β-OH). ^{13}C NMR (100 MHz, DMSO-d_6) δ: 11.1 (C-18), 18.0 (C-19), 20.6, 23.0, 25.5, 29.5, 29.7, 30.6, 31.1, 34.8, 35.2, 36.3, 42.4, 49.3, 50.0, 64.3 (C-3), 64.4 (C-4), 65.9 (C-5), 79.9 (C-17).

4β,5β-Epoxyandrostane-3β,17β-diyl acetate (45)

To a stirred solution of **44** (985.5 mg, 3.22 mmol) in pyridine (10 mL) at room temperature, acetic anhydride (1.5 mL, 15.9 mmol) was added. The reaction was stirred until complete transformation of the starting material (8 h, TLC). Pyridine was evaporated under vacuum and to the remaining residue DCM (200 mL) was added. The organic phase was washed with 10% aq HCl (3x 100 mL), 10% aq $NaHCO_3$ (3x 100 mL) and water (3x 100 mL), dried over anhyd Na_2SO_4, filtered and concentrated to dryness. The crude obtained was purified by silica gel 60 column chromatography (hexane/ethyl acetate) affording 1.26 g (64%) of **45**. $Mp_{(petroleum\ ether/ethyl\ acetate)}$ 101-103,5 ºC. IR (ATR) υ_{max} cm^{-1}: 1726 (C=O), 1372 and 1240 (C-O). ^1H NMR (400 MHz, $CDCl_3$) δ: 0.80 (3H, s, 18-H_3), 1.05 (3H, s, 19-H_3), 2.04 (3H, s, 17-CH_3COO), 2.09 (3H, s, 3-CH_3COO), 3.16 (1H, d, $J_{4\alpha\text{-}3\alpha}$=3.6 Hz, 4α-H), 4.59 (1H, dd, $J_{17\alpha\text{-}16\alpha}$=9.0 Hz, $J_{17\alpha\text{-}16\beta}$=8.1 Hz, 17α-H), 5.12 (1H, ddd, $J_{3\alpha\text{-}2}$=5.6 Hz, $J_{3\alpha\text{-}2}$=3.8 Hz, $J_{3\alpha\text{-}4\alpha}$=3.6 Hz, 3α-H).$^{13}C$ NMR (100 MHz, $CDCl_3$) δ: 11.9 (C-18), 18.4 (C-19), 20.9, 21.1, 21.2, 22.5, 23.5, 27.5, 29.5, 29.8, 31.1, 34.9, 35.9, 36.7, 42.6, 48.9, 50.4, 61.3 (C-4), 66.6 (C-5), 68.9 (C-3), 82.6 (C-17), 170.9 (OC=O), 171.1 (OC=O).

5α-Hydroxy-4-oxoandrostane-3β,17β-diyl acetate (46)

Preparation of **46** was performed by adapting a described strategy.[51]

To a stirred solution of **45** (776.4 mg, 1.99 mmol) in butanone (12 mL) at room temperature, a 75% aq trioxide chromium solution (2.1 mL) was added dropwise. The reaction mixture was stirred until complete transformation of the starting material (1 h 15 min, TLC). Water (300 mL) was added and the aqueous phase was extracted with ethyl acetate (4x 100 mL). The organic layer was washed with 10% aq $NaHCO_3$ (3x 100 mL) and water (3x 100 mL), dried over anhyd Na_2SO_4, filtered and concentrated to dryness giving an oil crude. This crude was purified by a silica gel 60 column chromatography (hexane/ethyl acetate) yielding 62% of the pure **46** as a white solid. $Mp_{(hexane/ethyl\ acetate)}$ 185-189 ºC. ^1H NMR (400 MHz, $CDCl_3$) δ: 0.77 (3H, s, 18-H_3), 0.79 (3H, s, 19-H_3), 2.03 (3H, s, 17-CH_3COO), 2.14

(3H, s, 3-CH_3COO), 4.59 (1H, dd, $J_{17\alpha\text{-}16\alpha}$=9.0 Hz, $J_{17\alpha\text{-}16\beta}$=7.9 Hz, 17α-H), 5.93 (1H, dd, $J_{3\alpha\text{-}2\beta}$=12.1 Hz, $J_{3\alpha\text{-}2\alpha}$=7.8 Hz, 3α-H). ^{13}C NMR (100 MHz, $CDCl_3$) δ: 12.0 (C-18), 15.1 (C-19), 20.8, 20.9, 21.1, 23.3, 24.5, 26.5, 27.5, 27.7, 29.3, 34.1, 36.8, 42.6, 44.0, 45.1, 50.1, 73.8 (C-3), 80.3 (C-5), 82.6 (C-17), 170.3 (OC=O), 171.2 (OC=O), 206.8 (C-4).

4-Oxoandrost-5-ene-3β,17β-diyl acetate (47)

Preparation of **47** was performed by adapting a described strategy.[52]

To a stirred and cooled (0 ºC) solution of **46** (1.2 g, 2.952 mmol) in anhyd pyridine (18 mL) under nitrogen atmosphere, thionyl chloride (1.4 mL) was added cautiously. After 25 min of reaction, water (20 mL) was added and the aqueous phase was extracted with DCM (3x 150 mL). The organic layer was washed with 10% aq HCl (3x 100 mL) and water (3x 100 mL), dried over anhyd $MgSO_4$, filtered and concentrated to dryness. The crude obtained was purified by silica gel 60 column chromatography (diethyl ether/petroleum ether 40-60 ºC) affording 840 mg (73%) of **47** as white crystals, after diethyl ether/methanol crystallization. $Mp_{(diethyl\ ether/\ methanol)}$ 93-97 ºC, [lit.[68] $_{(diethyl\ ether/\ acetone)}$ 102-103 ºC]. IR (ATR) υ_{max} cm^{-1}: 1727 (OC=O), 1699 (C_4=O), 1624 (C=C), 1232 and 1245 (C-O). ^{1}H NMR (300 MHz, $CDCl_3$) δ: 0.82 (3H, s, 18-H_3), 1.0 (3H, s, 19-H_3), 2.05 (3H, s, 17-CH_3COO), 2.18 (3H, s, 3-CH_3COO), 4.63 (1H, dd, $J_{17\alpha\text{-}16\alpha}$=9.0 Hz, $J_{17\alpha\text{-}16\beta}$=7.8 Hz, 17α-H), 5.21 (1H, dd, $J_{3\alpha\text{-}2\beta}$=12.3 Hz, $J_{3\alpha\text{-}2\alpha}$=7.2 Hz, 3α-H), 6.36 (1H, dd, $J_{6\text{-}7\alpha}$=5.1 Hz, $J_{6\text{-}7\beta}$=2.5 Hz, 6-H). ^{13}C NMR (75.5 MHz, $CDCl_3$) δ: 11.9 (C-18), 20.6, 20.8 (C-19), 21.1, 21.3, 23.4, 25.5, 27.4, 30.9, 31.1, 34.5, 36.5, 39.1, 42.4, 48.9, 50.7, 76.0 (C-17), 82.4 (C-3), 133.5 (C-6), 144.6 (C-5), 170.1 (OC=O), 171.1 (OC=O), 197.7 (C-4).

6-Allyl-4-oxoandrostane-3β,17β-diyl acetate (48)

To a stirred and cooled (-78 ºC) solution of **47** (490.0 mg, 1.261 mmol) in anhyd DCM (25 mL) under nitrogen atmosphere, titanium tetrachloride ($TiCl_4$) (0.17 mL, 1.545 mmol) was added. After 10 min of reaction, a solution of allyltrimethylsilane (0.37 mL, 2.302 mmol) in anhyd DCM (3 mL) was carefully added and the reaction solution was stirred for 20 min. Water (10 mL) was added, the aqueous phase

was extracted with DCM (3x 100 mL) and the organic layer was washed with water (3x 100 mL), dried with anhyd Na_2SO_4 and concentrated yielding an oily residue, which was purified by silica gel column chromatography (diethyl ether/ petroleum ether 40-60 ºC) affording the pure **48** as a clear oil (300 mg, 55%). IR (ATR) υ_{max} cm^{-1}: 1724 (C=O), 1645 (C=C), 1246 (C-O). ^{1}H NMR (300 MHz, $CDCl_3$) δ: 0.82 (3H, s, 18-H_3), 0.90 (3H, s, 19-H_3), 2.05 (3H, s, 17-CH_3COO), 2.17 (3H, s, 3-CH_3COO), 4.62 (1H, dd, $J_{17\alpha\text{-}16\alpha}$=9.0 Hz, 17α-H), 4.97 (2H, b m, $W_{1/2}$ *ca.* 25 Hz, -CH=C$\underline{H}_2$), 5.15 (1H, dd, $J_{3\alpha\text{-}2\beta}$=11.7 Hz, $J_{3\alpha\text{-}2\alpha}$=7.4 Hz, 3α-H), 5.78 (1H, m, $W_{1/2}$ *ca.* 42 Hz, -C$\underline{H}$=CH_2). ^{13}C NMR (75.5 MHz, $CDCl_3$) δ: 12.2 (C-18), 18.4 (C-19), 20.7, 21.0, 21.2, 23.5, 27.4, 27.7, 30.2, 32.5, 33.3, 34.3, 36.7, 38.0, 42.4, 42.7, 49.9, 54.9, 59.3 (C-5), 76.0 (C-17), 82.6 (C-3), 115.1 (-CH=$\underline{C}H_2$), 139.2 (-$\underline{C}$H=CH_2), 170.2 (OC=O), 171.2 (OC=O), 205.2 (C-4).

6α-Allyl-4,17β-dihydroxyandrost-4-en-3-one (49)

To a stirred solution of 5% aq NaOH, methanol and acetone [10/20/20] (10 mL) at room temperature, **48** (143 mg, 0.332 mmol) was added and the resulting mixture was stirred until complete transformation of the starting material (3 h 30 min, TLC). Water (300 mL) was added and the aqueous phase was extracted with ethyl acetate (3x 100 mL). The organic layer was washed with 5% aq HCl (3x 100 mL) and water (3x 100 mL) and dried with anhyd Na_2SO_4 leading to a crude which, after diethyl ether/*n*-hexane crystallization afforded the pure **49** as white crystals (87 mg, 76%). $Mp_{(ethyl\ acetate)}$ 154-156 ºC. IR (KBr disk) υ_{max} cm^{-1}: 3394 (O-H), 3045 (=C-H), 1665 (C=O), 1621 (C=C), 1154 (C_4-O), 1070 (C_{17}-O). ^{1}H NMR (300 MHz, $CDCl_3$) δ: 0.81 (3H, s, 18-H_3), 1.26 (3H, s, 19-H_3), 3.23 (1H, dd, $J_{6\beta\text{-}7\alpha}$=12.9 Hz, $J_{6\beta\text{-}7\beta}$=7.8 Hz, 6β-H), 3.66 (1H, dd, *J*=8.4 Hz, *J*=8.4 Hz, 17α-H), 5.00 (2H, b m, $W_{1/2}$ *ca.* 23 Hz, -CH=C$\underline{H}_2$), 5.78 (1H, b m, $W_{1/2}$ *ca.* 40 Hz, -C$\underline{H}$=CH_2), 6.15 (1H, s, 4-OH, disappears on adding D_2O). ^{13}C NMR (75.5 MHz, $CDCl_3$) δ: 11.1 (C-18), 20.2 (C-19), 20.5, 23.4, 29.9, 30.4, 31.9, 33.0 (2 carbons), 36.4, 36.8, 37.5, 38.9, 42.7, 50.5, 53.6, 81.7 (C-17), 116.1 (-CH=$\underline{C}H_2$), 137.4 (-$\underline{C}$H=CH_2), 142.1 (C-5), 142.3 (C-4), 194.0 (C-3).

Biochemistry

Preparation of Placental Microsomes

The human placental microsomes were obtained as previously described.[17-19] After delivery from a local hospital, human placenta were placed in cold 67 mM potassium phosphate buffer (pH 7.4) containing 1% KCl. The cotyledon tissue was separated and homogenized in a Polytron homogenizer with 67 mM potassium phosphate buffer (pH 7.4) containing 0.25 M sucrose and 0.5 mM dithiothreitol (DTT, 1:1, w/v). The homogenate was centrifuged at 5,000g for 30 min and the supernatant was centrifuged at 20,000g for 30 min and after, at 54,000g for 45 min to yield the microsomal pellet. After ultra-centrifugation, the microsomes were washed and resuspended in 67 mM potassium phosphate buffer (pH 7.4) containing 0.25 M sucrose, 20% glycerol and 0.5 mM DTT, and stored at -80 ºC. All the procedures were carried out at 0-4 ºC. Using bovine serum albumin (BSA) as a standard, the protein content was calculated by the Bio-Rad protein assay (Bio- Rad Labs, Munich, Germany).

Aromatase Assay Procedure

Aromatase activity was evaluated according to Thompson and Siiteri[55] and Heidrich *et al.*[69] method with some modifications,[17-19] by measuring the tritiated H_2O released from [1β-^{3}H] androstenedione (Perkin-Elmer Life Sciences, Boston, MA, USA), during the aromatization process. The compounds were dissolved in DMSO (Sigma-Aldrich Co., Saint Louis, USA) and stock solutions were prepared and stored at -20 °C. Prior the assays, compounds were diluted in 67 mM potassium phosphate buffer (pH 7.4). It was performed a screening assay to determine the percentage of aromatase inhibition for each compound. For the aromatization reaction it was used 20 μg of microsomal protein, 40 nM of [1β-^{3}H] androstenedione (1 μCi) and 2 μM of each compound in a final reaction volume of 500 μL. The reaction was initiated by the addition of NADPH (150 μM) (Sigma-Aldrich Co., Saint Louis, USA) and incubations were performed in a shaking water bath at 37 °C for 15 min. For the ones that presented an aromatase inhibition higher than 80% it was determined the IC_{50} value using the described reaction mixture but with 100 nM (1 μCi) of [1β-^{3}H] androstenedione and different

concentrations of the compounds (0.01 – 2 μM). The compounds that presented an IC_{50} value lower than 0.1 μM were submitted to kinetic studies. For the kinetic studies and to minimize the time-dependent loss of the initial aromatization rate, 5 min of incubation time was used, and assays were performed with different concentrations of [1β-^{3}H] androstenedione (10-30 nM) and different concentrations of compounds (0.02 – 0.4 μM). All the aromatase reactions were terminated by the addition of 250 μL of 20% trichloroacetic acid. The mixture was transferred to microcentrifuge tubes containing a charcoal-dextran pellet, vortexed, and incubated for 1 h. After centrifugation at 14,000g for 10 min, the supernatants were transferred to new charcoal-dextran pellets, incubated for 10 min, and subsequently pelleted by a new centrifugation cycle. The supernatant containing the tritiated water product was mixed with a liquid scintillation cocktail (ICN Radiochemicals, Irvine, CA, USA) and counted in a liquid scintillation counter (LS-6500, Beckman Coulter, Inc., Fullerton, CA). All the experiments were carried out in triplicate in three independent experiments. As a reference AI it was used exemestane (1 μM) (Sequoia Research Products Ltd., Pangbourne, UK) and formestane (0.5 μM) (Sigma-Aldrich Co., Saint Louis, USA).

In cell aromatase assay

It this study, for the compounds that presented an aromatase inhibition in placental microsomes higher than 80%, it was also evaluated their anti-aromatase activity in an ER-positive (ER^+) aromatase-overexpressing human breast cancer cell line (MCF-7aro), according to the Thompson and Siiteri[70] and Zhou et al.[71] methods with modifications.[21, 22] These cells were prepared by stable transfection of MCF-7 cells with the human placental aromatase gene and Geneticin selection,[71, 72] reason why they correspond to a good model to study AIs in ER^+ breast cancer.[56] They were maintained with Eagles's minimum essential medium (MEM) supplemented with 1 mmol/L sodium pyruvate, 1% penicillin-streptomycin-amphotericin B, 100 μg/mL G418 and 10% heat-inactivated fetal bovine serum (FBS) (Gibco Invitrogen Co., Paisley, Scotland, UK). Briefly, confluent MCF-7aro cells plated in a 24-well plate were cultured in serum-free medium containing the inhibitors at 10 μM, with 50 nM of [1β-^{3}H]

androstenedione as substrate and also 500 nM of progesterone (that was used to suppress 5α-reductase activity, which also uses androgen as substrate) and incubated at 37 ºC for 1 h. The aromatase reaction was finished by addition of 100 μL of 20% trichloroacetic acid (TCA). The aromatase inhibitory activity was evaluated as previously described.[21, 22] All experiments were carried out in triplicate in three independent experiments. Formestane and exemestane at 1 μM were used as reference AIs.

Molecular Modelling

Protein preparation and ligands conformational search

The crystal structure of the human placental aromatase was downloaded from the Protein Data Bank with the PDB ID: 4GL7.[28] This model was selected since the aromatase enzyme is complexed with a designed androstene-derived inhibitor having a C6-alkynyloxy side chain protruding into the opening access tunnel, which is bordered by Phe221, His480, Val313 and acts as an entry and exit way for steroidal scaffold inhibitors, substrate and water molecules. The crystallographic ligand was then removed and hydrogen atoms were then added with the Protein Preparation Wizard.[73] In addition, given the pH-dependent binding of androstenedione and exemestane that directly interact with Asp309,[74] which plays a critical role in the substrate binding and catalysis,[74, 75] the PROPKA 3.0 web server[76] was used to predict the protein protonation state at physiological pH of 7.4. According to the PROPKA 3.0 web server,[75] the predicted pKa for Asp309 residue was 8.49, comparable with literature data,[74] so Asp309 was considered in its carboxylate form for docking calculations.[77, 78] The tridimensional structure of the most active **11**, **12**, **13**, **14** and less active **4**, **7a**, **7b**, **8** and **21** compounds was built using the Maestro graphical user interface[79] and treated with the LigPrep tool[80] using the MMFF force field. For each ligand a conformational search was performed using the ConfGen tool,[81] in order to clarify the influence of the hydroxyl group at C-4 with the allyl side chain in position C-6α and C-7α. (Supporting Information, Figure S1 and Tables S1-S4).

Molecular Docking

Both the protein and the ligands structures, prepared as described above, were then submitted to the software FLAP (Fingerprint for Ligand and Protein) ver. 2.2.0[82-84] to perform docking calculations with the FLAPdock tool.[61] FLAP is based on the Molecular Interaction Fields (MIFs) similarities calculated by GRID.[85-87] In particular, the aromatase binding site was searched by the FLAPsite utility[17, 62] and it corresponded to the active site cavity, containing the heme group and the opening access channel (Supporting Information, Figure S2). On this pocket, GRID MIFs (Molecular Interaction Fields) were computed considering the H probe as the active site shape, N1 probe as hydrogen-bond donor, O probe as hydrogen-bond acceptor and the DRY probe as hydrophobic. The resolution was set up to the default value of 0.75Å. Subsequently, compounds **4**, **7a**, **7b**, **8**, **11**, **12**, **13**, **14** and **21**, were used to generate the appropriate FLAP file format to be submitted to docking calculation with FLAPdock tool,[61] reporting only the five best ligand poses. All the FLAPdock parameters were setting as their defaults, except for accuracy level that was set to high. The FLAPdock algorithm is a fragment-based approach consisting in subsequent placements of each ligand fragment within the receptor active site till a gradual incremental construction of the molecule. In a first step, poses are scored according to the FLAP field similarities, then a second scoring step takes into account the Lennard-Jones and dielectric corrected Coulombic energetic terms.[61] A preliminary validation of the computational docking protocol has been performed by evaluating the capability of FLAPdock[61] to reproduce the crystallographic pose of the androstene-derived ligand complexed in the PDB ID: 4GL7[28] (Supporting Information, Figure S7). The best FLAPdock S-score poses were energy minimized using the OPLS 2005 force field and 5000 iteration steps. All figures were rendered using PyMOL (http://www.pymol.org).

Supporting Information Available:

This material is available free of charge via the Internet at http://pubs.acs.org

SMILE strings, aromatase % inhibition, IC_{50}, inhibition type, K_i, real affinity (K_m/K_i) (CSV)

Conformational search details about dihedrals and angles values adopted by **11**, **12**, **13** and **14**. Binding pocket of aromatase as identified by the FLAPSite tool. FLAPdock poses of the inactive compounds **4**,

7a, **7b**, **8** and **21**. X-Ray binding conformation of androstenedione (PDB ID: 3EQM) and exemestane (PDB ID: 3S7S). FLAPdock re-docking results of the androstene-derived ligand 6β-(pent-2-yn-1-yloxy)androst-1,4-diene-3,17-dione complexed in the PDB ID: 4GL7 model.

Chromatograms with HPLC traces for key compounds **9** and **13**.

Description of the experimental procedures for the synthesis of the compounds **9**, **23**, **37a**, **37b** and **40**.

Corresponding Authors

*E-mail: Elisiário J. Tavares da Silva (etavares@ff.uc.pt), Fernanda M. F. Roleira (froleira@ff.uc.pt)

ORCID

Fernanda M. F. Roleira: 0000-0003-4229-5882

Carla Varela: 0000-0002-9824-4753

Cristina Amaral: 0000-0003-1594-2095

Saul C. Costa: 0000-0003-1476-7790

Georgina Correia-da-Silva: 0000-0001-5787-9018

Federica Moraca: 0000-0002-1077-1971

Giosuè Costa: 0000-0003-0947-9479

Stefano Alcaro: 0000-0002-0437-358X

Natércia A. A. Teixeira: 0000-0002-3664-1120

Elisiário J. Tavares da Silva: 0000-0002-0390-3403

Author Contributions

The manuscript was written through contributions of all authors. All authors have given approval to the final version of the manuscript.

Acknowledgments

The authors thank to FCT (Fundação para a Ciência e Tecnologia) for financial support and for the Post-Doc grant of Cristina Amaral (SFRH/BPD/98304/2013). This work was supported by the project (UID/MULTI/04378/2013–535 POCI/01/0145/FEDER/007728) from FCT/MEC, through national funds and co-financed by FEDER, under the Partnership Agreement PT2020.

NMR data was collected at the UC-NMR facility which is supported in part by FEDER – European Regional Development Fund through the COMPETE Programme (Operational Programme for Competitiveness) and by National Funds through FCT – Fundação para a Ciência e a Tecnologia (Portuguese Foundation for Science and Technology) through grants REEQ/481/QUI/2006, RECI/QEQ-QFI/0168/2012, CENTRO-07-CT62-FEDER-002012, and Rede Nacional de Ressonância Magnética Nuclear (RNRMN)."

Abbreviations

AI/AIs, aromatase inhibitors; DRY, hydrophobic probe; ER^+: estrogen receptor-positive; FLAP, fingerprints for ligands and proteins (molecular software by Molecular Discovery Inc.); GRID, software created by Professor Peter Goodford; MCF-7aro cells: ER^+ aromatase-overexpressing breast cancer cell line; MIFs, Molecular Interaction Fields; MMFF, Merck Molecular Force Field; H, active site shape, N1, hydrogen bond donor probe; O, hydrogen bond acceptor probe; DRY, hydrophobic probe; PYMOL, Python enhanced molecular graphics tool; SEM, standard error of the mean.

Authors will release the atomic coordinates upon article publication.

References and Notes

1. Ferlay, J.; Soerjomataram, I.; Dikshit, R.; Eser, S.; Mathers, C.; Rebelo, M.; Parkin, D. M.; Forman, D.; Bray, F. Cancer Incidence and Mortality Worldwide: Sources, Methods and Major Patterns in GLOBOCAN 2012. *International Journal of Cancer* **2015**, 136, E359-E386.

2. Chan, H. J.; Petrossian, K.; Chen, S. Structural and Functional Characterization of Aromatase, Estrogen Receptor, and their Genes in Endocrine-Responsive and –Resistant Breast Cancer Cells. *Journal of Steroid Biochemistry and Molecular Biology* **2016**, 161, 73-83.

3. Cardoso, F.; Costa, A.; Senkus, E.; Aapro, M.; André, F.; Barrios, C. H.; Bergh, J.; Bhattacharyya, G.; Biganzoli, L.; Cardoso, M. J.; Carey, L.; Corneliussen-James, D.; Curigliano, G.; Dieras, V.; El Saghir, N.; Eniu, A.; Fallowfield, L.; Fenech, D.; Francis, P.; Gelmon, K.; Gennari, A.; Harbeck, N.; Hudis, C.; Kaufman, B.; Krop, I.; Mayer, M.; Meijer, H.; Mertz, S.; Ohno, S.; Pagani, O.; Papadopoulos, E.; Peccatori, F.; Penault-Llorca, F.; Piccart, M. J.; Pierga, J. Y.; Rugo, H.; Shockney, L.; Sledge, G.; Swain, S.; Thomssen, C.; Tutt, A.; Vorobiof, D.; Xu, B.; Norton, L.; Winer, E. 3rd ESO–ESMO International Consensus Guidelines for Advanced Breast Cancer (ABC 3). *Annals of Oncology* **2017**, 28, 16-33.

4. Dutta, U.; Pant, K. Aromatase Inhibitors: Past, Present and Future in Breast Cancer Therapy. *Medical Oncology* **2008**, 25, 113-124.

5. Sobral, A. F.; Amaral, C.; Correia-da-Silva, G.; Teixeira, N. Unravelling Exemestane: From Biology to Clinical Prospects. *Journal of Steroid Biochemistry and Molecular Biology* **2016**, 163, 1-11.

6. Augusto, T. V.; Correia-da-Silva, G.; Rodrigues, C. M. P.; Teixeira, N.; Amaral, C. Acquired Resistance to Aromatase Inhibitors: Where we Stand! *Endocrine-Related Cancer* **2018**, 25, R283-R301.

7. Lv, W.; Liu, J. Z.; Skaar, T. C.; Flockhart, D. A.; Cushman, M. Design and Synthesis of Norendoxifen Analogues with Dual Aromatase Inhibitory and Estrogen Receptor Modulatory Activities. *Journal of Medicinal Chemistry* **2015**, 58, 2623-2648.

8. Lv, W.; Liu, J. Z.; Skaar, T. C.; O'Neill, E.; Yu, G.; Flockhart, D. A.; Cushman, M. Synthesis of Triphenylethylene Bisphenols as Aromatase Inhibitors that also Modulate Estrogen Receptors. *Journal of Medicinal Chemistry* **2016**, 59, 157-170.

9. Kang, H.; Xiao, X.; Huang, C.; Yuan, Y.; Tang, D.; Dai, X.; Zeng, X. Potent Aromatase Inhibitors and Molecular Mechanism of Inhibitory Action. *European Journal of Medicinal Chemistry* **2018**, 143, 426-437.

10. Yadav, M. R.; Barmade, M. A.; Tamboli, R. S.; Murumkar, P. R. Developing Steroidal Aromatase Inhibitors - An Effective Armament to Win the Battle Against Breast Cancer. *European Journal of Medicinal Chemistry* **2015**, 105, 1-38.

11. Yardley, D. A.; Noguchi, S.; Pritchard, K. I.; Burris, H. A.; Baselga, J.; Gnant, M.; Hortobagyi, G. N.; Campone, M.; Pistilli, B.; Piccart, M.; Melichar, B.; Petrakova, K.; Arena, F. P.; Erdkamp, F.; Harb, W. A.; Feng, W. T.; Cahana, A.; Taran, T.; Lebwohl, D.; Rugo, H. S. Everolimus Plus Exemestane in Postmenopausal Patients with HR^+ Breast Cancer: BOLERO-2 Final Progression-Free Survival Analysis. *Advances in Therapy* **2013**, 30, 870-884.

12. Piccart, M.; Hortobagyi, G. N.; Campone, M.; Pritchard, K. I.; Lebrun, F.; Ito, Y.; Noguchi, S.; Perez, A.; Rugo, H. S.; Deleu, I.; Burris, H. A.; Provencher, L.; Neven, P.; Gnant, M.; Shtivelband, M.; Wu, C.; Fan, J.; Feng, W.; Taran, T.; Baselga, J. Everolimus Plus Exemestane for Hormone-Receptor-Positive, Human Epidermal Growth Factor Receptor-2-Negative Advanced Breast Cancer: Overall Survival Results from BOLERO-2. *Annals of Oncology* **2014**, 25, 2357-2362.

13. Miki, Y.; Suzuki, T.; Hatori, M.; Igarashi, K.; Aisaki, K.; Kanno, J.; Nakamura, Y.; Uzuki, M.; Sawai, T.; Sasano, H. Effects of Aromatase Inhibitors on Human Osteoblast and Osteoblast-Like Cells: A Possible Androgenic Bone Protective Effects Induced by Exemestane. *Bone* **2007**, 40, 876-887.

14. Goss, P. E.; Qi, S.; Josse, R. G.; Pritzker, K. P. H.; Mendes, M.; Hu, H.; Waldman, S. D.; Grynpas, M. D. The Steroidal Aromatase Inhibitor Exemestane Prevents Bone Loss in Ovariectomized Rats. *Bone* **2004**, 34, 384-392.

15. Goss, P. E.; Hershman, D. L.; Cheung, A. M.; Ingle, J. N.; Khosla, S.; Stearns, V.; Chalchal, H.; Rowland, K.; Muss, H. B.; Linden, H. M.; Scher, J.; Pritchard, K. I.; Elliott, C. R.; Badovinac-Crnjevic, T.; St Louis, J.; Chapman, J. A. W.; Shepherd, L. E. Effects of Adjuvant Exemestane *versus* Anastrozole on Bone Mineral Density for Women with EarlyBreast Cancer (MA.27B): A Companion Analysis of a Randomised Controlled Trial. *Lancet Oncology* **2014**, 15, 474-482.

16. Cepa, M.; da Silva, E. J. T.; Correia-Da-Silva, G.; Roleira, F. M. F.; Teixeira, N. A. A. Structure-Activity Relationships of New A,D-Ring Modified Steroids as Aromatase Inhibitors: Design, Synthesis, and Biological Activity Evaluation. *Journal of Medicinal Chemistry* **2005**, 48, 6379-6385.

17. Varela, C.; da Silva, E. J. T.; Amaral, C.; da Silva, G. C.; Baptista, T.; Alcaro, S.; Costa, G.; Carvalho, R. A.; Teixeira, N. A. A.; Roleira, F. M. F. New Structure-Activity Relationships of A- and D-Ring Modified Steroidal Aromatase Inhibitors: Design, Synthesis, and Biochemical Evaluation. *Journal of Medicinal Chemistry* **2012**, 55, 3992-4002.

18. Varela, C. L.; Amaral, C.; Correia-da-Silva, G.; Carvalho, R. A.; Teixeira, N. A.; Costa, S. C.; Roleira, F. M. F.; Tavares-da-Silva, E. J. Design, Synthesis and Biochemical Studies of New 7-alpha-Allylandrostanes as Aromatase Inhibitors. *Steroids* **2013**, 78, 662-669.

19. Varela, C. L.; Amaral, C.; da Silva, E. T.; Lopes, A.; Correia-da-Silva, G.; Carvalho, R. A.; Costa, S. C. P.; Roleira, F. M. F.; Teixeira, N. Exemestane Metabolites: Synthesis, Stereochemical Elucidation, Biochemical Activity and Anti-Proliferative Effects in a Hormone-Dependent Breast Cancer Cell Line. *European Journal of Medicinal Chemistry* **2014**, 87, 336-345.

20. Varela, C. L.; Amaral, C.; Correia-da-Silva, G.; Costa, S. C.; Carvalho, R. A.; Costa, G.; Alcaro, S.; Teixeira, N. A. A.; Tavares-da-Silva, E. J.; Roleira, F. M. F. Exploring New Chemical Functionalities to Improve Aromatase Inhibition of Steroids. *Bioorganic & Medicinal Chemistry* **2016**, 24, 2823-2831.

21. Amaral, C.; Varela, C.; Azevedo, M.; da Silva, E. T.; Roleira, F. M. F.; Chen, S.; Correia-da-Silva, G.; Teixeira, N. Effects of Steroidal Aromatase Inhibitors on Sensitive and Resistant Breast Cancer Cells: Aromatase Inhibition and Autophagy. *Journal of Steroid Biochemistry and Molecular Biology* **2013**, 135, 51-59.

22. Amaral, C.; Varela, C. L.; Mauricio, J.; Sobral, A. F.; Costa, S. C.; Roleira, F. M. F.; Tavares-da-Silva, E. J.; Correia-da-Silva, G.; Teixeira, N. Anti-Tumor Efficacy of New 7-alpha-Substituted Androstanes as Aromatase Inhibitors in Hormone-Sensitive and Resistant Breast Cancer Cells. *Journal of Steroid Biochemistry and Molecular Biology* **2017**, 171, 218-228.

23. Amaral, C.; Lopes, A.; Varela, C. L.; da Silva, E. T.; Roleira, F. M. F.; Correia-da-Silva, G.; Teixeira, N. Exemestane Metabolites Suppress Growth of Estrogen Receptor-Positive Breast Cancer Cells by Inducing Apoptosis and Autophagy: A Comparative Study with Exemestane. *International Journal of Biochemistry & Cell Biology* **2015**, 69, 183-195.

24. Levina, I. S. Substituted Androstanes as Aromatase Inhibitors. *Uspekhi Khimii* **1998**, 67, 1068-1093.

25. Snider, C. E.; Brueggemeier, R. W. Potent Enzyme-Activated Inhibition of Aromatase by a 7-alpha-Substituted C-19 Steroid. *Journal of Biological Chemistry* **1987**, 262, 8685-8689.

26. Brodie, A. M. H.; Garrett, W. M.; Hendrickson, J. R.; Tsaimorris, C. H.; Marcotte, P. A.; Robinson, C. H. Inactivation of Aromatase *In vitro* by 4-Hydroxy-4-androstene-3,17-dione and 4-Acetoxy-4-androstene-3,17-dione and Sustained Effects *In vivo*. *Steroids* **1981**, 38, 693-702.

27. Numazawa, M.; Oshibe, M. 6-Alkyl- and 6-Arylandrost-4-ene-3,17-diones as Aromatase Inhibitors - Synthesis and Structure-Activity-Relationships. *Journal of Medicinal Chemistry* **1994**, 37, 1312-1319.

28. Ghosh, D.; Lo, J.; Morton, D.; Valette, D.; Xi, J. L.; Griswold, J.; Hubbell, S.; Egbuta, C.; Jiang, W. H.; An, J.; Davies, H. M. L. Novel Aromatase Inhibitors by Structure-Guided Design. *Journal of Medicinal Chemistry* **2012**, 55, 8464-8476.

29. Ghosh, D.; Griswold, J.; Erman, M.; Pangborn, W. Structural Basis for Androgen Specificity and Oestrogen Synthesis in Human Aromatase. *Nature* **2009**, 457, 219-223.

30. Ghosh, D.; Egbuta, C.; Lo, J. Testosterone Complex and Non-Steroidal Ligands of Human Aromatase. *Journal of Steroid Biochemistry and Molecular Biology* **2018**, 181, 11-19.

31. Annen, K.; Hofmeister, H.; Laurent, H.; Wiechert, R. A Simple Method for 6-Methylenation of 3-Oxo-delta-4-Steroids. *Synthesis-Stuttgart* **1982**, 34-40.

32. Burn, D.; Kirk, D. N.; Petrow, V. Modified Steroid Hormones. 38. Some Transformations of Steroidal 3-Alkoxy-6-formyl-3,5-dienes and Related Compounds. *Tetrahedron* **1965**, 21, 1619-1624.

33. McKenna, J.; Norymberski, J. K.; Stubbs, R. D. Partial Reduction of Steroid Hormones and Related Substances. 3. The Reaction of alpha,beta-Unsaturated Ketones with Zinc in Acetic Acid. *Journal of the Chemical Society* **1959**, 2502-2509.

34. da Silva, E. J. T.; Sá e Melo, M. L.; Neves, A. S. C. Novel Approach to the Synthesis of the Aromatase Inhibitor 4-Hydroxyandrost-4-ene-3,17-dione (4-OHA). *Journal of the Chemical Society, Perkin Transactions 1* **1996**, 1649-1650.

35. da Silva, E. J. T.; Roleira, F. M. F.; Melo, M.; Neves, A. S. C.; Paixao, J. A.; de Almeida, M. J.; Silva, M. R.; Andrade, L. C. R. X-Ray and Deuterium Labeling Studies on the Abnormal Ring Cleavages of a 5beta-Epoxide Precursor of Formestane. *Steroids* **2002**, 67, 311-319.

36. Paixao, J. A.; Andrade, L. C. R.; Almeida, M. J. d.; Tavares da Silva, E. J.; Fernandes Roleira, F. M.; Sa e Melo, M. L.; Campos Neves, A. S. 5[alpha]-Androst-3-en-17-one. *Acta Crystallographica Section E* **2001**, 57, o189-o191.

37. Li, C.; Qiu, W. W.; Yang, Z. F.; Luo, J. A.; Yang, F.; Liu, M. Y.; Xie, J.; Tang, J. Stereoselective Synthesis of Some Methyl-Substituted Steroid Hormones and Their *in vitro* Cytotoxic Activity Against Human Gastric Cancer Cell Line MGC-803. *Steroids* **2010**, 75, 859-869.

38. Martynow, J.; Krupa, M.; Les, A.; Kutner, A.; Szelejewski, W. Optimization of Copper(I)-Catalyzed 1,6-Conjugate Addition of a Methyl Group to 17beta-Acetoxy-4,6-estradien-3-one. *Organic Process Research & Development* **2004**, 8, 846-851.

39. Hanson, J. R.; Hitchcock, P. B.; Liman, M. D.; Nagaratnam, S. Facial Selectivity in the Hydroboration of Androst-4-enes. *Journal of the Chemical Society-Perkin Transactions 1* **1995**, 2183-2187.

40. Hoveyda, A. H.; Evans, D. A.; Fu, G. C. Substrate-Directable Chemical-Reactions. *Chemical Reviews* **1993**, 93, 1307-1370.

41. Numazawa, M.; Kamiyama, T.; Tachibana, M.; Oshibe, M. Synthesis and Structure-Activity Relationships of 6-Substituted Androst-4-ene Analogs as Aromatase Inhibitors. *Journal of Medicinal Chemistry* **1996**, 39, 2245-2252.

42. Numazawa, M.; Mutsumi, A.; Asano, N.; Ito, Y. A Time-Dependent Inactivation of Aromatase by 19-Substituted Androst-4-ene-3,6,17-triones. *Steroids* **1993**, 58, 40-46.

43. Rasmusson, G. H.; Arth, G. E. *Selective Oxidations of Hydroxysteroids. In Organic Reactions in Steroid Chemistry; Fried, J. Edwards, J. A., Eds.* Van Nostrand Reinhold Company: New York, 1972.

44. da Silva, E. J. T.; Melo, M.; Neves, A. S. C.; Paixao, J. A.; Andrade, L. C. R.; Almeida, M. J. M.; Costa, M. M. R. Expedient Synthesis of Lactone Analogues of Formestane as New Potential Aromatase Inhibitors. *Journal of the Chemical Society-Perkin Transactions 1* **1997**, 3487-3489.

45. Corey, E. J.; Venkateswarlu, A. Protection of Hydroxyl Groups as *tert*-Butyldimethylsylil Derivatives. *Journal of the American Chemical Society* **1972**, 94, 6190-6191.

46. Zinczuk, J.; Bacigaluppo, J. A.; Colombo, M. I.; Cravero, R. M.; Gonzalez-Sierra, M.; Ruveda, E. A. An Efficient and Environmentally Benign Chemical Synthesis of Testolactone. *Journal of the Brazilian Chemical Society* **2003**, 14, 970-974.

47. Djerassi, C.; Rosenkranz, G.; Romo, J.; Kaufmann, S.; Pataki, J. Steroids. 7. Contribution to the Bromination of delta-4-3-Ketosteroids and a New Partial Synthesis of the Natural Estrogens. *Journal of the American Chemical Society* **1950**, 72, 4534-4540.

48. Julian, P. L.; Bauer, L.; Bell, C. L.; Hewitson, R. E. Mechanism of Reaction of 2ζ,6β-Dibromocholest-4-ene-3-one with Potassium Acetate. *Journal of the American Chemical Society* **1969**, 91, 1690-1696.

49. Fieser, L. F.; Fieser, M.; Rajagopalan, S. Absorption Spectroscopy and the Structures of the Diosterols. *Journal of Organic Chemistry* **1948**, 13, 800-806.

50. Labrie, F.; Merand, Y. Aromatase Inhibitors. *WO9112206-A; August 22* **1991**.

51. Flaih, N.; Hanson, J. R.; Hitchcock, P. B. Neighboring-Group Participation in the Chromium Trioxide Oxidation of Steroidal 4,5-Epoxides - X-Ray Molecular-Structure of 4-beta,6-beta,17-beta-Triacetoxy-3-beta,5-alpha-dihydroxyandrostane. *Journal of the Chemical Society-Perkin Transactions 1* **1991**, 1085-1089.

52. Holland, H. L.; Kumaresan, S.; Tan, L.; Njar, V. C. O. Synthesis of 6-Hydroximino-3-Oxo-Steroids, A New Class of Aromatase Inhibitor. *Journal of the Chemical Society-Perkin Transactions 1* **1992**, 585-587.

53. Sakurai, H. Reactions of Allylsilanes and Application to Organic Synthesis. *Pure and Applied Chemistry* **1982**, 54, 1-22.

54. Huang, S. L.; Omura, K.; Swern, D. Oxidation of Sterically Hindered Alcohols to Carbonyls with Dimethyl Sulfoxide-Trifluoroacetic Anhydride. *Journal of Organic Chemistry* **1976**, 41, 3329-3331.

55. Thompson, E. A.; Siiteri, P. K. Involvement of Human Placental Microsomal Cytochrome P-450 in Aromatization. *Journal of Biological Chemistry* **1974**, 249, 5373-5378.

56. Itoh, T.; Karlsberg, K.; Kijima, I.; Yuan, Y. C.; Smith, D.; Ye, J.; Chen, S. Letrozole-, Anastrozole-, and Tamoxifen-Responsive Genes in MCF-7Aro Cells: a Microarray Approach. *Mol Cancer Res* **2005**, 3, 203-218.

57. Amaral, C.; Borges, M.; Melo, S.; da Silva, E. T.; Correia-da-Silva, G.; Teixeira, N. Apoptosis and Autophagy in Breast Cancer Cells Following Exemestane Treatment. *PLoS One* **2012**, 7, e42398.

58. Wang, X.; Chen, S. U. Aromatase Destabilizer: Novel Action of Exemestane, a Food and Drug Administration-Approved Aromatase Inhibitor. *Cancer Research* **2006**, 66, 10281-10286.

59. Lombardi, P. The Irreversible Inhibition of Aromatase (Oestrogen Synthetase) by Steroidal Compounds. *Current Pharmaceutical Design* **1995**, 1, 23-50.

60. Lombardi, P. Exemestane, a New Steroidal Aromatase Inhibitor of Clinical Relevance. *Biochimica Et Biophysica Acta-Molecular Basis of Disease* **2002**, 1587, 326-337.

61. Siragusa, L.; Luciani, R.; Borsari, C.; Ferrari, S.; Costi, M. P.; Cruciani, G.; Spyrakis, F. Comparing Drug Images and Repurposing Drugs with BioGPS and FLAPdock: The Thymidylate Synthase Case. *Chemmedchem* **2016**, 11, 1653-1666.

62. Henrich, S.; Salo-Ahen, O. M. H.; Huang, B.; Rippmann, F.; Cruciani, G.; Wade, R. C. Computational Approaches to Identifying and Characterizing Protein Binding Sites for Ligand Design. *Journal of Molecular Recognition* **2010**, 23, 209-219.

63. Ryan, K. J. Biological Aromatization of Steroids. *Journal of Biological Chemistry* **1959**, 234, 268-272.

64. Numazawa, M.; Yamada, K.; Nitta, S.; Sasaki, C.; Kidokoro, K. Role of Hydrophilic Interaction in Binding of Hydroxylated 3-Deoxy C-19 Steroids to the Active Site of Aromatase. *Journal of Medicinal Chemistry* **2001**, 44, 4277-4283.

65. Nagaoka, M.; Watari, Y.; Yajima, H.; Tsukioka, K.; Muroi, Y.; Yamada, K.; Numazawa, M. Structure-Activity Relationships of 3-Deoxy Androgens as Aromatase Inhibitors. Synthesis and Biochemical Studies of 4-Substituted 4-Ene and 5-Ene Steroids. *Steroids* **2003**, 68, 533-542.

66. Cepa, M.; da Silva, E. J. T.; Correia-da-Silva, G.; Roleira, F. M. F.; Teixeira, N. A. A. Synthesis and Biochemical Studies of 17-Substituted Androst-3-enes and 3,4-Epoxyandrostanes as Aromatase Inhibitors. *Steroids* **2008**, 73, 1409-1415.

67. Marsh, D. A.; Brodie, H. J.; Garrett, W.; Tsaimorris, C. H.; Brodie, A. M. H. Aromatase Inhibitors - Synthesis and Biological Activity of Androstenedione Deriviatives. *Journal of Medicinal Chemistry* **1985**, 28, 788-795.

68. Templeton, J. F.; Kumar, V. P. S.; Elsheikh, A. A. M.; Zeglam, T. H.; Marat, K. Molecular Rearrangement of 3-Substituted 4-Chloro-4,5-epoxide Systems in Ring-A of Steroids. *Journal of the Chemical Society-Perkin Transactions 1* **1988**, 1961-1971.

69. Heidrich, D. D.; Steckelbroeck, S.; Klingmuller, D. Inhibition of Human Cytochrome P450 Aromatase Activity by Butyltins. *Steroids* **2001**, 66, 763-769.

70. Thompson, E. A., Jr.; Siiteri, P. K. Utilization of Oxygen and Reduced Nicotinamide Adenine Dinucleotide Phosphate by Human Placental Microsomes During Aromatization of Androstenedione. *J Biol Chem* **1974**, 249, 5364-5372.

71. Zhou, D. J.; Pompon, D.; Chen, S. A. Stable Expression of Human Aromatase Complementary DNA in Mammalian Cells: A Useful System for Aromatase Inhibitor Screening. *Cancer Res* **1990**, 50, 6949-6954.

72. Sun, X. Z.; Zhou, D.; Chen, S. Autocrine and Paracrine Actions of Breast Tumor Aromatase. A Three-Dimensional Cell Culture Study Involving Aromatase Transfected MCF-7 and T-47D Cells. *J Steroid Biochem Mol Biol* **1997**, 63, 29-36.

73. Sastry, G. M.; Adzhigirey, M.; Day, T.; Annabhimoju, R.; Sherman, W. Protein and Ligand Preparation: Parameters, Protocols, and Influence on Virtual Screening Enrichments. *Journal of Computer-Aided Molecular Design* **2013**, 27, 221-234.

74. Di Nardo, G.; Breitner, M.; Bandino, A.; Ghosh, D.; Jennings, G. K.; Hackett, J. C.; Gilardi, G. Evidence for an Elevated Aspartate pK(a) in the Active Site of Human Aromatase. *The Journal of Biological Chemistry* **2015**, 290, 1186-1196.

75. Sen, K.; Hackett, J. C. Coupled Electron Transfer and Proton Hopping in the Final Step of CYP19-Catalyzed Androgen Aromatization. *Biochemistry* **2012**, 51, 3039-3049.

76. Sondergaard, C. R.; Olsson, M. H. M.; Rostkowski, M.; Jensen, J. H. Improved Treatment of Ligands and Coupling Effects in Empirical Calculation and Rationalization of pK(a) Values. *Journal of Chemical Theory and Computation* **2011**, 7, 2284-2295.

77. Caporuscio, F.; Rastelli, G.; Imbriano, C.; Del Rio, A. Structure-Based Design of Potent Aromatase Inhibitors by High-Throughput Docking. *Journal of Medicinal Chemistry* **2011**, 54, 4006-4017.

78. Brincat, J. P.; Carosati, E.; Sabatini, S.; Manfroni, G.; Fravolini, A.; Raygada, J. L.; Pate, D.; Kaatz, G. W.; Cruciani, G. Discovery of Novel Inhibitors of the NorA Multidrug Transporter of Staphylococcus aureus. *Journal of Medicinal Chemistry* **2011**, 54, 354-365.

79. Schrödinger Release 2016-3: Maestro, Schrödinger, LLC, New York, NY, **2016**.

80. Schrödinger Release 2016-3: LigPrep, Schrödinger, LLC, New York, NY, **2016**.

81. Watts, K. S.; Dalal, P.; Murphy, R. B.; Sherman, W.; Friesner, R. A.; Shelley, J. C. ConfGen: A Conformational Search Method for Efficient Generation of Bioactive Conformers. *Journal of Chemical Information and Modeling* **2010**, 50, 534-546.

82. Baroni, M.; Cruciani, G.; Sciabola, S.; Perruccio, F.; Mason, J. S. A Common Reference Framework for Analyzing/Comparing Proteins and Ligands. Fingerprints for Ligands and Proteins (FLAP): Theory and Application. *Journal of Chemical Information and Modeling* **2007**, 47, 279-294.

83. Artese, A.; Cross, S.; Costa, G.; Distinto, S.; Parrotta, L.; Alcaro, S.; Ortuso, F.; Cruciani, G. Molecular Interaction Fields in Drug Discovery: Recent Advances and Future Perspectives. *Wiley Interdisciplinary Reviews-Computational Molecular Science* **2013**, 3, 594-613.

84. Spyrakis, F.; Benedetti, P.; Decherchi, S.; Rocchia, W.; Cavalli, A.; Alcaro, S.; Ortuso, F.; Baroni, M.; Cruciani, G. A Pipeline To Enhance Ligand Virtual Screening: Integrating Molecular Dynamics and Fingerprints for Ligand and Proteins. *Journal of Chemical Information and Modeling* **2015**, 55, 2256-2274.

85. Goodford, P. J. A Computational-Procedure for Determining Energetically Favorable Binding-Sites on Biologically Important Macromolecules. *Journal of Medicinal Chemistry* **1985**, 28, 849-857.

86. Ortuso, F.; Langer, T.; Alcaro, S. GBPM: GRID-Based Pharmacophore Model: Concept and Application Studies to Protein-Protein Recognition. *Bioinformatics* **2006**, 22, 1449-1455.

87. Moraca, F.; Amato, J.; Ortuso, F.; Artese, A.; Pagano, B.; Novellino, E.; Alcaro, S.; Parrinello, M.; Limongelli, V. Ligand Binding to Telomeric G-quadruplex DNA Investigated by Funnel-

metadynamics Simulations. *Proceedings of the National Academy of Sciences of the United States of America* **2017**, 114, E2136-E2145.

Captions of figures and schemes

Figure 1 – Aromatase inhibitors in clinical use.

Figure 2 – Graphical representation of the dose-dependency of the % of aromatase inhibition for AIs **9**, **12**, **13** and **15**, in microsomes, in order to evaluate the IC_{50} (μM) values. Data are presented as a percentage of the tritiated water control and correspond to three independent experiments carried out in triplicate.

Figure 3 – Lineweaver−Burk and Dixon plots of inhibitor **9** (A, B) and inhibitor **13** (C, D). To determine the apparent inhibition constant (Ki) and the type of inhibition, different concentrations of inhibitors (0, 0.02, 0.05, 0.1 and 0.2 μM), with [1β-^{3}H] androstenedione as substrate at 10, 20, and 30 nM, were used. Each point represents the mean of three independent determinations done in triplicate.

Figure 4 – Energy minimized FLAPdock predicted pose of compound **13** (pink sticks) against human placental aromatase (PDB ID: 4GL7). The 3-keto oxygen of the A-ring benzoquinone moiety is much closer to the carboxylate Asp309, while the 17-keto oxygen engages one hydrogen bond with Met374. It can be observed how the C-6α allyl side chain is well accommodated within the access channel. Protein residues are displayed as light-orange lines. Hydrogen bonds are represented as dashed black lines. Heme group is displayed as violet lines. Atomic distances are displayed as dashed magenta lines. Ligands hydrogen atoms are not displayed for clarity reasons.

Figure 5 – Energy minimized FLAPdock predicted pose of compound **11** (cyan sticks) against human placental aromatase (PDB ID: 4GL7). The simultaneous presence of such functional hydroxyl group at C-4 and the allyl side chain in C-6α, leads the 3-keto oxygen of the A-ring farther from Asp309 (5.0 Å). This is mainly due to steric hindrance reasons. Protein residues are displayed as light-orange lines.

Hydrogen bonds are represented as dashed black lines. Heme group is displayed as violet lines. Atomic distances are displayed as dashed magenta lines. Ligands hydrogen atoms are not displayed for clarity reasons.

Figure 6 – Energy minimized FLAPdock predicted pose of compound **12** (light-green sticks) against human placental aromatase (PDB ID: 4GL7). The presence of the hydroxyl group at C-4 and the allyl side chain at C-7α, improves the inhibition activity because the A-ring finds closer to Asp309 with respect to compound **11**. Protein residues are displayed as light-orange lines. Hydrogen bonds are represented as dashed black lines. Heme group is displayed as violet lines. Atomic distances are displayed as dashed magenta lines. Ligands hydrogen atoms are not displayed for clarity reasons.

Figure 7 – Energy minimized FLAPdock predicted pose of compound **14** (brown sticks) against human placental aromatase (PDB ID: 4GL7). It is evident that the substitution of the allyl side chain from C-6α to C-7α mainly affects the A-ring binding geometries. The 3-keto oxygen atom of the A-ring is farther to the OD2 atom of Asp309. This is mainly due to the steric hindrance of the allyl side chain with Leu477 and Ser478 residues. Protein residues are displayed as light-orange lines. Hydrogen bonds are represented as dashed black lines. Heme group is displayed as violet lines. Atomic distances are displayed as dashed magenta lines. Ligands hydrogen atoms are not displayed for clarity reasons.

Scheme 1 – C-6 and C-7 methyl series of steroidal aromatase inhibitors.

Scheme 2 – **Synthesis of aromatase inhibitors 1a, 3a and 9**. Reagents and conditions: (i) anhyd sodium acetate, formaldehyde dimethyl acetal, phosphoryl chloride, anhyd chloroform, reflux, 10 h; (ii) cyclohexene, 5% Pd-C, ethanol, reflux, 3 h 15 min; (iii) zinc dust, glacial acetic acid, reflux, 5 h 15 min; (iv) HCOOOH, DCM, rt, 9 h 30 min.

Scheme 3 – Synthesis of aromatase inhibitors 2a/2b, 4, 6, 8 and 10a. Reagents and conditions: (i) chloranil, *tert*-butanol, reflux, 7h; (ii) CuBr, Me_3Al, TMSCl, anhyd THF, rt, 24 h; (iii) CF_3COOH, CH_3CN, CH_3COOH, $NaBH_4$, anhyd DCM, rt, 3 h 40 min; (iv) Jones reagent, acetone, 0 ºC, 5 min; (v) *m*-CPBA, DCM, rt, 19 h 20 min; (vi) zinc dust, glacial acetic acid, reflux, 22 h; (vii) HCOOOH, DCM, rt, 8 h.

Scheme 4 – Synthesis of aromatase inhibitors 5, 9, 7a and 7b. Reagents and conditions: (i) $NaBH_4$, methanol, 0 ºC, 1 h 45 min; (ii) *m*-CPBA, DCM, rt, 2 h 15 min; (iii) CH_3MgBr, anhyd THF, reflux 46 h 30 min; (iv) Jones reagent, acetone, 0 ºC, 5 min; (v) HCl/CH_3COOH, rt, 5 h 45 min; (vi) CF_3COOH, CH_3CN, CH_3COOH, $NaBH_4$, anhyd DCM, rt, 2 h; (vii) HCOOOH, DCM, rt, 6 h.

Scheme 5 – C-6 and C-7 allyl series of steroidal aromatase inhibitors.

Scheme 6 – Synthesis of aromatase inhibitors 13, 15 and 17. Reagents and conditions: (i) *tert*-butyldimethylsilyl chloride, imidazole, dimethylformamide, rt, 2 h; (ii) allylmagnesium bromide, anhyd THF, reflux, 40 min; (iii) HCl/Ethanol, rt, 25 h; (iv) Jones reagent, acetone/dioxane, 0 ºC, 5 min; (v) HCl/CH_3COOH, rt, 17 h 30 min; (vi) DDQ, benzoic acid, toluene, reflux, 18 h 30 min; (vii) CF_3COOH, CH_3CN, CH_3COOH, $NaBH_4$, anhyd DCM, rt, 1 h 30 min..

Scheme 7 – Synthesis of aromatase inhibitor 12. Reagents and conditions: (i) Br_2 in CH_3COOH, diethyl ether, 0º C, 30 min; (ii) CH_3COOK/ethanol, acetone, reflux, 30 min; (iii) HCl/ethanol, reflux, 1 h 30 min; (iv) $(CH_3CO)_2O$, pyridine, rt, 2 h; (v) Allyl-$Si(CH_3)_3$, $TiCl_4$, anhyd DCM, -78 ºC, 30 min.

Scheme 8 – Synthesis of aromatase inhibitor 11. Reagents and conditions: (i) $NaBH_4$, methanol, rt, 2 h 40 min; (ii) HCOOOH, DCM, rt, 4 h; (iii) $(CH_3CO)_2O$, pyridine, rt, 8 h; (iv) 75% aq CrO_3, butanone, rt, 1 h 15 min; (v) $SOCl_2$, anhyd pyridine, 0 ºC, 25 min; (vi) Allyl-$Si(CH_3)_3$, $TiCl_4$, anhyd DCM, -78 ºC,

20 min, (vii) 5% NaOH, methanol, acetone, rt, 3 h 30 min; (viii) anhyd DMSO, TFAA, TEA, anhyd DCM, - 60 ºC, 3 h.

Scheme 9 – C-6 and C-7 hydroxyl series of steroidal aromatase inhibitors.

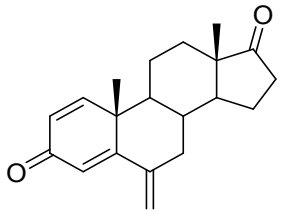

Exemestane

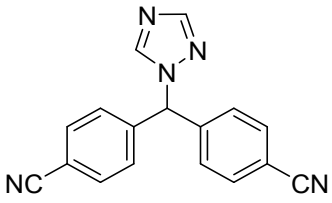

Letrozole

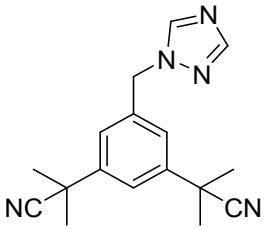

Anastrozole

Figure 1

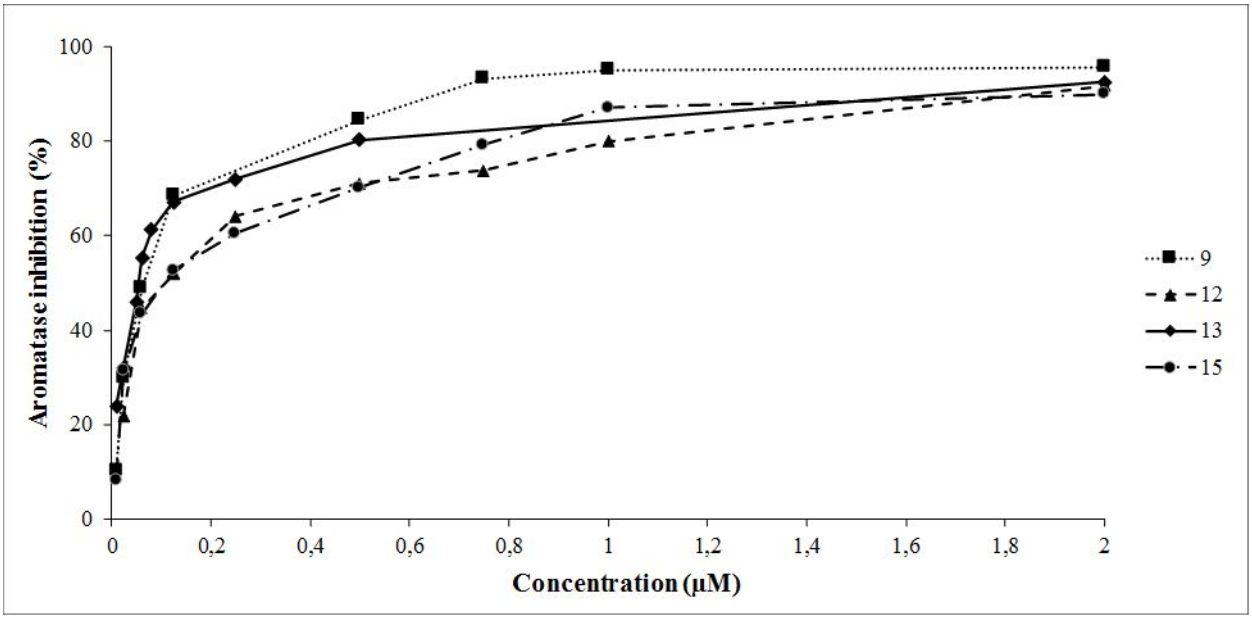
Aromatase inhibition (%)
100
80
60
40
20
0
0
0,2
0,4
0,6
0,8
1
1,2
1,4
1,6
1,8
2
Concentration (µM)
9
12
13
15

Figure 2

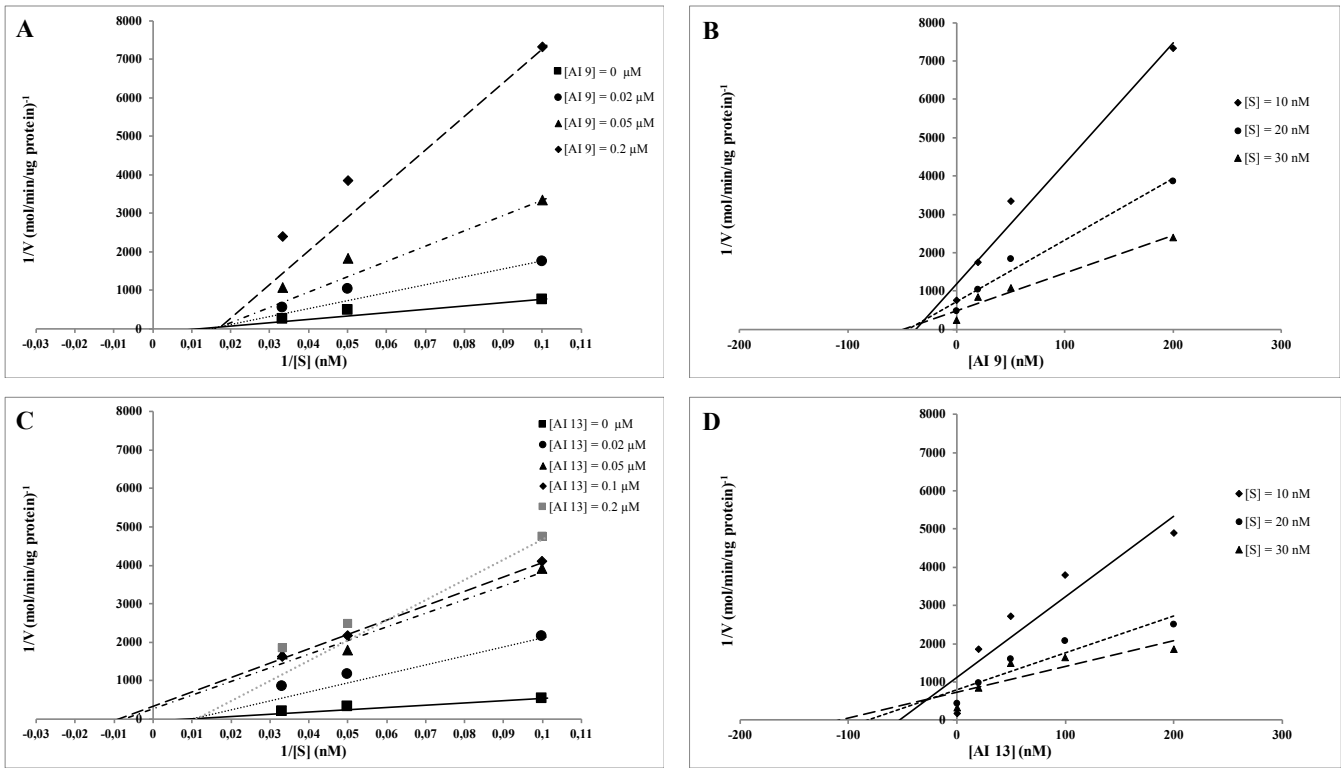
A
1/V (mol/min/ug protein)-1
1/[S] (nM)
[AI 9] = 0 µM
[AI 9] = 0.02 µM
[AI 9] = 0.05 µM
[AI 9] = 0.2 µM
B
1/V (mol/min/ug protein)-1
[AI 9] (nM)
[S] = 10 nM
[S] = 20 nM
[S] = 30 nM
C
1/V (mol/min/ug protein)-1
1/[S] (nM)
[AI 13] = 0 µM
[AI 13] = 0.02 µM
[AI 13] = 0.05 µM
[AI 13] = 0.1 µM
[AI 13] = 0.2 µM
D
1/V (mol/min/ug protein)-1
[AI 13] (nM)
[S] = 10 nM
[S] = 20 nM
[S] = 30 nM

Figure 3

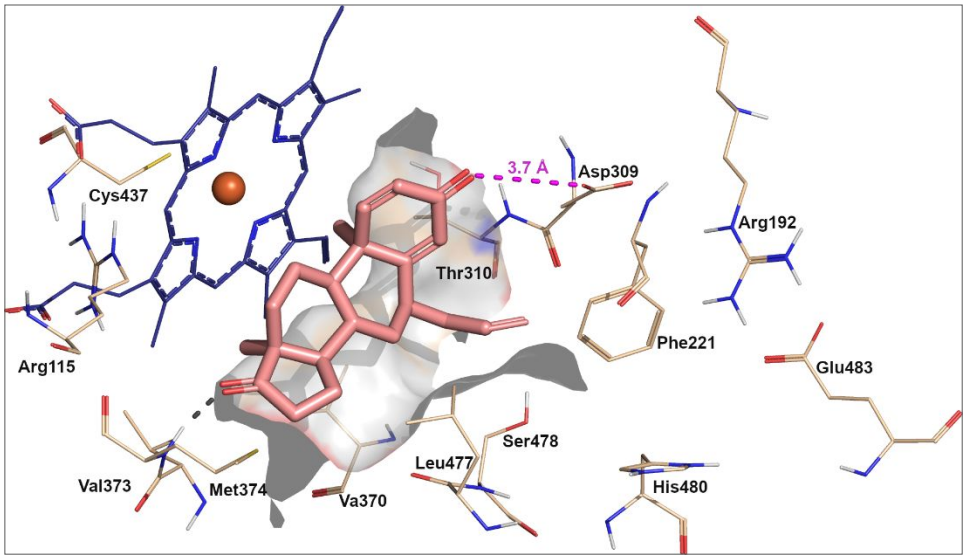
3.7 A
Asp309
Cys437
Arg192
Thr310
Phe221
Arg115
Glu483
Ser478
Leu477
Val373
Met374
Va370
His480

Figure 4

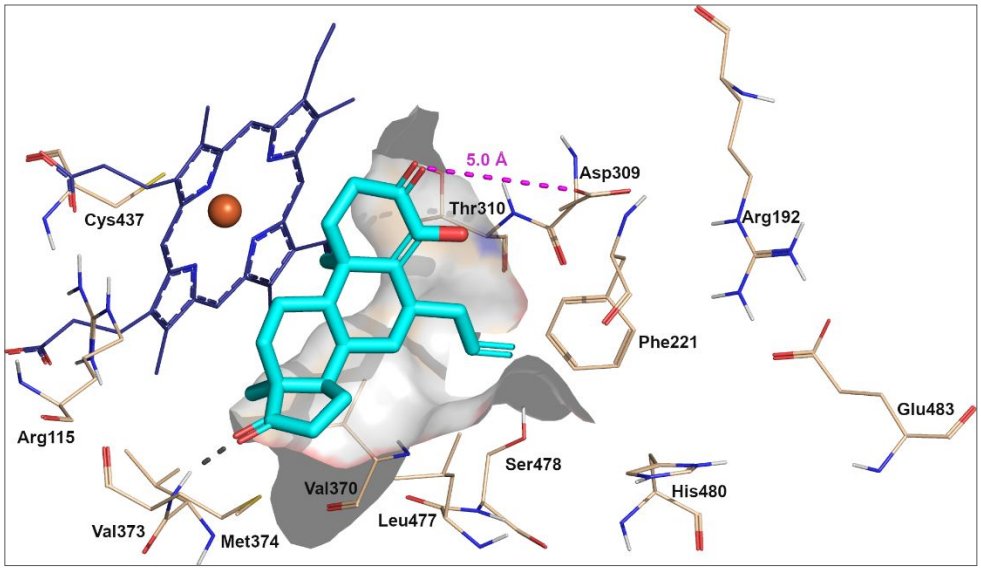
5.0 Å
Asp309
Thr310
Cys437
Arg192
Phe221
Glu483
Arg115
Ser478
Val370
His480
Leu477
Val373
Met374

Figure 5

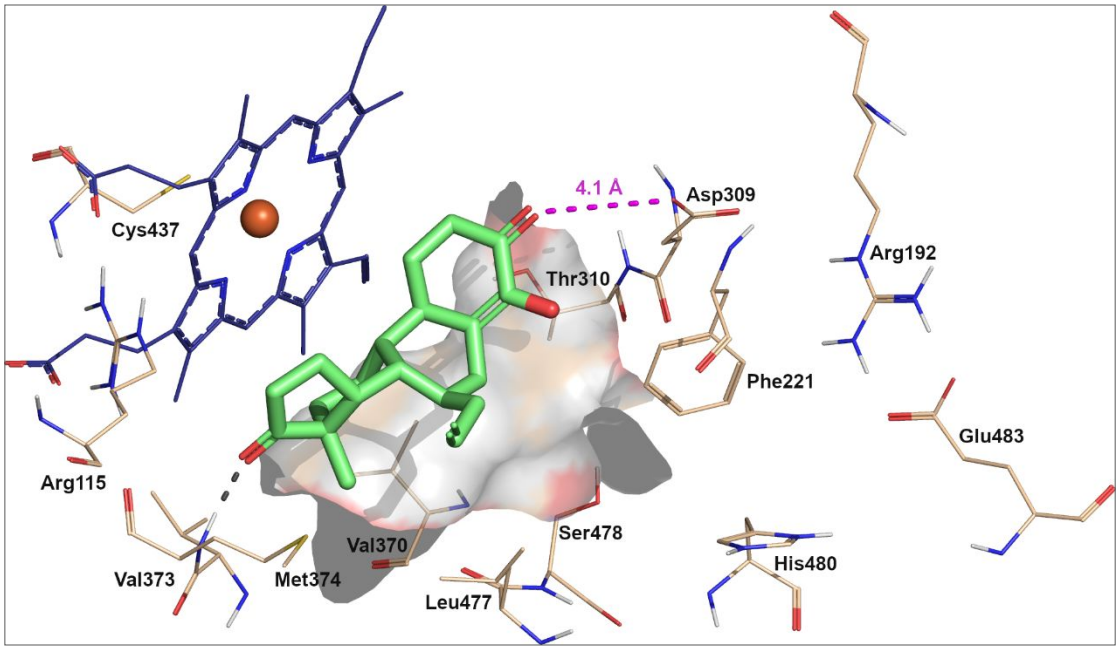
4.1 Å
Asp309
Cys437
Thr310
Arg192
Phe221
Glu483
Arg115
Val370
Ser478
His480
Val373
Met374
Leu477

Figure 6

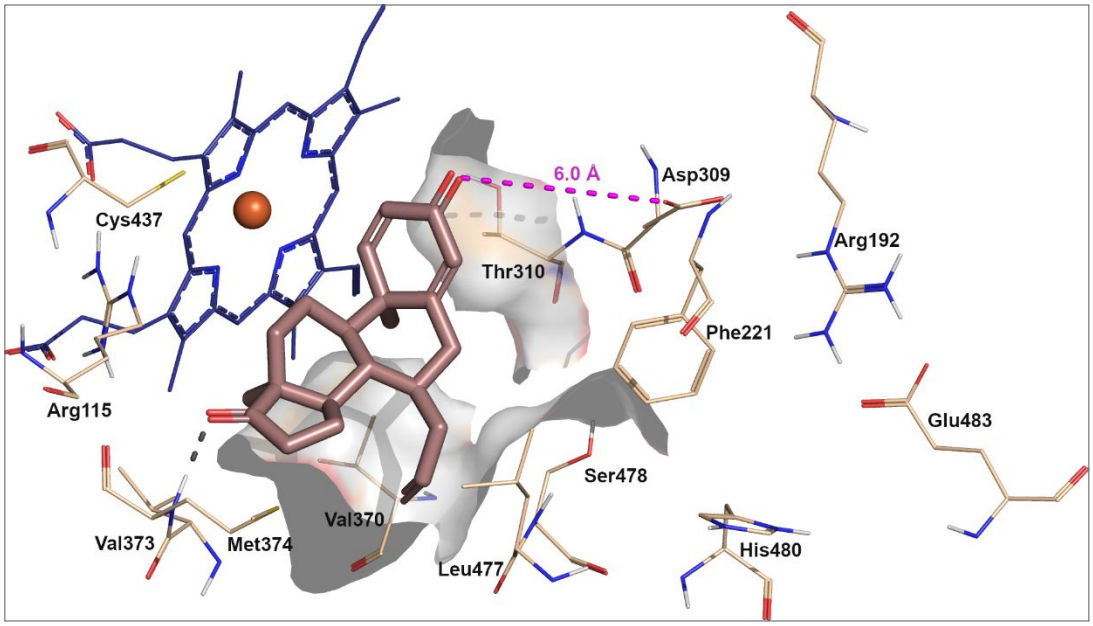
6.0 Å
Asp309
Cys437
Thr310
Arg192
Phe221
Arg115
Glu483
Ser478
Val370
Val373
Met374
Leu477
His480

Figure 7

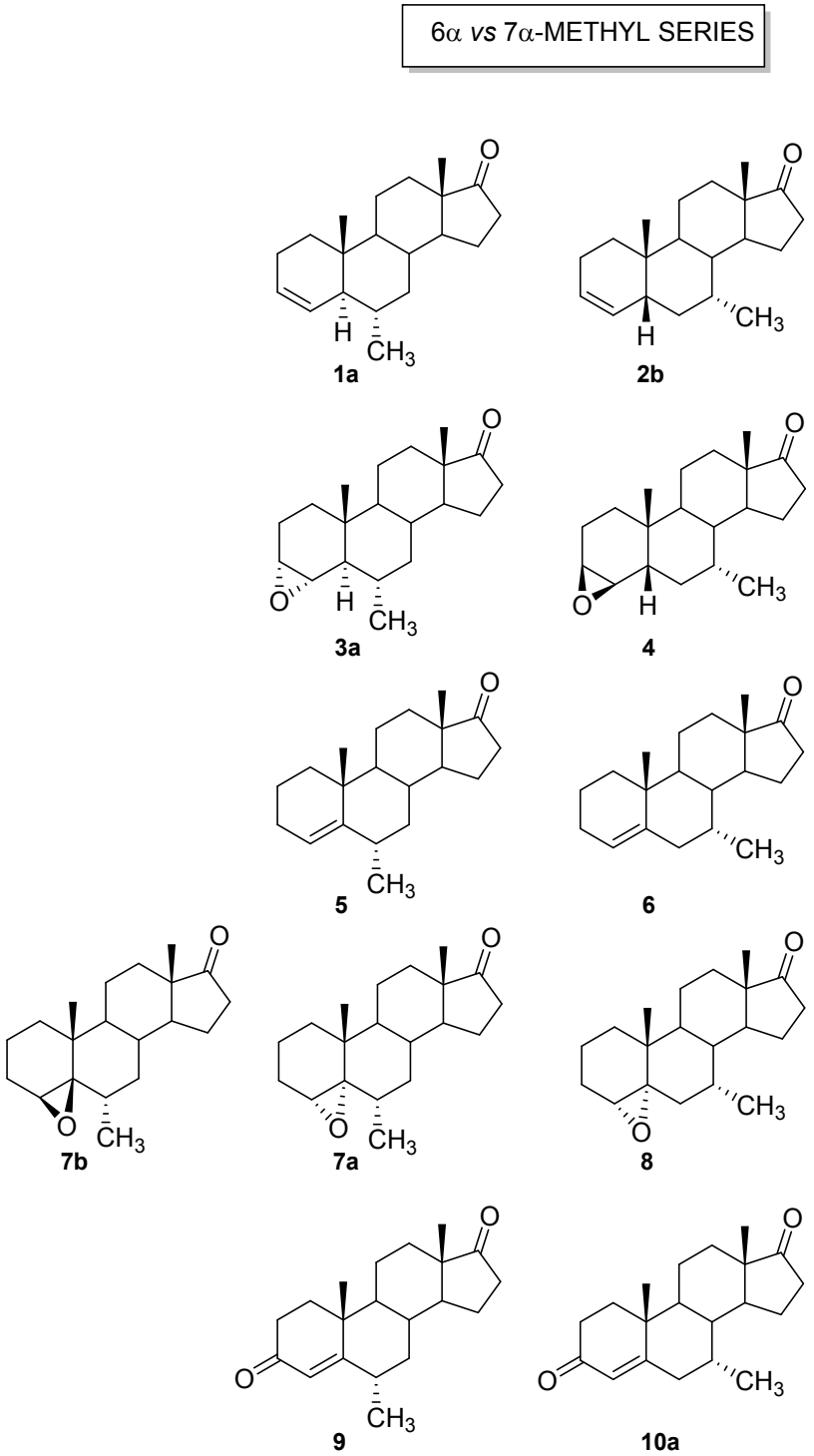

Scheme 1

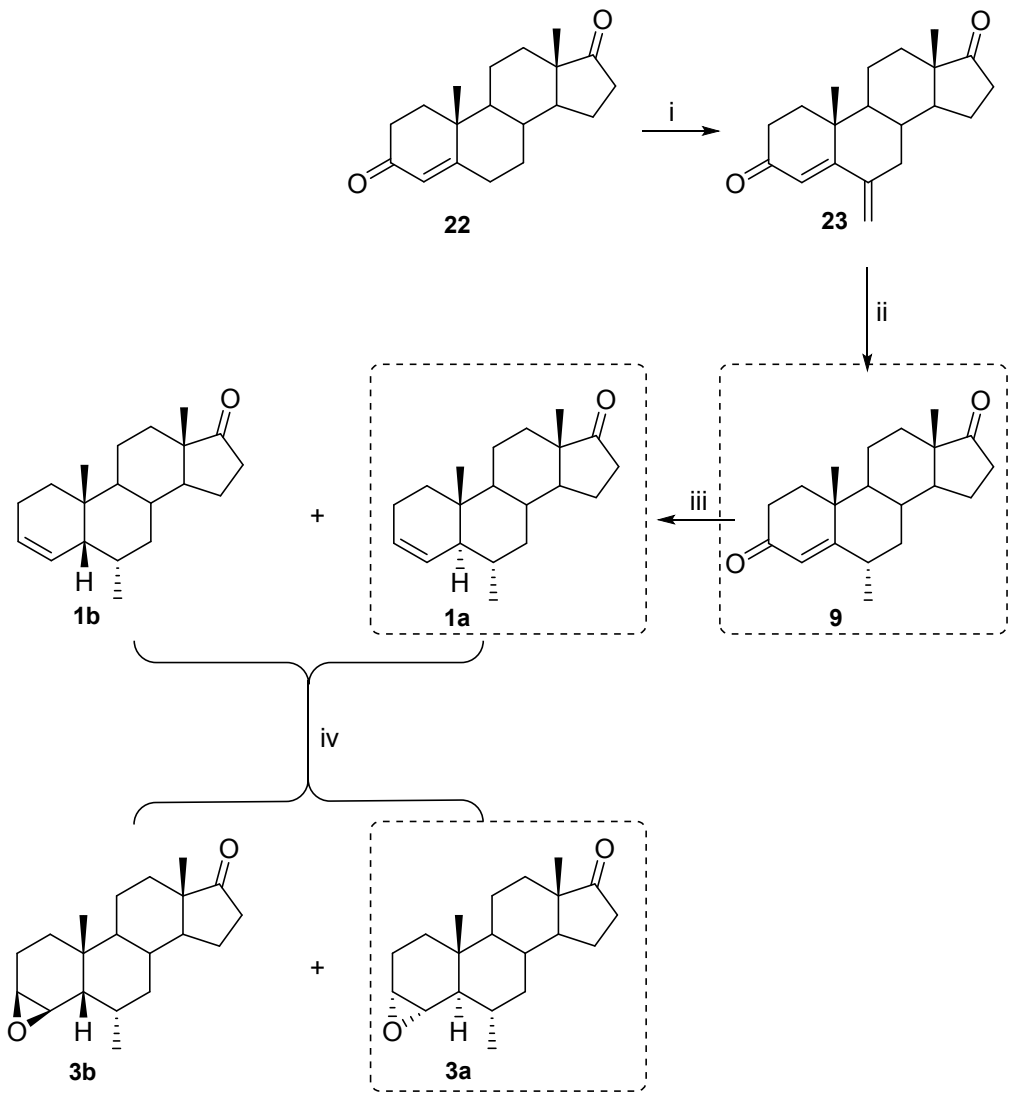

Scheme 2

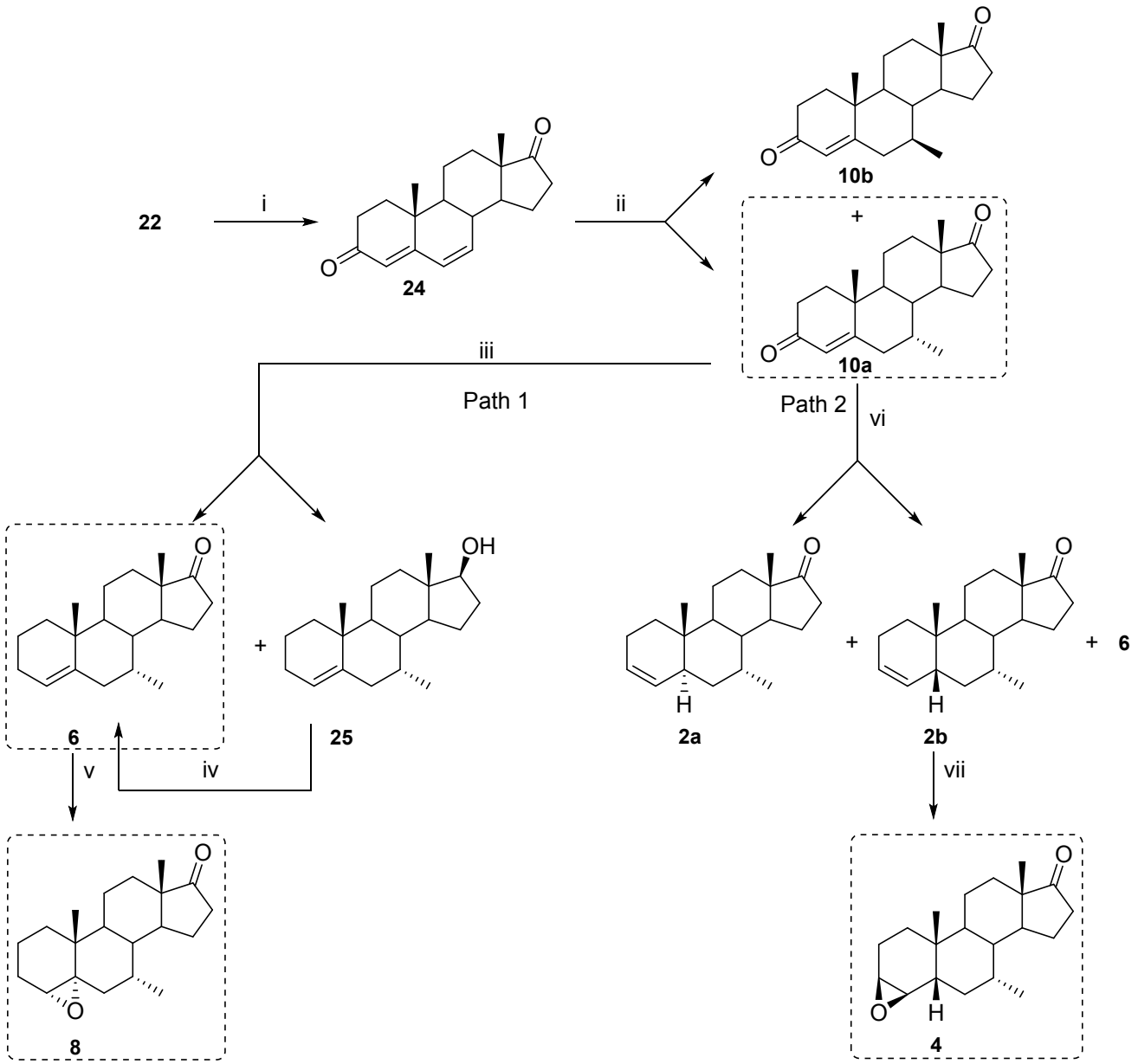

Scheme 3

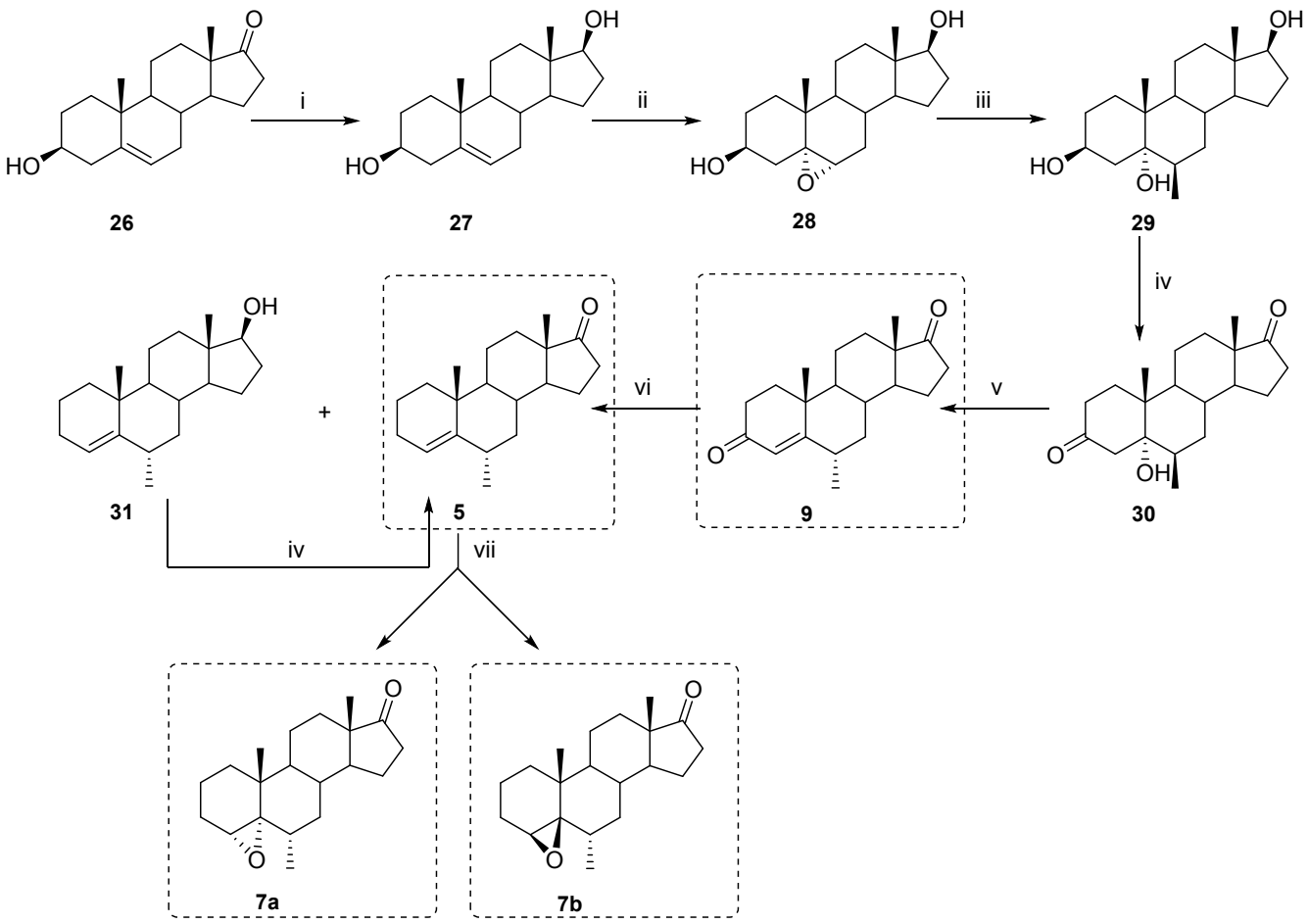

Scheme 4

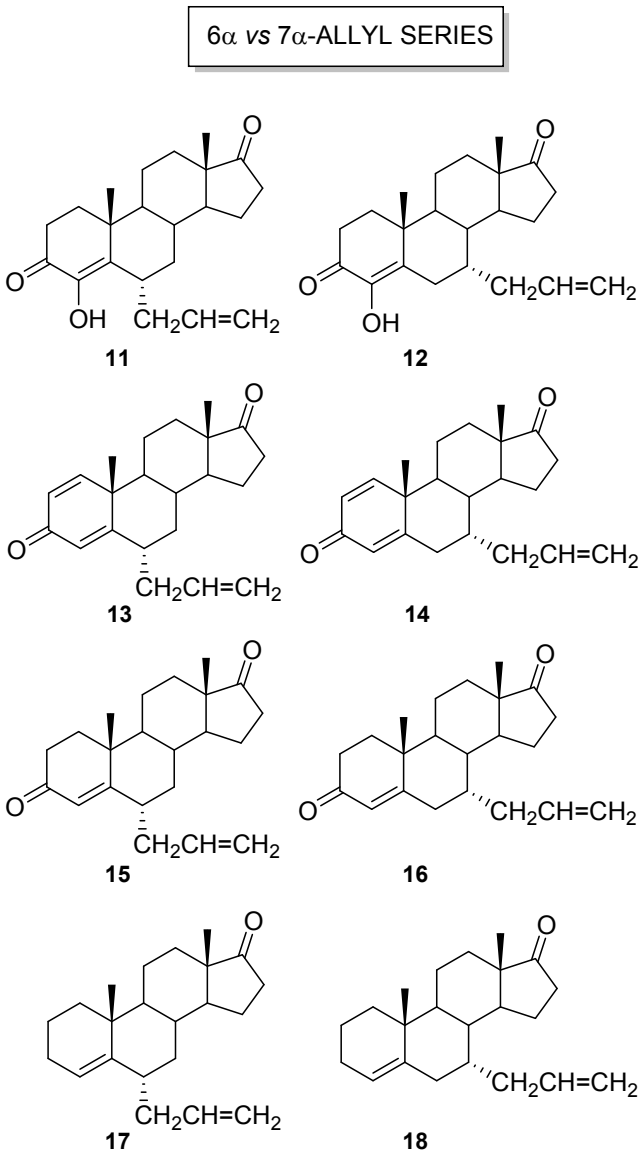

Scheme 5

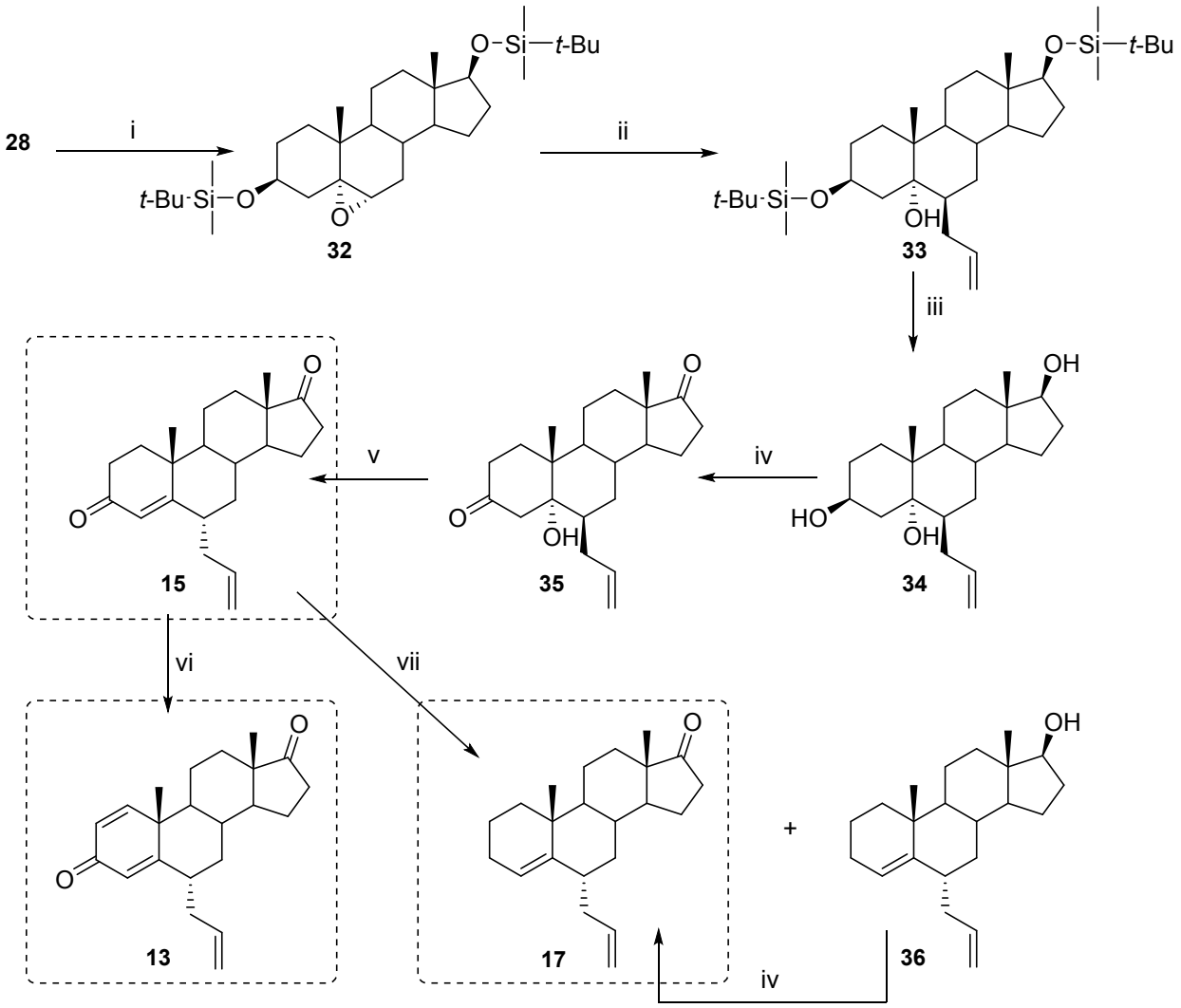
28
i
ii
iii
iv
v
vi
vii
iv
32
33
34
35
15
13
17
36
+
O-Si—t-Bu
t-Bu·Si—O
OH
HO
O

Scheme 6

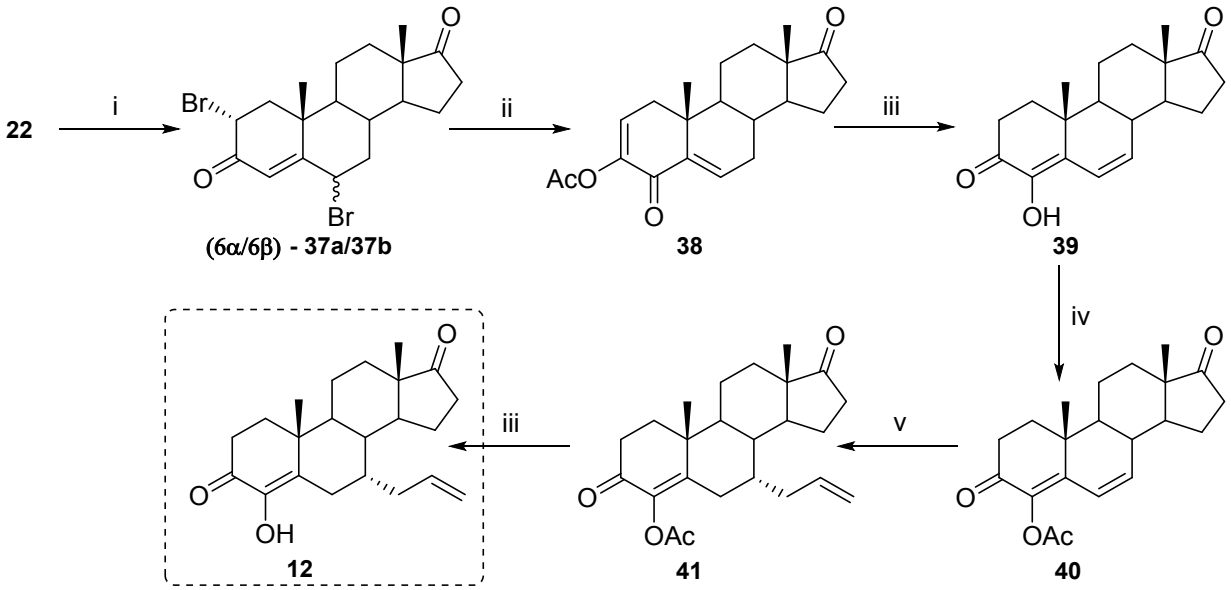
22
i
Br
O
Br
(6α/6β) - 37a/37b
ii
AcO
O
38
iii
O
OH
39
iv
O
OAc
40
v
O
OAc
41
iii
O
OH
12

Scheme 7

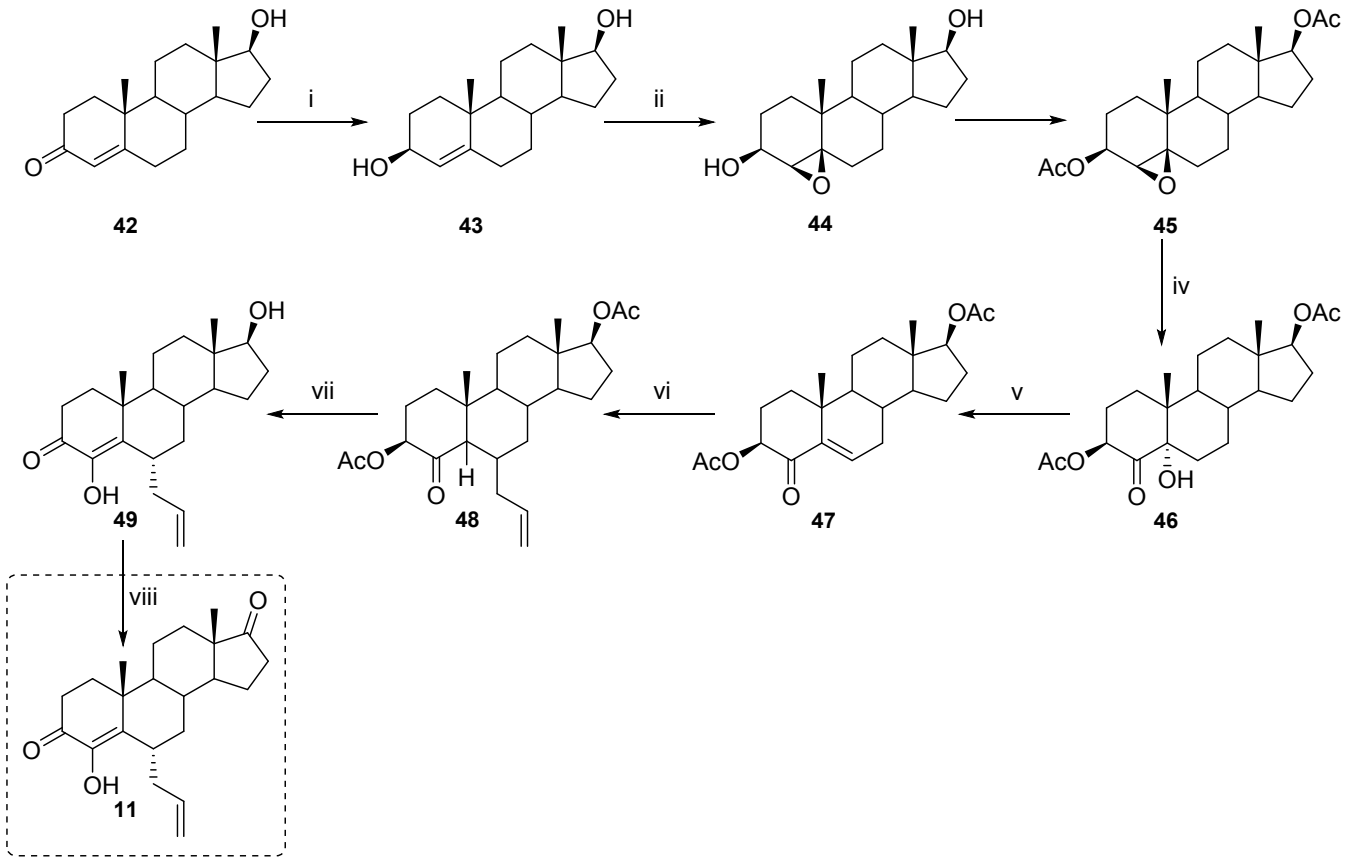
OH
O
42
i
OH
HO
43
ii
OH
HO
O
44
OAc
AcO
O
45
iv
OAc
AcO
OH
O
46
v
OAc
AcO
O
47
vi
OAc
AcO
O
H
48
vii
OH
O
OH
49
viii
O
O
OH
11

Scheme 8

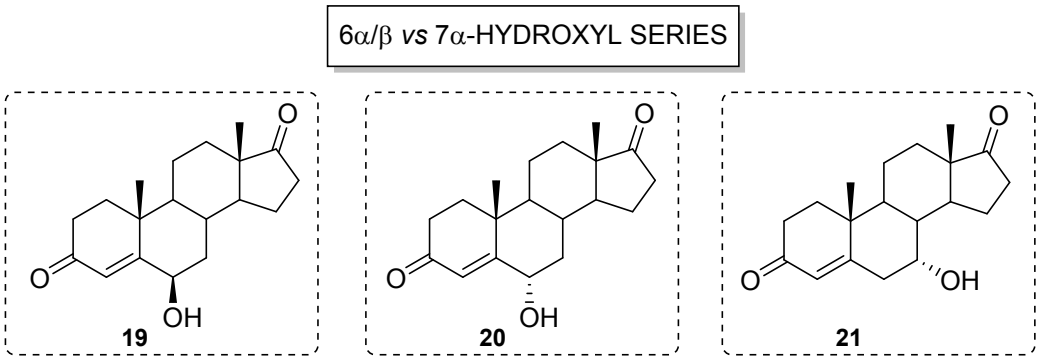

Scheme 9

Table 1 – *In vitro* aromatase inhibition of different steroidal compounds with A- and B-ring modifications in human placental microsomes and in ER^+ breast cancer cells.

Compounds	Human placental microsomes		MCF-7aro cells
	Aromatase Inhibition[a] (%) ± SEM	IC_{50}[b] (μM)	Aromatase Inhibition[c] (%) ± SEM
1a	93.47 ± 1.1	0.560 ± 0.018	88.71 ± 3.0
2b*	89.61 ± 1.4	0.510 ± 0.051	-
3a	96.72 ± 0.4	0.175 ± 0.008	84.21 ± 3.2
4	13.66 ± 3.1	-	-
5	96.72 ± 0.4	0.170 ± 0.009	crystals
6	97.39 ± 1.1	0.405 ± 0.012	89.53 ± 1.9
7a	58.69 ± 2.9	-	-
7b	76.15 ± 2.4	-	-
8	64.89 ± 4.5	-	-
9	98.73 ± 0.1	0.060 ± 0.005	98.56 ± 0.7
10a	94.35 ± 0.5	0.270 ± 0.026	90.77 ± 0.4
11	90.13 ± 0.4	0.520 ± 0.075	80.74 ± 2.4
12	91.80 ± 1.4	0.110 ± 0.006	crystals
13	97.59 ± 0.1	0.055 ± 0.003	99.21 ± 1.1
14	94.49 ± 1.0[d]	0.470 ± 0.05[d]	96.26 ± 0.6
15	97.18 ± 0.4	0.105 ± 0.013	96.52 ± 1.7
16	83.14 ± 1.9[d]	0.590 ± 0.047[d]	92.57 ± 2.5
17	92.39 ± 1.2	0.210 ± 0.011	84.14 ± 3.4
18	84.29 ± 3.3[d]	0.745 ± 0.063[d]	74.74 ± 3.9
19	88.58 ± 2.2	0.840 ± 0.025	88.22 ± 1.5
20	90.65 ± 2.3	0.880 ± 0.065	88.43 ± 2.6
21	49.83 ± 1.9	-	-
Formestane (F)	99.22 ± 0.1	0.042 ± 0.001[e]	97.14 ± 0.4
Exemestane (Exe)	98.91 ± 0.6	0.050 ± 0.009[f]	99.62 ± 0.07

[a]Concentrations of 40 nM [1β-^{3}H] androstenedione, 20 μg protein from human placental microsomes, 150 μM NADPH, 2 μM of the compounds and 15 min incubation were used. [b]Concentrations of 100 nM [1β-^{3}H] androstenedione, 20 μg protein from human placental microsomes, 150 μM NADPH, different concentrations (0.01 – 2 μM) of the compounds and 15 min incubation were used. [c]Concentrations of 50 nM [1β-^{3}H] androstenedione, confluent MCF-7aro cells, 10 μM of the compounds and 1 h of incubation were used. Results represent the mean ± S.E.M. of three different experiments performed in triplicate. Formestane (F) and exemestane (Exe) were used as reference AIs. [d]IC_{50} value according to ref 18. [e]IC_{50} value according to ref 17. [f]IC_{50} value according to ref 19. *The results presented for compound **2b** refers to a mixture (7.6:2.4) of **2b** with **6**.

Table 2 – Kinetic Studies for the steroidal AIs **9** and **13**

Compounds	Type of inhibition	Kinetic studies[a] Vm (mol/min/μg prot)	Ki (μM)	Real affinity (Km/Ki) (nM)
9	Competitive reversible	0.0191 ± 0.0009	0.025	2.53 ± 0.10
13	Competitive irreversible	-	0.0225	2.81 ± 0.06

[a]Concentrations of 10, 20 and 30 nM of [1β-^{3}H]androstenedione, 20 μg of protein from human placental microsomes, 150 μM NADPH, different concentrations of the compounds (0.02 – 0.4 μM) and 5 min of incubation were used. Apparent inhibition constants (Ki) were obtained by Dixon Plot. Inhibition type was based on analysis of the Lineweaver−Burk plot. The experiments were performed in triplicate in three independent experiments.

Table of Contents graphic